Přiložený dokument 1

Increasing Veno-Arterial Extracorporeal Membrane Oxygenation Flow Reduces Electrical Impedance of the Lung Regions in Porcine Acute Heart Failure

Michaela POPKOVÁ[1], Eduard KURIŠČÁK[1], Pavel HÁLA[1,2], David JANÁK[1,3], Leoš TEJKL[1], Jan BĚLOHLÁVEK[4], Petr OŠŤÁDAL[2], Petr NEUŽIL[1,2], Otomar KITTNAR[1], Mikuláš MLČEK[1]

[1]Department of Physiology, First Faculty of Medicine, Charles University, Prague, Czech Republic, [2]Department of Cardiology, Na Homolce Hospital, Prague, Czech Republic, [3]Department of Cardiovascular Surgery, Second Faculty of Medicine, Charles University and University Hospital Motol, Prague, Czech Republic, [4]Second Department of Medicine – Cardiovascular Medicine, First Faculty of Medicine, Charles University and General University Hospital, Prague, Czech Republic

Received January 6, 2020
Accepted April 22, 2020
Epub Ahead of Print June 25, 2020

Summary

Veno-arterial extracorporeal membrane oxygenation (VA ECMO) is a technique used in patients with severe heart failure. The aim of this study was to evaluate its effects on left ventricular afterload and fluid accumulation in lungs with electrical impedance tomography (EIT). In eight swine, incremental increases of extracorporeal blood flow (EBF) were applied before and after the induction of ischemic heart failure. Hemodynamic parameters were continuously recorded and computational analysis of EIT was used to determine lung fluid accumulation. With an increase in EBF from 1 to 4 l/min in acute heart failure the associated increase of arterial pressure (raised by 44 %) was accompanied with significant decrease of electrical impedance of lung regions. Increasing EBF in healthy circulation did not cause lung impedance changes. Our findings indicate that in severe heart failure EIT may reflect fluid accumulation in lungs due to increasing EBF.

Key words

Extracorporeal membrane oxygenation • Electrical impedance tomography • Pulmonary edema • Swine

Corresponding author

Mikuláš Mlček, Department of Physiology, First Faculty of Medicine, Charles University, Albertov 5, 128 00 Prague 2, Czech Republic. E-mail: mikulas.mlcek@lf1.cuni.cz

Introduction

Veno-arterial extracorporeal membrane oxygenation (VA ECMO) is a lifesaving method used in patients with severe circulatory failure refractory to conventional management (Abrams *et al.* 2014, Makdisi and Wang 2015). It can substitute lungs and support circulation since it enables blood gas exchange (oxygenation and carbon dioxide extraction), improves tissue perfusion (Hala *et al.* 2016, Lequier *et al.* 2017), and serves as a bridge of the critical period (Ostadal *et al.* 2018). Blood is bypassed from the native circulation through percutaneous venous cannula to the gas exchange unit and after being oxygenated, it is returned into the descending aorta. Blood from VA ECMO is thus mixed with the blood pumped by the left ventricle (LV). Recent papers have discussed the negative effects of increased afterload on the LV function (Fuhrman *et al.* 1999, Soleimani and Pae 2012, Ostadal *et al.* 2015, Brechot *et al.* 2017, Donker *et al.* 2019, Hála *et al.* 2020), which may lead to LV distension, a rise in the end-diastolic volume, end-systolic volume, end-diastolic pressure, and in left atrial pressure. Progression into pulmonary edema may consequently occur (Fuhrman *et al.* 1999, Burkhoff *et al.* 2015, Ostadal *et al.* 2015, Ostadal *et al.* 2018, Donker *et al.* 2019). Furthermore, clinical work by Kim

Fax +420 241 062 164, e-mail: physres@fgu.cas.cz, www.biomed.cas.cz/physiolres

et al. (2018) recently described how excessive cumulative fluid balance during early phases of ECMO increases the risk of mortality.

Pulmonary edema is a serious complication of VA ECMO, especially in patients with severely impaired left ventricular function. Therefore, it often requires urgent intervention (Fuhrman *et al.* 1999, Brechot *et al.* 2017, Donker *et al.* 2019). Currently, standard diagnostic procedures to detect pulmonary edema are based on clinical examination, lung ultrasound, echocardiography, chest radiography, and hemodynamics assessment. However, these methods are lacking the sensitivity to quantify fluid volumes (Cardinale *et al.* 2014) and may require repeated evaluations. Real-time diagnostic methods (e.g. transpulmonary thermodilution) are also available, however, requiring additional invasive procedure and lacking high sensitivity (Sobota *et al.* 2019).

Electrical impedance tomography (EIT) is a bedside, non-invasive, radiation-free, and real-time imaging technique based on the assessment of tissue resistivity. This is best represented by the physical quantity called impedance, obtained by probing the tissue with skin electrodes injecting a weak alternating current (excitation frequency ranges from tens to hundreds of kHz). Currently, it is being used for bedside monitoring of regional lung ventilation and the distribution of air within the lungs, especially in patients with acute lung injury and acute respiratory distress syndrome (Frerichs *et al.* 2017, Bachmann *et al.* 2018). Due to the air space in the alveoli, native resistivity of lung tissue is high and electrical impedance varies considerably with breathing cycles reaching peak values during inspiration. Conversely, impedance of plasma is low and therefore increased volume of fluid in lungs has a considerable effect on decreasing tissue electrical impedance. Sobota *et al.* (2019) and Becher *et al.* (2019) recently demonstrated in both animal experiments and clinical practice that intravenous administration of fluids has a significant effect on the lung impedance. Therefore, EIT can serve as a suitable method for bedside evaluation of small fluid changes in the lungs (Adler *et al.* 1997, Noble *et al.* 2000). Moreover, the diagnostic potential of EIT can be further increased using advanced signal analysis, which allows for the evaluation of the regional perfusion and heart work (Borges *et al.* 2012, Reinius *et al.* 2015).

The purpose of this pilot study was to evaluate the acute fluid changes in the lungs during VA ECMO support. Lung impedance changes were registered during incremental increases in VA ECMO blood flow under both healthy and failing heart conditions. We present a new computational analysis of the raw EIT data which detects minor changes in fluid content specifically within the lung tissue.

Methods

Experimental protocol was reviewed and approved by the Institutional Animal Expert Committee of the Fist Faculty of Medicine, Charles University and was performed at the University experimental laboratory, Department of Physiology, First Faculty of Medicine, Charles University, Prague, Czech Republic, in accordance with Act No 246/1992 Coll. on the protection of animals against cruelty. All animals were treated and cared in accordance with the European Guidelines on Laboratory Animal Care.

Animal model

Eight healthy female pigs (*Sus scrofa domestica*), weight 57±2 kg, were included in this study. After 12 hours of fasting, animals were premedicated with midazolam (0.2-0.4 mg/kg IM) and ketamine (15-25 mg/kg IM), then marginal ear vein access was secured, and induction of anesthesia was achieved by intravenous application of propofol (2 mg/kg IV). The animals were positioned into the dorsal recumbency before the endotracheal intubation was performed (tube 7-8 mm). Mechanical ventilation was operated by Hamilton G5 ventilator (Hamilton Medical AG, Switzerland), set to volume control ventilation described in more detail in the ECMO protocol section. The position of the animals was stable during the whole experiment.

Total intravenous anesthesia was maintained during the experiment. Propofol (6-10 mg/kg/h) and midazolam (0.1-0.2 mg/kg/h) were combined with opiate analgesia (morphine 0.1-0.3 mg/kg/h), and the depth of anesthesia was confirmed by controlling reflexes, muscle tone, and cardiovascular reactions. Continuous infusions of heparin (50-80 UI/kg/h) was set to prevent thrombosis. Infusion of Ringer's solution and 0.9 % saline was kept within range 5-10 ml/kg/h to maintain central venous pressure (CVP) around 5 mmHg before the ECMO implantation. Foley catheter was inserted through the urethra to the urinary bladder to monitor urine production.

Experimental preparation and monitoring

A triple lumen central venous catheter was placed percutaneously through the external jugular vein for CVP monitoring, as well as for fluid and anesthetics administration. The femoral artery was cannulated to measure systemic blood pressure. A balloon Swan-Ganz catheter was inserted into the pulmonary artery via the femoral vein to simultaneously record pulmonary artery pressure, mixed venous oxygen saturation (SvO_2), and cardiac output (CCO Combo Catheter, Vigilance II, Edwards Lifesciences, USA), whereas pulmonary capillary wedge pressure (PCWP) was measured upon completion of each ECMO flow step. The right carotid artery was surgically exposed, and an ultrasound flow probe was placed around the vessel (4PSB or 6PSB, Transonic Systems, USA) to continuously measure the blood flow. Regional tissue oxygenation (rSO_2) was monitored by near-infrared spectroscopy (INVOS Oximeter, Medtronic, USA) with sensors placed on forehead and right forelimb, to evaluate head and peripheral tissue oxygen saturation.

Electrical impedance tomography

Swisstom EIT-Pioneer set (Swisstom, AG, Switzerland) was used to measure the electrical impedance tomography of the thorax. The sensor belt, fitted with 32 evenly distributed electrodes, was placed around the circumference of the thorax and its position was verified by X-ray to ensure its proper position above the diaphragm around both lungs and the heart. Alternating electrical current of single frequency (3 mA, 200 kHz) was applied through pairs of electrodes and corresponding voltages were measured on the remaining electrodes. The pattern of the injecting and sensing electrodes was rearranged automatically, achieving apparent rotatory movement of probing electrodes around the chest, resembling the way the computed tomography image is obtained. This allows for the real-time (update rate 50 Hz) reconstruction of the tissue impedance, generating a 64x64 pixel matrix every 20 ms, and so creating a dynamic 2D image of the thoracic tomographic plane.

Veno-arterial extracorporeal membrane oxygenation

Extracorporeal membrane oxygenation in veno-arterial setting (VA ECMO) was used. The dosage of heparin was set to keep activated clotting time at 200-300 s. ECMO cannulas were introduced by Seldinger technic through punctures of the ipsilateral femoral vein and artery. The tip of the inflow venous cannula (21 Fr) was placed near the right atrium and the arterial outflow cannula (15 Fr) was placed in the descending aorta. The

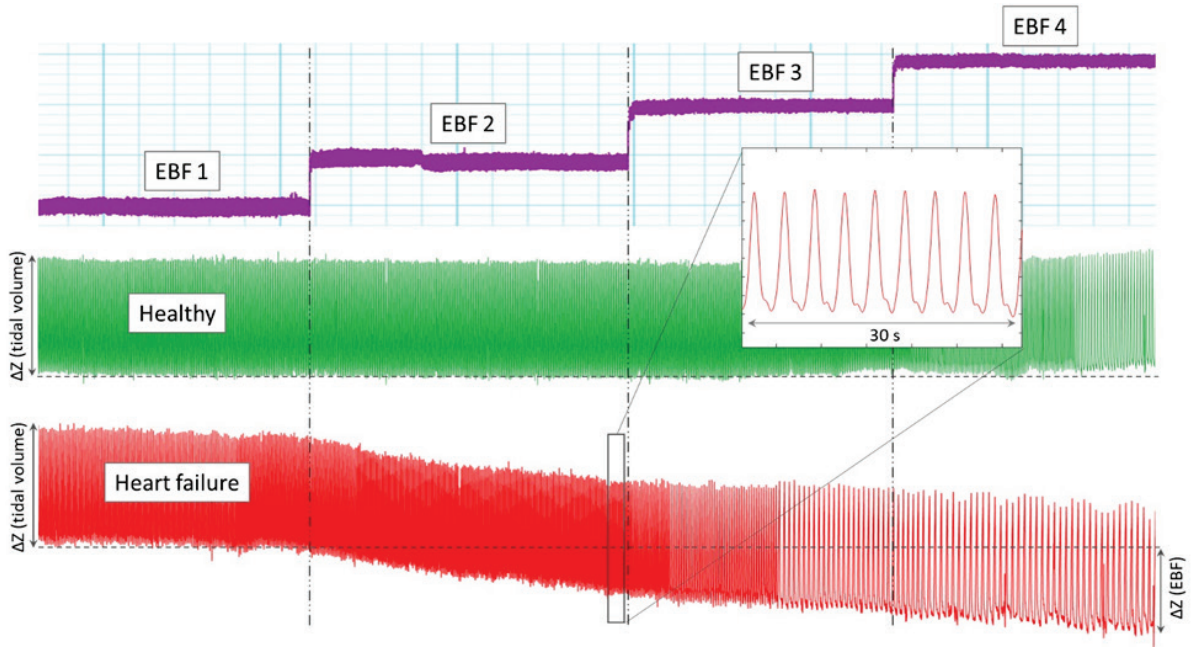

Fig. 1. Representative example of EIT waveforms from one animal. Stepwise changes with increasing VA ECMO flows (purple) are aligned with electrical impedance for both healthy (green) and heart failure (red) conditions. Electrical impedance waveforms represent impedance of lung regions during breathing cycles. End-expiratory impedance was evaluated at the end of each EBF step and with increasing EBF it did not change in healthy condition but decreased significantly in heart failure. ΔZ (tidal volume) represents the change in electrical impedance during breathing cycle (tidal volume), whereas ΔZ (EBF) represents change in impedance with increased EBF (EBF 1 to EBF 4 l/min). ΔZ (EBF) is approximately 60 % of the ΔZ (tidal volume) in this animal.

position of both cannulas was verified by fluoroscopy. Extracorporeal blood flow (EBF) was measured by the flow probe (ME 9PXL, Transonic, USA) attached to the outflow cannula. Blood gas parameters were monitored continuously in the blood leaving the oxygenator (CDI® Blood Parameter Monitoring System 500, Terumo Cardiovascular System Corporation, USA). The oxygen and air flow were adjusted to maintain arterial pO_2 at 150-200 mmHg and pCO_2 at 35-45 mmHg.

ECMO protocol

After the introduction of VA ECMO, the defined protocol (Fig. 1) with increasing EBF was applied to healthy cardiovascular system (before the induction of HF). Lung-protective ventilation was set to volume control: tidal volume (V_T) 6-7 ml/kg, positive end-expiratory pressure (PEEP) 5-6 cmH_2O, peak inspiratory pressure PIP < 25 cmH_2O, fraction of inspired oxygen (FiO_2) 30 %. V_T and PEEP were kept constant during the protocol and the respiratory rate was adjusted to maintain end-tidal CO_2 ($etCO_2$) 35-45 mmHg. Administration of intravenous infusions was constant throughout the protocol (5-6 ml/kg/h). VA ECMO flow was increased stepwise with 20 ml/kg/min increments, starting at 20 ml/kg/min (referred to as EBF 1 l/min) and reaching up to 80 ml/kg/min (EBF 4 l/min). Each step lasted 8-12 min. At the end of each step lung impedance and hemodynamic parameters were obtained by averaging end-expiratory values during 30 s.

Heart failure

A model of acute HF was used in our experiment. Based on previous publications (Suzuki *et al.* 2008, Ishikawa *et al.* 2014, Li *et al.* 2014) and our own experience (Ostadal *et al.* 2016, Janak *et al.* 2017, Hala *et al.* 2018, Lacko *et al.* 2018), an ischemic HF model was induced by fluoroscopically controlled proximal occlusion of the left anterior descending coronary artery (LAD) with a balloon-tip catheter (balloon 4 x 20 mm or 5 x 20 mm). Amiodarone was administered (150-300 mg IV) prior to the occlusion. LAD occlusion lasted for 40-50 min. In case the ventricular fibrillation (VF) occurred, the ECMO flow of 60 ml/kg/min was used to substitute the systemic circulation. Defibrillation was then performed after the balloon deflation. Moreover, if MAP dropped below 50 mmHg, continuous infusion of norepinephrine (0.01-0.1 mcg/kg/min) was started and titrated at the lowest rate to maintain MAP 50-60 mmHg.

Subsequently, identical VA ECMO protocol as described above was applied to conditions of acute ischemic heart failure, and hemodynamic and lung impedance values were compared to those acquired with the healthy circulation.

Electrical impedance data analysis

As mentioned above, the 64x64 pixel matrix of impedances was continuously generated throughout the whole experiment with an update rate of 50 Hz, creating a dynamic, real-time, cross-sectional, 2D thorax map, at the position of the EIT sensor belt. In time domain, each pixel of that matrix represents the time-course of reconstructed electrical impedance of corresponding thorax tissue region. To filter out frequencies higher than those related to breathing, we rejected all frequencies above 1 Hz by low-pass filter. Furthermore, to isolate the lung regions, we filtered out other chest areas, by discarding pixels (matrix elements) that were more than 0.8π cycle out of breathing phase, as viewed from the 0π phase pixel representing the center of the lungs (Fig. 2).

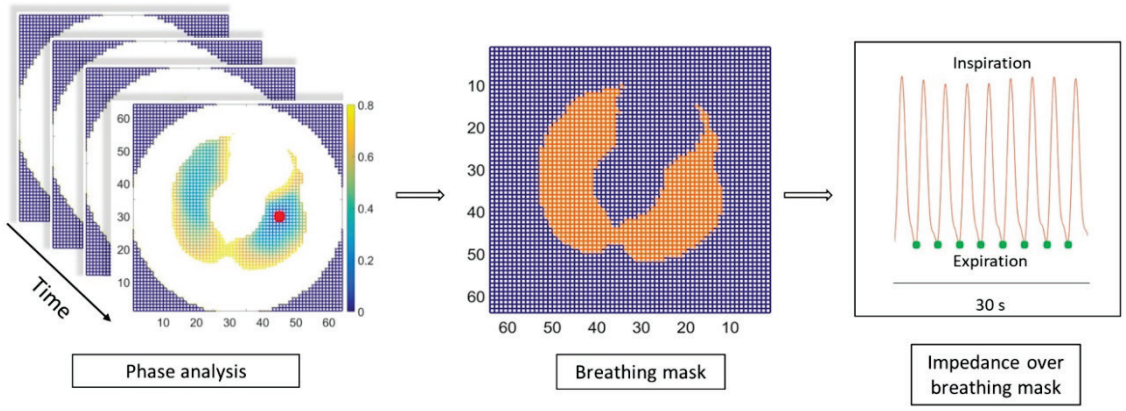

Fig. 2. Analysis of EIT signal. To the left, 64x64 impedance matrix and corresponding colorbar map show the phase delay from the reference pixel of zero phase (red dot), representing the center of the left lung. In the middle, resulting breathing mask (orange) defines pixels which were analyzed at expiration (green dots), averaged over this mask region, and normalized to the EIT value obtained at EBF 1 l/min. EBF – extracorporeal blood flow, EIT – electrical impedance tomography.

Pixels being less than 0.8π from the 0π reference point set up the breathing mask at the beginning of each experiment. Then, the impedance was averaged over this mask region only (summing all impedances of those pixels, divided by the number of pixels in the mask), giving us the course of impedance of whole lungs in time. These EIT values registered at the end of expiration averaged over the last 30 s of each EBF step, were further processed. To eliminate interindividual variability of absolute lung impedance, values of lung impedance were rescaled by normalization. Within the time frame of one ECMO protocol, impedance values taken at various EBF steps were normalized with respect to the EBF of 1 l/min (assigned with reference impedance set to 1).

Statistical analysis

Except the electrical impedance, recordings were sampled at 400 Hz by PowerLab A/D converted and continuously recorded by LabChart Pro Software (ADInstruments, Australia). EIT data were analyzed in MATLAB (The MathWorks, USA) and normalized to baseline value measured at 1 l/min of EBF. Statistical analyses were performed in GraphPad Prism 7 (GraphPad Software, USA) and Excel (Microsoft, USA).

All results are expressed as mean ± standard error of mean (SEM). The differences among individual levels of EBF were analyzed using a repeated-measures one-way ANOVA with Tukey's multiple comparison test or using the Friedman test with Dunn's multiple comparison test (for data sets without normal distribution). Success in heart failure induction was verified using the Wilcoxon signed-rank test. A P value of <0.05 was considered statistically significant.

Table 1. Hemodynamic parameters of heart failure induced by myocardial ischemia.

		Healthy	Heart failure	P value	*Change*
$_pCO$	*l/min*	5.5 ± 0.7	2.9 ± 0.3	< 0.01	-47 %
MAP	*mmHg*	76 ± 5	51 ± 4	< 0.01	-33 %
Carotid flow	*ml/min*	419 ± 37	248 ± 22	< 0.05	-41 %
SvO_2	*%*	76 ± 3	59 ± 6	< 0.01	-23 %
rSO_2 head	*%*	72 ± 2	54 ± 3	< 0.05	-25 %

Values expressed as mean ± SEM. Last column presents the relative change between healthy and heart failure. Parameters were obtained with 1 l/min of EBF before start of the ECMO protocol. EBF – extracorporeal blood flow, ECMO – extracorporeal membrane oxygenation, MAP – mean arterial pressure, $_pCO$ – cardiac output measured using a pulmonary artery catheter, rSO_2 head – regional tissue oxygenation measured on forehead, SvO_2 – mixed venous oxygen saturation.

Results

Hemodynamic characteristics of the model before (healthy) and after the acute heart failure (HF) induction are summarized in Table 1. Ventricular fibrillation occurred in all animals within the first ten minutes of LAD occlusion. It was successfully terminated by an external defibrillation. HF induction had a significant effect on all major hemodynamic parameters: cardiac output decreased from 5.5±0.7 to 2.9±0.3 l/min (P<0.01), MAP from 76±5 to 51±4 mmHg (P<0.01), carotid flow from 419±37 to 248±22 ml/min (P<0.05), and mixed venous oxygen saturation and rSO_2 on forehead decreased by 23 % and 25 %, respectively (for both P<0.05). All these parameters were obtained with 1 l/min of EBF support, before the start of each ECMO protocol. Moreover, five animals required norepinephrine administration (0.01-0.1 ml/kg/min) during EBF 1 to prevent severe hypotension. In these animals, norepinephrine was discontinued after MAP reached 60 mmHg.

VA ECMO effects on hemodynamics and electrical impedance are detailed in Table 2 and Figure 3. With the same VA ECMO protocol applied to the healthy and the heart failure conditions, we have observed different effects on electrical impedance of the lung regions. With increasing EBF from 1 to 4 l/min the normalized lung impedance did not change in the healthy circulation but declined with each EBF step in HF group – from 1±0.0 to 0.986±0.009, 0.979±0.014, and 0.974±0.017 (for EBF 1 to 4 l/min, P<0.001). Figure 1 shows an example of full trends of electrical impedance over the ECMO protocol in healthy and HF conditions.

In stepwise ECMO protocol applied to the

Table 2. Comparison of the effects of extracorporeal blood flow on hemodynamic parameters and electrical impedance of lungs in healthy circulation and heart failure conditions.

	l/min	**EBF 1 Healthy**	**EBF 2 Healthy**	**EBF 3 Healthy**	**EBF 4 Healthy**	**P value Healthy**
MAP	*mmHg*	75 ± 5	84 ± 5	*87 ± 6	**92 ± 6	< 0.01
Carotid flow	*ml/min*	395 ± 26	425 ± 30	*456 ± 31	435 ± 38	< 0.05
MPAP	*mmHg*	29 ± 4	27 ± 4	*24 ± 3	**23 ± 3	< 0.001
PCWP	*mmHg*	5.4 ± 0.9	5.4 ± 0.9	5.1 ± 0.5	4.4 ± 0.6	< 0.05
CVP	*mmHg*	4.4 ± 0.5	3.9 ± 0.5	3.3 ± 0.6	*2.6 ± 0.7	< 0.01
SvO_2	*%*	76 ± 3	80 ± 3	*82 ± 2	*83 ± 3	< 0.01
rSO_2 head	*%*	72 ± 2	73 ± 2	*76 ± 2	**76 ± 1	< 0.01
rSO_2 limb	*%*	69 ± 2	69 ± 2	69 ± 2	70 ± 2	ns
EIT		1.000	0.999 ± 0.006	1.006 ± 0.007	1.006 ± 0.009	ns
	l/min	**EBF 1 Heart failure**	**EBF 2 Heart failure**	**EBF 3 Heart failure**	**EBF 4 Heart failure**	**P value Heart failure**
MAP	*mmHg*	52 ± 5	53 ± 5	60 ± 4	**74 ± 6	< 0.01
Carotid flow	*ml/min*	258 ± 28	310 ± 43	319 ± 23	**410 ± 34	< 0.01
MPAP	*mmHg*	32 ± 4	29 ± 5	25 ± 3	25 ± 3	ns
PCWP	*mmHg*	8.3 ± 1.9	8.8 ± 2.0	10.5 ± 2.1	*10.3 ± 1.8	< 0.001
CVP	*mmHg*	7.5 ± 0.5	6.5 ± 0.5	6.0 ± 0.5	*5.1 ± 0.4	< 0.01
SvO_2	*%*	56 ± 6	67 ± 4	*74 ± 3	****84 ± 4	< 0.0001
rSO_2 head	*%*	52 ± 4	54 ± 5	61 ± 3	**66 ± 3	< 0.01
rSO_2 limb	*%*	58 ± 3	61 ± 2	62 ± 3	**65 ± 3	< 0.01
EIT		1.000	0.986 ± 0.003	**0.9785 ± 0.005	***0.9744 ± 0.006	< 0.001

Values expressed as mean ± SEM. Values significantly different to 1 l/min (EBF 1) are marked with * for P<0.05, ** for P<0.01, *** for P<0.001, **** for P<0.0001. The P values reflect the whole EBF trend statistics. CVP – central venous pressure, EBF – extracorporeal blood flow, EIT – electrical impedance normalized to EBF 1, MAP – mean arterial pressure, MPAP – mean pulmonary artery pressure, PCWP – pulmonary capillary wedge pressure, ns – non-significant, rSO_2 – regional tissue oxygenation, SvO_2 – mixed venous oxygen saturation.

healthy circulation, with increasing EBF (from EBF 1 to 4 l/min) MAP increased from 75±5 to 92±6 mmHg (P<0.01) and mean carotid flow from 395±26 to 435±38 ml/min (P<0.05). MPAP decreased from 29±4 to 23 ± 3 mmHg (P < 0.001), PCWP decreased mildly from 5.4 ± 0.9 to 4.4 ± 0.6 mmHg (P < 0.05), and transpulmonary pressure gradient (TPG) from 24 ± 4 to 18 ± 3 mmHg (P < 0.01). SvO_2 increased from 76 ± 3 % to 83 ± 3 % (P < 0.01). Regional tissue oxygenation increased on forehead from 72 ± 2 % to 76 ± 1 % (P < 0.01) and did not change significantly on forelimb. With increasing EBF, the CVP gradually fell from 4.4 ± 0.5 to 2.6 ± 0.7 mmHg (P < 0.001).

Effects of the same ECMO protocol applied to HF model were considerably stronger. From EBF 1 to 4 l/min MAP increased from 52 ± 5 to 74 ± 6 mmHg (P < 0.01) and carotid flow increased from 258 ± 28 to 410 ± 34 ml/min (P < 0.01). MPAP did not change significantly, nevertheless PCWP increased from 8.3 ± 1.9 to 10.3 ± 1.8 mmHg (P < 0.001), and TPG decreased from 27 ± 4 mmHg to 15 ± 5 mmHg (P < 0.05). SvO_2 improved from 56 ± 6 % to 84 ± 4 % (P < 0.0001), rSO_2 on forehead increased from 52 ± 4 % to 66 ± 3 % (P < 0.01), and on forelimb from 58 ± 3 % to 65 ± 3 % (P < 0.01). CVP decreased from 7.5 ± 0.5 to 5.1 ± 0.4 mmHg (P <0.01).

V_T and PEEP were set constant during the whole protocol to minimize the influence of lung air content to the EIT measurement. Nevertheless, for EBF 1 to 4 l/min mean airway pressure decreased in both groups, from 10.0 ± 0.3 to 9.1 ± 0.4 cmH_2O (P < 0.001) in healthy circulation and from 9.9 ± 0.5 to 8.9 ± 0.3 cmH_2O (P < 0.05) in HF model. With increasing EBF, static lung compliance decreased in healthy circulation group from 31 ± 2 to 30 ± 2 ml/cmH_2O (P < 0.001) but did not change in HF model.

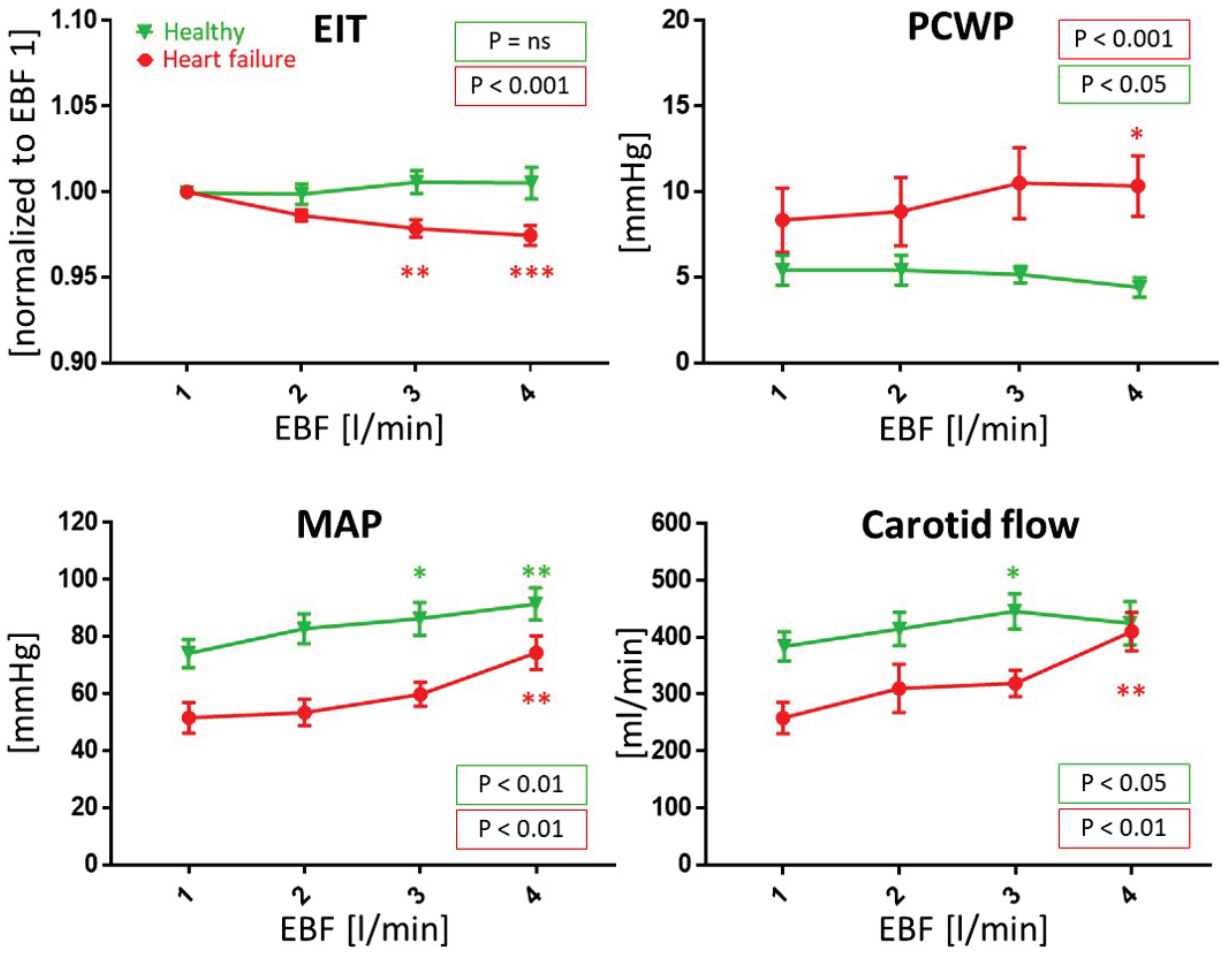

Fig. 3. The effect of veno-arterial membrane oxygenation blood flow (EBF) on selected hemodynamic parameters and EIT in a porcine model of healthy (green triangles) and heart failure (red dots) conditions. Means and SEMs shown here have descriptive meaning, for details of P values see the Methods. Values significantly different to 1 l/min (EBF 1) are marked with * for P<0.05, ** for P<0.01, *** for P<0.001. The two P values in the legend reflect the whole EBF trend statistics. EBF – extracorporeal blood flow, EIT – electrical impedance of lung regions normalized to EBF 1 (1 l/min), MAP – mean arterial pressure, PCWP – pulmonary capillary wedge pressure, ns – non-significant.

Discussion

Recent studies have reported the effect of increasing VA ECMO flow on the LV overload under severe heart failure condition. However, not enough attention has been paid to pulmonary edema which may consequently occur. The primary aim of this study was to evaluate the ability of EIT to distinguish even small changes in fluid content within the lung tissue related to VA ECMO operation. For this purpose, we have developed a custom-build algorithm for EIT signal analysis and together with other hemodynamic and oximetry parameters we used it to compare the effects of VA ECMO on healthy versus heart failure circulation.

Electrical impedance tomography for pulmonary fluid detection

Our key finding is that in a failing circulation supported by VA ECMO, the electrical impedance of pulmonary regions reduces with increasing EBF (1-4 l/min). This was significantly different from a healthy heart with identical ECMO support where there was no change in pulmonary region impedance (Fig. 3). Impedance is affected by numerous parameters such as pulmonary aeration, fluid infusion rate, patient movement, and electrodes position, so care was taken that these were kept constant. This is discussed in more detail here.

The changes of thoracic electrical impedance associated with the breathing cycle are one order of magnitude larger than the changes induced by the heart-lung perfusion cycle or the fluid accumulation. Thus, several approaches have been proposed to separate lung regions and perfusion-related changes as well. This mainly includes auto-detection of the pulmonary region based on methods of identifying regions of interest such

as frequency-based or statistic-based methods (Ferrario *et al.* 2012, Frerichs *et al.* 2017). However, some of these reconstructions do not correspond well to the expected lung anatomy. Isophase analysis, i.e. finding the regions of the same breathing phase (Riedel *et al.* 2009, Graf and Riedel 2017), realized by our own algorithm and area-averaging of the impedance signal identified more relevant breathing regions.

Volume control lung-protective ventilation with constant tidal volume (V_T) and constant PEEP was used to eliminate the effect of variable functional residual capacity and V_T on electrical impedance, revealing thus much more delicate impedance effects caused by parameters like fluid accumulation in lungs. In heart failure conditions, the static lung compliance did not change significantly throughout the protocol, thus we assume that there was no influence of air volume on end-expiratory electrical impedance. In healthy condition there was a small decrease of static lung compliance (0.9 ml/cm H_2O) accompanied with no impedance decrease. This result was not expected but its magnitude had no significant effect on the outcome. We hypothesize that it could be consequence of overall pulmonary deterioration often seen during general anesthesia.

The effect of fluid administration was minimized by keeping IV infusions constant throughout the protocol (5-6 ml/kg/h), eliminating possible effects on the lung impedance. We suppose that constant lung impedance measured during running infusions indicates balanced fluid intake and loss.

Under constant ventilation and constant fluid infusions, we assume that the decrease in pulmonary region impedance during VA ECMO can be interpreted as an indirect marker of fluid accumulation. Increasing EBF generates higher afterload (represented by the rise in MAP – see Fig. 3) that impedes ventricular emptying of failing LV. This may be supported by the observation of LV filling pressure elevation (PCWP) despite significant reduction of preload (CVP) caused by ECMO drainage from the central veins.

Extracorporeal membrane oxygenation in healthy circulation

Interesting outputs of the study are the findings regarding the effects of increasing VA ECMO flow on healthy circulation. Our data indicate that even for the highest EBF (80 ml/kg/min), which is about 75 % of the resting cardiac output, the overall hemodynamics and oxygenation changed only little. In healthy circulation, MAP increased by 23 %, carotid blood flow increased by 10 %, rSO_2 on the forehead by 7 %, on the forelimb by 1 %, and SvO_2 by 9 %. Thus, increased blood flow caused by VA ECMO could have been balanced by regulatory mechanisms, such as shunting the blood through arterio-venous anastomoses and by reducing cardiac output. Since carotid flow (a correlate for the global blood flow) increased only by 10 %, the latter option might be more involved. Indeed, during increasing of EBF from 1 to 4 l/min, we noticed a significant decrease in CVP (by 41 %) and in MPAP (by 22 %). The TPG decreased in healthy as well as in the HF groups. This is likely a consequence of increased venous drainage by VA ECMO inflow cannula.

Aside from decreasing preload, VA ECMO increases left ventricular afterload. However, in healthy animals MAP increased only by 23 % (Table 2). Furthermore, the electrical impedance in the pulmonary region did not change during EBF stepwise increases. Thus, we assume that fluids were neither depleted nor accumulated in the lungs in healthy animals due to VA ECMO operation. This was contrary to the observations in the HF condition.

An unexpected observation was the decrease in pulmonary compliance (40 to 32 ml/cmH_2O) soon after the VA ECMO insertion during the preparatory phase. This could be related to high pulmonary vasoreactivity of swine lungs that was triggered by the contact of blood with the extracorporeal circuit.

Extracorporeal membrane oxygenation in heart failure

In all animals we have succeeded in inducing moderate to severe acute heart failure with severe hypotension, hypoperfusion, increased filling pressures of both left and right ventricle (i.e. increased PCWP and CVP, respectively), and impaired oxygenation (Table 1). During the HF induction, the static lung compliance further decreased (32 to 25 ml/cmH_2O). This could have been caused by the onset of heart failure.

Recent studies have discussed EBF influence on a failing systemic circulation and our hemodynamic results are consistent with their findings (Burkhoff *et al.* 2015, Ostadal *et al.* 2015). In our study systemic hemodynamics and oximetry parameters increased considerably with increasing EBF from 1 to 4 l/min, MAP by 44 %, carotid flow by 59 %, SvO_2 by 49 % (Table 2). The maximal EBF that was achieved in all animals was 80 ml/kg/min (4 l/min). Only such high flow allowed for almost complete restoration of

hemodynamics and oxygen delivery, demonstrated by rSO_2 and SvO_2. Both these parameters are used also clinically to monitor patients supported with VA ECMO since they are not dependent on the pulsatility of blood flow. The interpretation of SvO_2 in terms of VA ECMO is rather complex as it is influenced by actual ratio of pulmonary and extracorporeal flows. In the settings of VA ECMO, the SvO_2 reflects both delivery of oxygen and its extraction (Doufle and Ferguson 2016), but SvO_2 values may vary in the venous blood of tissues supplied by native and extracorporeal circulation (Ostadal *et al.* 2018).

Despite reduced CVP and hence decreased right ventricular output caused by increasing VA ECMO drainage of the central veins, there was significant increase in the already elevated PCWP (Fig. 3). PCWP reflects both LV preload and LV cardiac output. If preload was reduced and PCWP increased, then this finding could again support the hypothesis that LV output (emptying) is compromised by increased LV afterload generated by increasing EBF. This is in accord with the findings from EIT discussed above.

Limitations

EIT is a highly sensitive method of fluid content monitoring as demonstrated above. The major EIT limitation is the dependence of impedance on several parameters that can change independently and might be difficult to separate in real-life scenarios. End-expiratory lung impedance can be influenced by other mechanisms than tidal volume and fluids, such as air trapping and/or air leaks. We consider air trapping was insignificant in our setup as no increase in intrinsic PEEP was noticed. Also, tidal volume and respiratory rate were low and there were no signs of airway obstruction. With adequate endotracheal cuff inflation, the air leak was only 2.1 % of tidal volume in both groups and thus should not have affected the end-expiratory lung impedance. Moreover, it is known that EIT lacks the ability to reliably provide results in absolute units that would be unambiguously interpreted and compared among the patients, which is why we reported normalized EIT values solving that problem. In a recent study Da Silva Ramos *et al.* (2018) showed, that the differences in body dimension have a significant influence on the electrical impedance. To minimize this effect, we included animals of similar body weight. We expect that additional implementation of features like ventilation gating (based on airway pressure and flow) and cardiac cycle gating (based on ECG) would, in future, broaden the spectrum of observed parameters and make our analysis more robust. Moreover, this could enable the estimation of relative changes in systolic impedance variation (Vonk-Noordegraaf *et al.* 2000). We do not have a direct proof of lung fluid accumulation, e.g. transpulmonary thermodilution (TPTD). Nevertheless, Sobota *et al.* (2019) demonstrated that EIT is more sensitive compared to the TPTD in identifying the changes in lung fluids, as TPTD may not reflect small changes of lung fluids. Previous works have suggested that the pulmonary edema usually occurs after days of VA ECMO running (Lequier *et al.* 2017) and our protocol covered only short periods. Further work is needed to observe long-term VA ECMO influence on electrical impedance to evaluate lung fluid accumulation.

Conclusion

In heart failure conditions, the reduction of lung tissue electrical impedance was observed when VA ECMO flow was increased. In healthy circulation with VA ECMO, this impedance change was not detected. Under constant ventilation and fluid infusion this can be interpreted as transient fluid content changes in the lungs. We conclude that EIT could be considered helpful in monitoring the VA ECMO therapy and its effects on lung fluid content.

Abbreviations

CVP, central venous pressure; EBF, extracorporeal blood flow; EIT, electrical impedance tomography; $etCO_2$, end-tidal CO_2; FiO_2, fraction of inspired oxygen; HF, heart failure; IM, intramuscular; IV, intravenous; LAD, left anterior descending coronary artery; LV, left ventricle; MAP, mean arterial pressure; MPAP, mean pulmonary artery pressure; PCWP, pulmonary capillary wedge pressure; $_pCO$, cardiac output; pCO_2, partial pressure of CO_2; pO_2, partial pressure of oxygen; PEEP, positive end-expiratory pressure; PIP, peak inspiratory pressure; rSO_2, regional oxygen saturation; SEM, standard error of the mean; SvO_2, mixed venous oxygen saturation; TPG, transpulmonary pressure gradient; TPTD, transpulmonary thermodilution; VA ECMO, veno-arterial extracorporeal membrane oxygenation; VF, ventricular fibrillation; V_T, tidal volume; ΔZ (tidal volume), change of electrical impedance during breathing cycle; ΔZ (EBF), change of electrical impedance during increasing EBF.

Conflict of Interest

There is no conflict of interest.

Acknowledgements

The authors wish to sincerely and gratefully acknowledge the advice and assistance of Jana Bortelová for help with animal care and of Jana Míšková, Tereza Vavříková, Alena Ehrlichová, Karel Kypta, Matěj Hrachovina, Vít Čapoun for technical support, and Alena Dohnalová for statistical analysis. This work was supported by Charles University research grant GA UK No. 538216 and SVV 260379.

References

ABRAMS D, COMBES A, BRODIE D: What's new in extracorporeal membrane oxygenation for cardiac failure and cardiac arrest in adults? Intens Care Med 40: 609-612, 2014. https://doi.org/10.1007/s00134-014-3212-0

ADLER A, AMYOT R, GUARDO R, BATES JH, BERTHIAUME Y: Monitoring changes in lung air and liquid volumes with electrical impedance tomography. J Appl Physiol (1985) 83: 1762-1767, 1997. https://doi.org/10.1152/jappl.1997.83.5.1762

BACHMANN MC, MORAIS C, BUGEDO G, BRUHN A, MORALES A, BORGES JB, COSTA E, RETAMAL J: Electrical impedance tomography in acute respiratory distress syndrome. Crit Care 22: 263, 2018. https://doi.org/10.1186/s13054-018-2195-6

BECHER T, WENDLER A, EIMER C, WEILER N, FRERICHS I: Changes in electrical impedance tomography findings of ICU patients during rapid infusion of a fluid bolus: a prospective observational study. Am J Respir Crit Care Med 199: 1572-1575, 2019. https://doi.org/10.1164/rccm.201812-2252LE

BORGES JB, SUAREZ-SIPMANN F, BOHM SH, TUSMAN G, MELO A, MARIPUU E, SANDSTROM M, PARK M, COSTA EL, HEDENSTIERNA G, AMATO M: Regional lung perfusion estimated by electrical impedance tomography in a piglet model of lung collapse. J Appl Physiol (1985) 112: 225-236, 2012. https://doi.org/10.1152/japplphysiol.01090.2010

BRECHOT N, DEMONDION P, SANTI F, LEBRETON G, PHAM T, DALAKIDIS A, GAMBOTTI L, LUYT CE, SCHMIDT M, HEKIMIAN G, CLUZEL P, CHASTRE J, LEPRINCE P, COMBES A: Intra-aortic balloon pump protects against hydrostatic pulmonary oedema during peripheral venoarterial-extracorporeal membrane oxygenation. Eur Heart J Acute Cardiovasc Care: 2048872617711169, 2017. https://doi.org/10.1177/2048872617711169

BURKHOFF D, SAYER G, DOSHI D, URIEL N: Hemodynamics of mechanical circulatory support. J Am Coll Cardiol 66: 2663-2674, 2015. https://doi.org/10.1016/j.jacc.2015.10.017

CARDINALE L, PRIOLA AM, MORETTI F, VOLPICELLI G: Effectiveness of chest radiography, lung ultrasound and thoracic computed tomography in the diagnosis of congestive heart failure. World J Radiol 6: 230-237, 2014. https://doi.org/10.4329/wjr.v6.i6.230

DA SILVA RAMOS FJ, HOVNANIAN A, SOUZA R, AZEVEDO LCP, AMATO MBP, COSTA ELV: Estimation of stroke volume and stroke volume changes by electrical impedance tomography. Anesth Analg 126: 102-110, 2018. https://doi.org/10.1213/ANE.0000000000002271

DONKER DW, BRODIE D, HENRIQUES JPS, BROOME M: Left ventricular unloading during veno-arterial ECMO: a review of percutaneous and surgical unloading interventions. Perfusion 34: 98-105, 2019. https://doi.org/10.1177/0267659118794112

DOUFLE G, FERGUSON ND: Monitoring during extracorporeal membrane oxygenation. Curr Opin Crit Care 22: 230-238, 2016. https://doi.org/10.1097/MCC.0000000000000309

FERRARIO D, GRYCHTOL B, ADLER A, SOLA J, BOHM SH, BODENSTEIN M: Toward morphological thoracic EIT: major signal sources correspond to respective organ locations in CT. IEEE Trans Biomed Eng 59: 3000-3008, 2012. https://doi.org/10.1109/TBME.2012.2209116

FRERICHS I, AMATO MB, VAN KAAM AH, TINGAY DG, ZHAO Z, GRYCHTOL B, BODENSTEIN M, GAGNON H, BOHM SH, TESCHNER E, STENQVIST O, MAURI T, TORSANI V, CAMPOROTA L, SCHIBLER A, WOLF GK, GOMMERS D, LEONHARDT S, ADLER A, and TREND study group: Chest electrical impedance tomography examination, data analysis, terminology, clinical use and recommendations: consensus statement of the TRanslational EIT developmeNt stuDy group. Thorax 72: 83-93, 2017. https://doi.org/10.1136/thoraxjnl-2016-208357

FUHRMAN P, HERNAN L, ROTTA A: Pathophysiology of cardiac extracorporeal membrane oxygenation. Artificial Organs 23: 966-969, 1999. https://doi.org/10.1046/j.1525-1594.1999.06484.x

GRAF M, RIEDEL T: Electrical impedance tomography: Amplitudes of cardiac related impedance changes in the lung are highly position dependent. PLoS One 12: e0188313, 2017. https://doi.org/10.1371/journal.pone.0188313

HALA P, MLCEK M, OSTADAL P, JANAK D, POPKOVA M, BOUCEK T, LACKO S, KUDLICKA J, NEUZIL P, KITTNAR O: Regional tissue oximetry reflects changes in arterial flow in porcine chronic heart failure treated with venoarterial extracorporeal membrane oxygenation. Physiol Res 65 (Suppl 5): S621-S631, 2016. https://doi.org/10.33549/physiolres.933532

HALA P, MLCEK M, OSTADAL P, JANAK D, POPKOVA M, BOUCEK T, LACKO S, KUDLICKA J, NEUZIL P, KITTNAR O: Tachycardia-induced cardiomyopathy as a chronic heart failure model in swine. J Vis Exp, 2018. https://doi.org/10.3791/57030

HÁLA P, MLČEK M, OŠŤÁDAL P, POPKOVÁ M, JANÁK D, BOUČEK T, LACKO S, KUDLIČKA J, NEUŽIL P, KITTNAR O: Increasing venoarterial extracorporeal membrane oxygenation flow puts higher demands on left ventricular work in a porcine model of chronic heart failure. J Translat Med 18: 75, 2020. https://doi.org/10.1186/s12967-020-02250-x

ISHIKAWA K, AGUERO J, TILEMANN L, LADAGE D, HAMMOUDI N, KAWASE Y, SANTOS-GALLEGO CG, FISH K, LEVINE RA, HAJJAR RJ: Characterizing preclinical models of ischemic heart failure: differences between LAD and LCx infarctions. Am J Physiol Heart Circ Physiol 307: H1478-1486, 2014. https://doi.org/10.1152/ajpheart.00797.2013

JANAK D, HALA P, MLCEK M, POPKOVA M, LACKO S, KUDLICKA J, KITTNAR O: Detection of microembolic signals in the common carotid artery using Doppler sonography in the porcine model of acute heart failure treated by veno-arterial extracorporeal membrane oxygenation. Physiol Res 66 (Suppl 4): S529-S536, 2017. https://doi.org/10.33549/physiolres.933806

KIM H, PAEK JH, SONG JH, LEE H, JHEE JH, PARK S, YUN HR, KEE YK, HAN SH, YOO TH, KANG SW, KIM S, PARK JT: Permissive fluid volume in adult patients undergoing extracorporeal membrane oxygenation treatment. Crit Care 22: 270, 2018. https://doi.org/10.1186/s13054-018-2211-x

LACKO S, MLCEK M, HALA P, POPKOVA M, JANAK D, HRACHOVINA M, KUDLICKA J, HRACHOVINA V, OSTADAL P, KITTNAR O: Severe acute heart failure - experimental model with very low mortality. Physiol Res 67: 555-562, 2018. https://doi.org/10.33549/physiolres.933774

LEQUIER L, LORUSSO R, MACLAREN G, PEEK G, BROHAN TV: Extracorporeal Life Support: The ELSO Red Book. ELSO, 2017.

LI X, SHAO D, WANG G, JIANG T, WU H, GU B, CAO K, ZHANG J, QI L, CHEN Y: Effects of different LAD-blocked sites on the development of acute myocardial infarction and malignant arrhythmia in a swine model. J Thorac Dis 6: 1271-1277, 2014. https://doi.org/10.3978/j.issn.2072-1439.2014.07.22

MAKDISI G, WANG IW: Extra Corporeal Membrane Oxygenation (ECMO) review of a lifesaving technology. J Thorac Dis 7: E166-176, 2015. https://doi.org/10.3978/j.issn.2072-1439.2015.07.17

NOBLE TJ, HARRIS ND, MORICE AH, MILNES P, BROWN BH: Diuretic induced change in lung water assessed by electrical impedance tomography. Physiol Meas 21: 155-163, 2000. https://doi.org/10.1088/0967-3334/21/1/319

OSTADAL P, BELOHLAVEK J, BALIK M, RIHA H: ECMO - Extracorporeal Membrane Oxygenation. Manual for use in adult patients. Czech Republic, Maxdorf, 2018.

OSTADAL P, MLCEK M, KRUGER A, HALA P, LACKO S, MATES M, VONDRAKOVA D, SVOBODA T, HRACHOVINA M, JANOTKA M, PSOTOVA H, STRUNINA S, KITTNAR O, NEUZIL P: Increasing venoarterial extracorporeal membrane oxygenation flow negatively affects left ventricular performance in a porcine model of cardiogenic shock. J Transl Med 13: 266, 2015. https://doi.org/10.1186/s12967-015-0634-6

OSTADAL P, MLCEK M, STRUNINA S, HRACHOVINA M, KRUGER A, VONDRAKOVA D, JANOTKA M, HALA P, KITTNAR O, NEUZIL P: Novel porcine model of acute severe cardiogenic shock developed by upper-body hypoxia. Physiol Res 65: 711-715, 2016. https://doi.org/10.33549/physiolres.933294

REINIUS H, BORGES JB, FREDEN F, JIDEUS L, CAMARGO ED, AMATO MB, HEDENSTIERNA G, LARSSON A, LENNMYR F: Real-time ventilation and perfusion distributions by electrical impedance tomography during one-lung ventilation with capnothorax. Acta Anaesthesiol Scand 59: 354-368, 2015. https://doi.org/10.1111/aas.12455

RIEDEL T, KYBURZ M, LATZIN P, THAMRIN C, FREY U: Regional and overall ventilation inhomogeneities in preterm and term-born infants. Intensive Care Med 35: 144-151, 2009. https://doi.org/10.1007/s00134-008-1299-x

SOBOTA V, MÜLLER M, ROUBÍK K: Intravenous administration of normal saline may be misinterpreted as a change of end-expiratory lung volume when using electrical impedance tomography. Scientific Reports 9: 5775, 2019. https://doi.org/10.1038/s41598-019-42241-7

SOLEIMANI B, PAE WE: Management of left ventricular distension during peripheral extracorporeal membrane oxygenation for cardiogenic shock. Perfusion 27: 326-331, 2012. https://doi.org/10.1177/0267659112443722

SUZUKI Y, LYONS JK, YEUNG AC, IKENO F: In vivo porcine model of reperfused myocardial infarction: in situ double staining to measure precise infarct area/area at risk. Catheter Cardiovasc Interv 71: 100-107, 2008. https://doi.org/10.1002/ccd.21329

VONK-NOORDEGRAAF A, 2ND, JANSE A, MARCUS JT, BRONZWAER JG, POSTMUST PE, FAES TJ, DE VRIES PM: Determination of stroke volume by means of electrical impedance tomography. Physiol Meas 21: 285-293, 2000. https://doi.org/10.1088/0967-3334/21/2/308

Přiložený dokument 2

Journal of Translational Medicine

RESEARCH

Open Access

Increasing venoarterial extracorporeal membrane oxygenation flow puts higher demands on left ventricular work in a porcine model of chronic heart failure

Pavel Hála[1,2*], Mikuláš Mlček[1], Petr Ošťádal[1,2], Michaela Popková[1], David Janák[1,3], Tomáš Bouček[1,4], Stanislav Lacko[1], Jaroslav Kudlička[1], Petr Neužil[1,2] and Otomar Kittnar[1]

Abstract

Background: Venoarterial extracorporeal membrane oxygenation (VA ECMO) is widely used in the treatment of circulatory failure, but repeatedly, its negative effects on the left ventricle (LV) have been observed. The purpose of this study is to assess the influence of increasing extracorporeal blood flow (EBF) on LV performance during VA ECMO therapy of decompensated chronic heart failure.

Methods: A porcine model of low-output chronic heart failure was developed by long-term fast cardiac pacing. Subsequently, under total anesthesia and artificial ventilation, VA ECMO was introduced to a total of five swine with profound signs of chronic cardiac decompensation. LV performance and organ specific parameters were recorded at different levels of EBF using a pulmonary artery catheter, a pressure–volume loop catheter positioned in the LV, and arterial flow probes on systemic arteries.

Results: Tachycardia-induced cardiomyopathy led to decompensated chronic heart failure with mean cardiac output of 2.9 ± 0.4 L/min, severe LV dilation, and systemic hypoperfusion. By increasing the EBF from minimal flow to 5 L/min, we observed a gradual increase of LV peak pressure from 49 ± 15 to 73 ± 11 mmHg (P = 0.001) and an improvement in organ perfusion. On the other hand, cardiac performance parameters revealed higher demands put on LV function: LV end-diastolic pressure increased from 7 ± 2 to 15 ± 3 mmHg, end-diastolic volume increased from 189 ± 26 to 218 ± 30 mL, end-systolic volume increased from 139 ± 17 to 167 ± 15 mL (all P < 0.001), and stroke work increased from 1434 ± 941 to 1892 ± 1036 mmHg*mL (P < 0.05). LV ejection fraction and isovolumetric contractility index did not change significantly.

Conclusions: In decompensated chronic heart failure, excessive VA ECMO flow increases demands and has negative effects on the workload of LV. To protect the myocardium from harm, VA ECMO flow should be adjusted with respect to not only systemic perfusion, but also to LV parameters.

Keywords: Extracorporeal membrane oxygenation, Heart failure, Swine, Hemodynamics, Heart ventricles, Artificial cardiac pacing

Background

Venoarterial extracorporeal membrane oxygenation (VA ECMO) represents a well-established method that can treat refractory but potentially recoverable cardiogenic shock and thus revert a dire prognosis. Temporarily, it

*Correspondence: pavel.hala@hotmail.com
[1] Department of Physiology, First Faculty of Medicine, Charles University, Albertov 5, 128 00 Prague, Czech Republic
Full list of author information is available at the end of the article

can fully substitute the functions of the lungs and heart to maintain sufficient gas exchange and systemic blood circulation [1, 2]. VA ECMO forms a circulatory bypass by draining blood from the right atrium, passing it through the gas exchange unit, and returning the oxygenated blood into the thoracic aorta. Benefits of VA ECMO on resuscitability, improved survival, and improved neurologic outcomes have been proved both in practice [3, 4] and in animal experiments [5–7].

However, it has also been observed that VA ECMO significantly affects systemic circulation and the workload of the heart [8–13]. Increasing VA ECMO blood flow seems to negatively impact left ventricular (LV) performance; hence, it has been suggested to use only the lowest possible rate of circulatory support to protect myocardial function [8, 10]. Several causes for this negative effect have been repeatedly suspected. During high bypass flow, the inflow of blood reaches the aortic root and increases the mean aortic pressure and the LV afterload. These factors, together with preload and coronary perfusion, play key roles in heart performance. In patients with reduced myocardial contractile reserve, the increase in LV wall tension and end-diastolic pressure (EDP) due to excess afterload opposes the coronary perfusion [14] and exacerbates heart insufficiency [15]. In structural heart diseases, additional mitral regurgitation may contribute to rise in left atrial pressure; consequently, pulmonary congestion may appear as a feared complication of VA ECMO [16–18].

Especially in this context of LV overload, evaluation of VA ECMO in experiments with heart failure (HF) models have become important before translations to clinical practice. LV performance has been studied on models with intact or acutely decompensated hearts [6, 8, 19–22], but to our knowledge, there have been no experimental studies on hemodynamic effects of VA ECMO in conditions of chronic HF and its decompensation. Even though a significant part of VA ECMO clinical applications is for circulatory decompensation developed on grounds of previously present chronic heart disease, we still lack evidence from corresponding experiments. Furthermore, retrospective clinical studies have also revealed that outcome of patients treated by ECMO differs according to the "acuteness or chronicity" of cardiac disease [23].

Although there are reasons why the use of chronic HF models is scarce—time-consuming preparations, instability of heart rhythm, high mortality rates, ethical questions—the advantages of using chronic HF models are evident as they offer prolonged neurohumoral activation, general systemic adaptation, functional changes of cardiomyocytes, and structural alterations of heart valves [24–27]. In this experimental work, a chronic HF animal model was developed by long-term fast cardiac pacing which produced tachycardia-induced cardiomyopathy (TIC). TIC was first recognized in 1913 [28] and later widely used in experiments [29]. It reliably mimics decompensated dilated cardiomyopathy with low cardiac output which persists also after cessation of pacing and allows investigation of chronic HF conditions [27, 30–32].

The aim of our study was to describe hemodynamic and LV performance changes in a swine model of decompensated chronic HF, supported by gradual increase in flow of VA ECMO. We focused on LV pressure and volume changes as well as myocardial contractility and work. It is expected that VA ECMO should be able to supply enough systemic blood circulation, but the details of the negative effects on LV performance have yet to be evaluated.

Methods

Animal model

According to previous studies, TIC as a form of dilated cardiomyopathy was generated by long-term rapid cardiac pacing [33–35]. Details of the methodology were recently described (Fig. 1) [32].

Five healthy crossbred female swine (*Sus scrofa* domestica) up to 6 months of age with initial weights of 37–46 kg were included in this study. After 1 day of fasting, general anesthesia was initiated with intramuscular administration of midazolam (0.3 mg/kg) and ketamine hydrochloride (15–20 mg/kg). Intravenous boluses of morphine (0.1–0.2 mg/kg) and propofol (2 mg/kg) were administered, and animals were preoxygenated and orotracheally intubated with a cuffed endotracheal tube. Total intravenous anesthesia was then continued by combination of propofol (6–12 mg/kg/h), midazolam (0.1–0.2 mg/kg/h), and morphine (0.1–0.2 mg/kg/h); all doses adjusted according to individual responses. Mechanical ventilation was provided by a Hamilton G5 closed-loop device (Hamilton Medical AG, Switzerland), set to adaptive support ventilation to maintain target end-tidal CO_2 of 38–42 mmHg and adequate oxygen saturation of 95–99%. All procedures were performed according to standard veterinary conventions.

Under aseptic conditions and antibiotic prophylaxis (cefazolin 1 g), a single pacing lead with active fixation was inserted transvenously by fluoroscopic guidance in the apical part of right ventricle and subcutaneously tunneled to connect with an in-house modified heart pacemaker (Effecta, Biotronik SE & Co. KG, Germany), which was then implanted into a dorsal subcutaneous pocket. These arrangements proved to prevent device-related complications and allowed a wide range of high rate pacing frequencies.

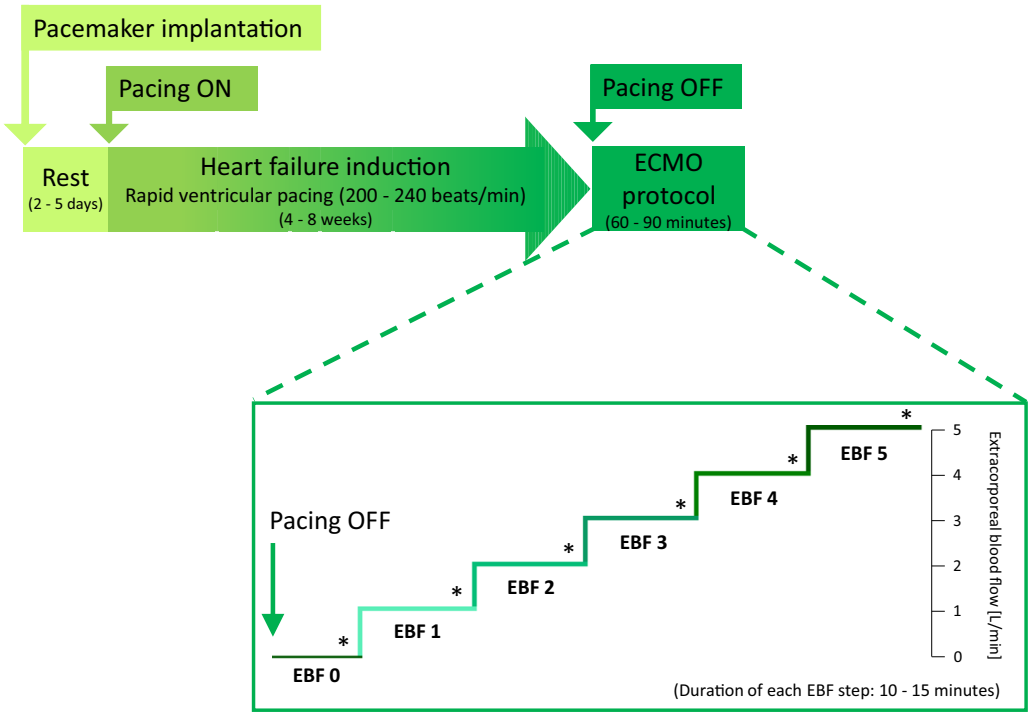

Fig. 1 Diagram of study protocol. After pacemaker implantation, rapid ventricular pacing for 4–8 weeks led to progressive heart failure induction. When pacing was stopped, ECMO protocol consisted of stepwise increase of EBF. Data sets were collected at each EBF step (asterisk). Timeframe durations are stated in each box. *EBF* extracorporeal blood flow

Additional permanent catheter (Groshong PICC, Bard AS, USA or Arteriofix, B. Braun, Germany) was inserted through the marginal ear vein, and animals were kept in a chronic care facility under veterinary care. They were provided with free access to water and continued antibiotic regimen of cefazolin for total of 5 days.

Pacing protocol and chronic heart failure induction

After the necessary resting period of 2–5 days, reserved for recovery from the surgical procedure, a rapid ventricular pacing was started. According to previous publications [36, 37] and our own experience [32], the pacing protocol was defined and started at a pacing rate of 200 beats/min. The frequency was then escalated to 220 beats/min after 1 week, to 240 beats/min the following week, and then sustained. Veterinary surveillance and clinical check-ups including pulse oximetry, rhythm control, and echocardiographic evaluations of myocardial contractility were performed regularly to assess the individual HF progression and pacing rate titration [25, 30]. In the case of excessive HF progression, the pacing rate was reduced for a week before increasing it again. Due to interindividual differences in response to fast pacing, time needed to produce chronic HF with profound signs of decompensation varied from 4 to 8 weeks.

At the end of pacing protocol, all animals presented consistently with symptoms of chronic HF—tachypnea, fatigue, spontaneous tachycardia of > 150 beats/min, and systolic murmurs. At further investigation, ascites, pericardial and pleural effusions, nonsustained ventricular tachycardias, dilation of all heart chambers, and significant mitral and tricuspid regurgitations were noticeable. Hemodynamics of failing circulation was denoted by arterial hypotension, and due to poor contractility and low stroke volume, cardiac output was reduced to approximately 50% of a healthy animal's expected normal value [38]. This model of tachycardia-induced cardiomyopathy matched well to poorly compensated dilated cardiomyopathy and was preserved also after the cessation of pacing [31]. Qualities of the prepared model including neurohumoral dynamics, peripheral vascular abnormalities, and cardiac dysfunction reflected human chronic HF [26].

Experimental preparation and hemodynamic monitoring

At this stage of decompensated chronic HF, again anesthesia and artificial ventilation were administered following principles described above, but dosing was adjusted due to low cardiac output.

Vital functions of anesthetized animals were monitored, and all invasive approaches commenced. Bilateral femoral veins and arteries, jugular vein, and left carotid artery were punctured, and intravascular accesses ensured by standard percutaneous intraluminal sheaths. Right carotid and subclavian arteries were surgically exposed, and circumjacent ultrasound flow probes of appropriate sizes attached (3PSB, 4PSB, or 6PSB, Scisense, Transonic Systems, USA), enabling continuous detection of blood flow velocities. Near-infrared spectroscopy (INVOS Oximeter, Somanetics, USA) with sensors placed on forehead and right forelimb was used to monitor cranial and peripheral regional tissue oxygen saturations (rSO_2).

Intravenous anticoagulation was initiated by unfractionated heparin bolus (100 IU/kg IV), followed by continual infusion, maintaining an activated clotting time (ACT) of 200–300 s (Hemochron Junior +, International Technidyne Corporation, USA), and a set of invasive monitoring equipment was introduced. A balloon Swan-Ganz catheter was placed through femoral vein to the pulmonary artery allowing thermodilution-derived continuous cardiac output, mixed venous oxygen saturation (SvO_2), pulmonary artery, and pulmonary wedge pressure assessments (CCO Combo Catheter; Vigilance II, Edwards Lifesciences, USA). Through the aortic valve, a pressure–volume catheter (7F VSL Pigtail, Scisense, Transonic Systems, USA) was introduced and positioned in the LV cavity. Central venous pressure (CVP) was measured via jugular vein and arterial pressure in femoral artery using fluid-filled pressure transducers (TruWave, Edwards Lifesciences, USA).

Intracardiac and transthoracic echocardiography probes (AcuNav IPX8, Acuson P5-1 and X300 ultrasound system, Siemens, USA) were used for 2D and color Doppler imaging. ECG, heart rate (HR), pulse oximetry, capnometry, rectal temperature, and SvO_2 were measured continuously; blood gas parameters were evaluated by a bedside analysis system (AVL Compact 3, Roche Diagnostics, Germany).

Left ventricular parameters and stroke work analysis, hemodynamic parameters

To register instant volume and pressure in the LV chamber, a pressure–volume (PV) conductance catheter was passed via left carotid arterial approach, retrogradely through the aortic valve into the LV. Its fluoroscopy and echocardiography guided position was set stable before the protocol started to obtain optimal PV loop morphology (Fig. 2). Volume measurements were calibrated by thermodilution-derived cardiac output at baseline.

Measured LV parameters included end-diastolic pressure and volume (EDP and EDV), end-systolic volume (ESV), LV peak pressure (LVPP), stroke work (SW; defined as LV pressure integral with respect to volume), and maximal positive change of LV pressure, defined as first time derivative of LV pressure (dP/dt_{max}). When normalized to EDV, $dP/dt_{max}/EDV$ represents a preload independent index of LV contractility [39–43].

Additional parameters were stroke volume (SV), left ventricular ejection fraction (EF), mean arterial flows in carotid and subclavian arteries, and their pulsatility indices.

ECMO

After intravenous systemic heparinization, extracorporeal circulation was maintained by a femoral VA ECMO system compounded of Levitronix Centrimag console (Thoratec, USA) with a centrifugal pump, hollow fiber microporous membrane oxygenator (QUADROX-i Adult, Maquet Cardiopulmonary, Germany), and tubing set with two percutaneous cannulas (Medtronic, USA) which were introduced by the Seldinger technique through punctures of the unilateral femoral vein and artery (Fig. 3). The tip of venous inlet cannula (23 Fr) was advanced to the right atrium, and the tip of arterial outlet cannula (18 Fr) reached the thoracic descending aorta, with both positions verified by fluoroscopy. Fully assembled ECMO circuit [44] was primed with saline solution, and extracorporeal blood flow (EBF) was initiated at flow rate of 300 mL/min to prevent thrombus formation inside ECMO circuit while having a neglectable impact

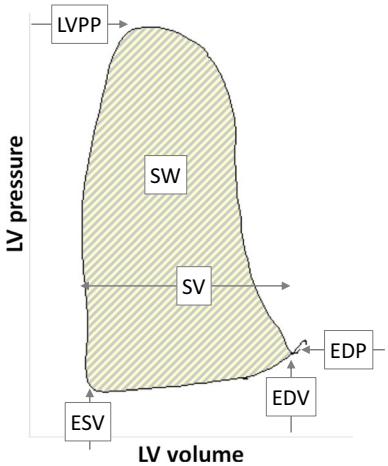

Fig. 2 Pressure–volume loop diagram example recorded by PV catheter. A single cardiac cycle is defined by left ventricular (LV) dimensions, pressures, and work. *ESV* end-systolic volume, *EDV* end-diastolic volume, *EDP* end-diastolic pressure, *LVPP* LV peak pressure, *SV* stroke volume, *SW* LV stroke work

on the systemic circulation. EBF was registered by a separate circumjacent flow probe (ME 9PXL, Transonic Systems, USA) attached to the ECMO outlet cannula.

Blood gas analysis was checked continuously (CDI Blood Parameter Monitoring System 500, Terumo Cardiovascular Systems Corporation, USA) throughout the whole experiment; the fraction of oxygen and air flow through the oxygenator were adjusted to maintain pO_2 100–120 mmHg, pCO_2 35–45 mmHg, and pH 7.35–7.45 in the blood leaving the oxygenator.

Experimental protocol and data acquisition

After instrumentation was completed and ventricular pacing discontinued, all animals were studied in sinus rhythm. Mechanical ventilation was adjusted to keep oxygen saturation above 95% and end-tidal CO_2 within range 38–42 mmHg. Crystalloid infusion was continuously administered (2.5–5.0 mL/kg/h) to reach and maintain a mean CVP at least 5 mmHg. ACT was kept between 200 and 300 s by intravenous heparin administration, and normothermia was maintained. No inotropic agents were used during the protocol.

Under conditions of profound chronic HF, the ECMO protocol was initiated. By changing the ECMO pump rotation speed, the EBF was set according to a standardized ramp protocol (Fig. 1). EBF was gradually increased by increments of 1 L/min every 10–15 min from minimal flow to 5 L/min, and these stepwise categories with constant EBF were referred to as EBF 0, 1, 2, 3, 4, and 5. At each step, animals were allowed to stabilize to a steady state condition in which parameters including PV loop data were recorded. Sets of data were then averaged from three end-expiratory time points. If present, premature beats were omitted from the analyses. At the completion of each study, the animals were euthanized, and a necropsy performed to look for potential cardiac anomalies.

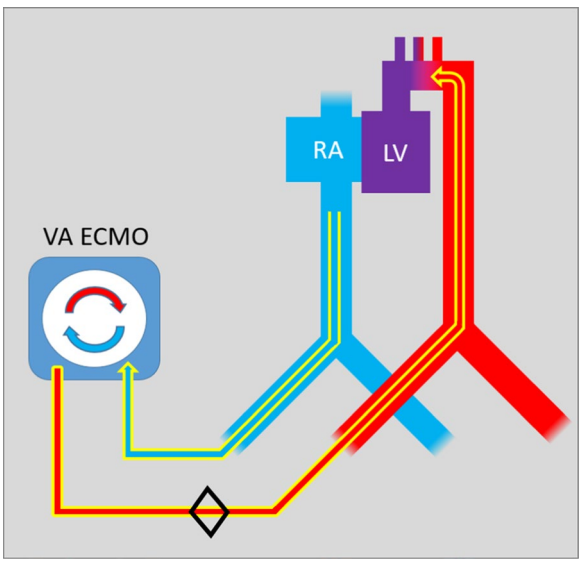

Fig. 3 Femoro-femoral VA ECMO scheme. Venous blood is drawn by inflow cannula from right atrium (RA). Then it continuous through the gas exchange unit by the force of centrifugal pump and oxygenated is returned to the descending part of thoracic aorta. *LV* left ventricle. Black diamond showing the placement of EBF flow probe

Statistical analysis

All data sets were tested for normality and are expressed as mean ± standard error of mean (SEM). Comparisons between different levels of EBF were analyzed—by using the Friedman test with Dunn's multiple comparison and linear regression with Pearson correlation and scatter plots were used for comparisons in between models. A two-sided P-value < 0.05 was considered statistically significant.

Recordings were sampled at 400 Hz by PowerLab A/D converter and continuously recorded to LabChart Pro Software (ADInstruments, Australia). Statistical analyses and graphical interpretations were performed in Prism 6 (GraphPad, USA) and Excel (Microsoft, USA).

Results

Detailed results are summarized in Table 1 and Fig. 4. In the all animals in our study, fast ventricular pacing for 4–8 weeks generated TIC with signs of decompensated HF which was denoted by baseline values of cardiac output 2.9 ± 0.4 L/min at rest, severe dilation of all heart chambers, valves insufficiency, and systemic hypotension. Left ventricular EF evaluated by echocardiography was below 30% in all animals; initial mean heart rate of sinus rhythm was 100 ± 19 beats/min; dyssynchrony of LV contraction was obvious. Baseline SvO_2 value of 62 ± 8% at rest corresponded with inadequate tissue oxygen delivery in our model, and elevated CVP underlined congestion.

After connecting VA ECMO, stepwise increments of EBF from minimal to maximal flow led to gradual and dramatic changes in LV hemodynamic parameters. LVPP increased by 49% from 49 ± 15 mmHg to 55 ± 13, 61 ± 13, 66 ± 12, 74 ± 10, and 73 ± 11 mmHg (for EBF 0 to 5, P = 0.001), and EDP increased by 114% from 7 ± 2 mmHg to 8 ± 2, 10 ± 2, 11 ± 3, 13 ± 2, and 15 ± 3 mmHg (for EBF 0 to 5, P < 0.001). Every escalation of EBF emphasized LV dilation. ESV increased severely by 20% from 139 ± 17 mL to 143 ± 16, 148 ± 18, 152 ± 19, 164 ± 15, and 167 ± 15 mL and EDV by 15% from 189 ± 26 mL to 194 ± 27, 203 ± 29, 209 ± 30, 217 ± 29, and 218 ± 30 mL (both for EBF 0 to 5, P < 0.001).

On the other hand, SV and EF changed only with less significant mean differences and both reached

Table 1 Hemodynamic and pressure–volume characteristics

Parameter	Units	VA ECMO blood flow						P	Relative change
		EBF 0	EBF 1	EBF 2	EBF 3	EBF 4	EBF 5		EBF 0–5 (%)
Ventricular hemodynamics									
LVPP	mmHg	49 ± 5	55 ± 13	61 ± 13	66 ± 12	74 ± 10*	73 ± 11*	0.001	49
EDP	mmHg	7 ± 2	8 ± 2	10 ± 2	11 ± 3	13 ± 2*	15 ± 3*	< 0.001	114
ESV	mL	139 ± 17	143 ± 16	148 ± 18	152 ± 19	164 ± 15*	167 ± 15*	< 0.001	20
EDV	mL	189 ± 26	194 ± 27	203 ± 29	209 ± 30	217 ± 29*	218 ± 30*	< 0.001	15
SV	mL	51 ± 20	51 ± 20	56 ± 20	59 ± 20	55 ± 21	52 ± 21	0.03	2
EF	%	25 ± 7	24 ± 6	26 ± 7	27 ± 7	23 ± 6	21 ± 6	0.18	− 16
HR	beats/min	101 ± 22	96 ± 19	93 ± 17	90 ± 13	90 ± 14	86 ± 14	0.34	− 15
SW	mmHg*mL	1434 ± 941	1595 ± 987	1867 ± 1102	2014 ± 1062	2105 ± 1060*	1892 ± 1036	0.04	32
dP/dt_{max}/EDV	mmHg/s/mL	2.2 ± 0.8	2.2 ± 0.6	2.4 ± 0.4	2.5 ± 0.4	2.8 ± 0.6	3 ± 0.9	0.94	36
Perfusion parameters									
Carotid flow	mL/min	211 ± 72	291 ± 62	314 ± 57	356 ± 57	447 ± 64*	479 ± 58*	< 0.001	127
Subclavian flow	mL/min	103 ± 49	128 ± 44	158 ± 40	208 ± 47	266 ± 47*	296 ± 54*	< 0.001	187
Cranial rSO_2	%	57 ± 6	60 ± 4	67 ± 5	69 ± 5	72 ± 4*	74 ± 3*	< 0.001	30
Forelimb rSO_2	%	37 ± 6	46 ± 5	58 ± 5	67 ± 6	72 ± 7*	77 ± 6*	< 0.001	108
SvO_2	%	62 ± 8	77 ± 3	81 ± 3	86 ± 4	89 ± 4*	89 ± 4*	< 0.001	44
CVP	mmHg	14 ± 2	11 ± 2	10 ± 2	8 ± 2*	9 ± 2*	8 ± 2*	0.001	− 43

For each step of increasing extracorporeal blood flow (EBF in L/min), hemodynamic values are expressed as mean ± SEM

LV left ventricle, *LVPP* LV peak pressure, *EDP* LV end-diastolic pressure, *ESV* LV end-systolic volume, *EDV* LV end-diastolic volume, *SV* stroke volume, *EF* LV ejection fraction, *HR* heart rate, *SW* LV Stroke work, dP/dt_{max}/*EDV* maximal time derivative of LV pressure change normalized to EDV, SvO_2 mixed venous oxygen saturation, *CVP* central venous pressure

Values significantly different from EBF 0 are marked with *

highest values at EBF 3 L/min. In detail, SV changed from 51 ± 20 mL to 51 ± 20, 56 ± 20, 59 ± 20, 55 ± 21, and 52 ± 21 mL (P = 0.03), and EF from 25 ± 7% to 24 ± 6, 26 ± 7, 27 ± 7, 23 ± 6, and 21 ± 6% (P = 0.18). Mean HR tended to decline with every increase in EBF—from 101 ± 22 beats/min to 96 ± 19, 93 ± 17, 90 ± 13, 90 ± 14, and 86 ± 14 beats/min (for EBF 0 to 5, P = 0.34).

Left ventricular SW was calculated from measured pressure–volume loops and exhibited significant flow-dependent increases from 1434 ± 941 mmHg∗mL to 1595 ± 987, 1867 ± 1102, 2014 ± 1062, 2105 ± 1060, and 1892 ± 1036 mmHg∗mL (EBF 0 to 5, P = 0.04). However, preload independent index of LV contractility represented by dP/dt_{max}/EDV ratio showed no consistent trend during the ECMO protocol—from 2.2 ± 0.8 mmHg/s/mL to 2.2 ± 0.6, 2.4 ± 0.4, 2.5 ± 0.4, 2.8 ± 0.6, and 3.0 ± 0.9 mmHg/s/mL (EBF 0 to 5, P = 0.94).

Arterial blood flow increased with every increase of EBF—in total by 127% in the carotid and by 187% in the subclavian artery, while pulsatility indices dropped significantly. SvO_2 increased to 77 ± 3% with EBF 1 and reached > 80% with all higher EBF steps (P < 0.001). Similarly, rSO_2 values were low at baseline but increased promptly with ECMO flow. With increasing EBF, the average value of CVP did gradually fall, but not under 7 mmHg, avoiding ECMO underfilling (P = 0.001).

Postmortem autopsies did not reveal any shunt or other cardiac anomaly, but myocardial hypertrophy (heart weight 471 ± 127 g).

Discussion

VA ECMO is being used as an ultimate method in cases of severe circulatory decompensation, but multiple clinical and experimental studies have documented adverse changes in LV function with the increased EBF [2, 8, 12, 18] for both cardiac [13] and respiratory [45] compromised patients. The incidences of these complications vary widely between 12 and 68% [13, 46–48] and are still believed to be underreported [13, 46].

The goal of our experiment was to assess the response of hemodynamic parameters and LV workload to different levels of EBF. We chose a porcine model of TIC, developed by long-term fast ventricular pacing, over weeks resulting in symptoms and signs of anatomical, functional, and neurohumoral profiles similar to human chronic HF. As far as we are informed, this study is unique in that it describes the hemodynamic effects

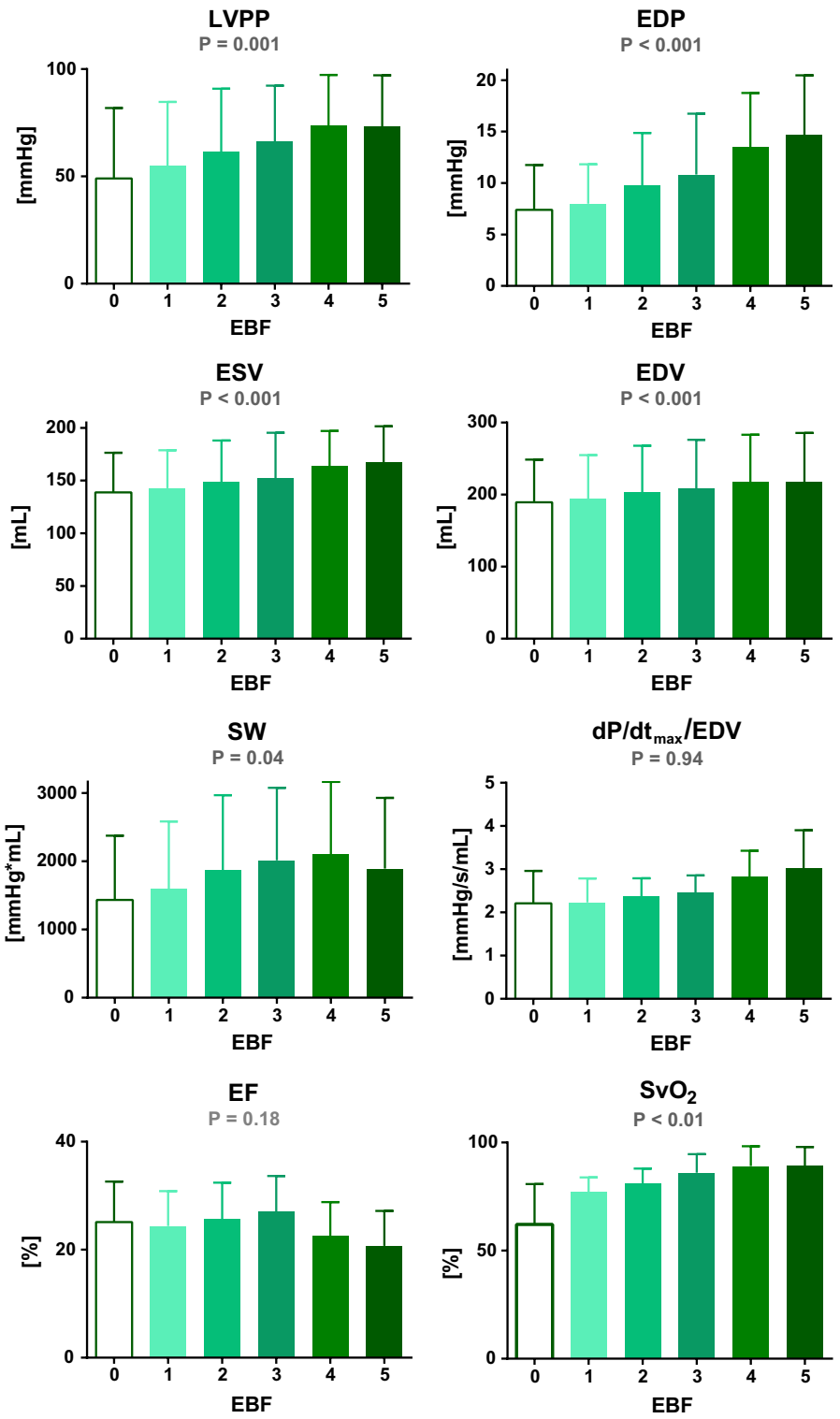

Fig. 4 Effects of venoarterial extracorporeal membrane oxygenation blood flow (EBF in L/min) on selected hemodynamic parameters in a porcine model of chronic heart failure. *LV* left ventricle, *LVPP* LV peak pressure, *EDP* LV end-diastolic pressure, *ESV* LV end-systolic volume, *EDV* LV end-diastolic volume, *SW* LV stroke work, $dP/dt_{max}/EDV$ maximal positive LV pressure change normalized to EDV, *EF* LV ejection fraction, SvO_2 mixed venous oxygen saturation

of VA ECMO in decompensated chronic HF model. An important feature of our protocol is also adequate lung ventilation which ensures that coronary arteries receive well-oxygenated blood during all rates of EBF. Therefore, reported changes in LV hemodynamics should not be attributed to coronary ischemia as a result of poor oxygenation.

With initiation of the extracorporeal circulation and stepwise increase of EBF, progressive dilation of LV was observed. Affected were both the end-diastolic (in total by 15% from EBF 0 to 5) and even more, the end-systolic volume (by 20%). This increase in LV dimensions was strongly pronounced between EBF 0 and EBF 4; by increasing the flow beyond this point, left ventricle did not significantly further dilate.

LV pressures demonstrated upward trends as well. LVPP increased by 49% but still remained abnormally low despite high EBF. LV EDP was initially elevated to 7 mmHg due to abnormal LV filling dynamics, but when compared to a model of acute heart failure [8], the EDP elevation during low EBF in TIC was pointedly lower (Figs. 5 and 6). This may be explained by the chronicity of our HF model which led to massive ventricular dilation without appreciable thickening of its wall, higher ventricular compliance, and thus less pronounced EDP elevation. With ECMO flows from EBF 0 to 5, EDP increased significantly further by over 114% leading to high preload and high end-diastolic wall tension, possibly opposing coronary perfusion [14].

On the other hand, SV and EF had a different course when increasing EBF. Both these measures of LV ejection showed increase from EBF 1 to EBF 3, but with higher EBF, their mean values decreased. Systolic ejection trended to maximum at middle levels and to minimum at the highest levels of VA ECMO support. Such a trend was not observed in acute cardiogenic shock model induced by regional myocardial hypoxemia where ejection continued to decline [8] but was observed in another model of global myocardial hypoxia supported by stepwise VA ECMO [49]. Interestingly, in the latter work, this trend was observed regardless of pulsatile or non-pulsatile ECMO flows.

SW, defined as the area of PV loop and representing the instant LV workload, was expected to be proportional to ventricular systolic pressure and SV [40, 41]. In our measurements, demands on the LV work measured by SW showed significant increase by 40% from EBF 0 to EBF 4, and with further escalation of ECMO flow to EBF 5, declined. In fact, SW is well respecting the trend of LVPP and SV.

The maximal positive LV pressure change is considered to be one of isovolumetric phase contractility indices. Due to severe LV dilation in our experiment, we used

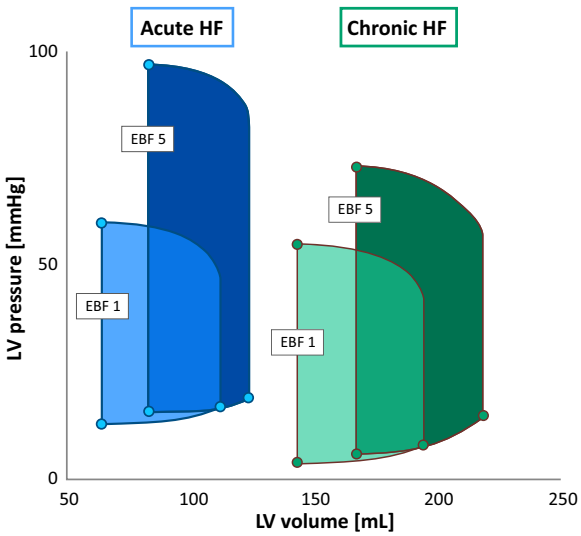

Fig. 5 Effect of increasing EBF on acute (blue) and chronic (green) heart failure. Averaged PV loops for EBF 1 and EBF 5 are demonstrating the change of LV parameters by increasing EBF. Acute heart failure data used from Ostadal et al. study [8]. *EBF* ECMO blood flow

this index normalized to EDV, dP/dt_{max}/EDV, as recommended for its high sensitivity for global inotropic state, irrespective of ventricular loading conditions [39, 41, 43]. It has been confirmed that its linear relation is affected less by afterload compared to the end-systolic PV ratio [43]. As expected, the initial value in our TIC model was significantly below normal. Further across the stepwise protocol of EBF, the ratio of dP/dt_{max}/EDV continued to increase but did not meet statistical significance. For isovolumetric phase of contraction, this could imply that LV did not lose its ability to contract. In individuals where the dP/dt_{max}/EDV ratio did not decrease with higher EBF, this could be explained by unrestricted or at least, sufficient coronary perfusion and secondarily by preserved potential of contractility. A similarly designed study reported hemodynamic effects of VA ECMO, but applied to healthy canine circulation [14]. Although they reported reduction of coronary flow with increasing EBF, myocardial oxygen consumption was not reduced. In a similar sense, our data did not indicate critically inadequate myocardial perfusion on any of EBF levels.

Blood propelled to the aortic root, especially potentiated by aortic and mitral regurgitations, often leads to increased left atrial pressure [15]. Yet, in none of our cases, progression into pulmonary edema was observed, which could be due to the short-term duration of extracorporeal support and sufficient right heart unloading.

The combination of increasing SW and not declining dP/dt_{max}/EDV ratio demonstrate increased demands on

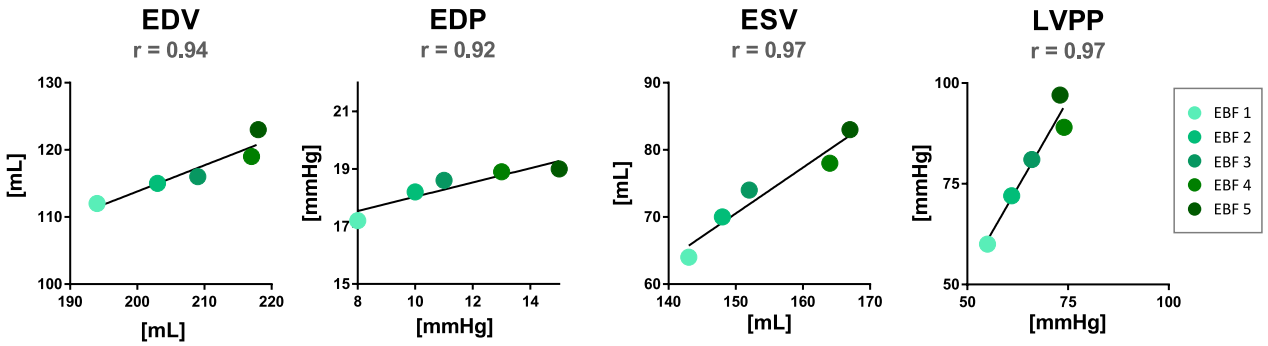

Fig. 6 Scatter plots of LV pressure–volume parameters showing effects of increasing EBF on chronic (horizontal axes) and on acute heart failure (vertical axes). Acute heart failure data used from Ostadal et al. 2015 study [8]. In each graph, both axis (horizontal and vertical) presented with identical scales. For all, $P < 0.05$

LV work, placed by the high afterload, and this increase in LV work occurs concurrently with LV dilation [41].

As the metabolic rate and hematocrit remain unchanged, systemic organ perfusion can be predicted by arterial flows and mixed venous blood saturation. We previously reported linear correlation of tissue saturation and regional arterial flow in VA ECMO support of chronic HF. Both tissue saturation and regional arterial flow demonstrated significant increases with respect to EBF [7]. Low initial value of SvO_2 improved already at level of EBF 1, suggesting sufficient systemic perfusion with only minor extracorporeal support. Not surprisingly, with every higher EBF step, average SvO_2 and carotid arterial flow rose, but the pulsatility index gradually decreased, demonstrating loss of aortic pulse pressure and the dominance of ECMO blood flow in systemic circulation [5, 7]. Practically, the value of regional tissue saturation together with SvO_2 have the potential to serve as additional methods to secure vital organ perfusion in ECMO therapy guidance.

A recent study by our group described hemodynamic effects of VA ECMO on an innovative animal model of acute HF induced by hypoxic coronary perfusion [8, 20], and these findings were later confirmed by computer modeling [9]. Similar to our current design, the effects of increasing EBF on LV were reported. Figure 5 is depicting PV loops of acute and chronic model reactions to VA ECMO flow which can offer insights into hemodynamic changes in both models.

In comparison to our current study, baseline ESV and EDV in acute HF were reported to be of far smaller dimensions (46% for ESV, 58% for EDV) and the effect of faster EBF was different in acute HF—by increasing EBF, ESV increased by 31% (64 ± 11 mL to 83 ± 14 mL, $P < 0.001$), but EDV only by 10% (112 ± 19 mL to 123 ± 20 mL, $P = 0.43$, both for EBF 1 to 5). Likewise, increase of LVPP was more pronounced (by 67%; from 60 ± 7 to 97 ± 8, $P < 0.001$), but changes of EDP were only mild (17.2 ± 1.4 to 19.0 ± 2.9, $P = 0.87$, both for EBF 1 to 5). In both experiments, SW followed the same trend, reaching the highest value at EBF 4, and HR declined with every increment of EBF.

In Fig. 6, PV characteristics of this acute model are plotted against our results. Values of EDV, ESV, EDP, and LVPP for corresponding EBF steps reveal linear relations with dissimilar slopes ($r = 0.94$, $r = 0.97$, $r = 0.92$, and $r = 0.97$, respectively, all $P < 0.05$).

In another model of acute HF generated by hypoxic myocardial perfusion, Shen et al. reported a decline of dP/dt_{max} and LVPP associated with VA ECMO flow, but in their settings all of the coronary vascular bed received hypoxemic blood [22].

When summarized, in our chronic HF model, EDP was lower at baseline but increased more with higher EBF, and end-diastolic dilation was more pronounced. EF and SV were proved to decline only in the case of acute hypoxic HF. One possible explanation is that in our protocol, high ECMO flow improves the coronary perfusion with oxygen rich blood, in contrast to the acute models, where a major portion of LV myocardium is perfused by constant flow of hypoxic blood, stunned, and therefore cannot keep pace and eject against increasing afterload. Long-term adaptation to chronic HF conditions with humoral activation during TIC model induction could be another possible explanation.

Although the impact of LV overload on clinical outcomes is mostly unknown and the literary evidence limited, it is expected that it negatively affects patients' recovery [13, 50] and in minority of patients, the status can further progress into pulmonary congestion or

edema [13, 17, 18, 50]. In addition, recent small clinical and experimental series have shown that the severity of LV overload and distention correlates well with the rate of EBF [8, 11, 51].

In clinical settings, echocardiography can serve as a method of choice to evaluate the ventricular response to volume loading during or while weaning from ECMO [11, 50, 51]. Assessments of SV and filling pressures, together with pulmonary wedge pressure, lung fluid accumulation, and regional saturations, are available measures which should be operated on daily basis [13, 50, 52]. Having these in hands, partial flows of extracorporeal support in conjunction with aggressive inotropic support have been suggested in effort to prevent LV overload [7, 8, 13].

In the presented study we showed how VA ECMO increases the demands on LV work and that despite significant increase of EDP, negative effect on load-independent contractility was not observed, suggesting sufficient myocardial oxygenated blood supply. Several methods have been proposed to unload the ventricles under VA ECMO therapy but are associated with increased rate of complications and the clinical evidence is limited to few single center small cohorts and case reports [13, 16–18, 50]. In a recent report, 15 out of 36 patients with LV distention on VA ECMO required some venting strategy to reduce wall stress [13]. It has also been shown that even a small venting catheter of 7 or 8 Fr in left atrium [47] or LV [16] seems sufficient and that its early applications result in lower mortality [18, 48]. However, the clinical relevance of these effects still remains uncertain.

We assume that to decrease the risk of LV overload, VA ECMO flow should be maintained at the lowest level securing adequate tissue perfusion.

Even though the study protocol was prepared carefully and the total number of studied animals was adequately reasonable, several limitations must be considered. First, real isovolumetric phase was absent on recorded PV loops, as it could only be seen in cases with intact heart valves. In real measurements, LV volume may never stay constant due to valve insufficiency. The aortic regurgitation in our experiments was caused by PV loop catheter and was not considered severe on echocardiography. Second, contractility indices are highly sensitive but are also known to have a low reproducibility for contractile status. Therefore, myocardial perfusion cannot be directly deducted. In future studies, coronary arterial flow or oxygen consumption should be assessed. A third limitation could be seen in the relatively brief duration of extracorporeal support used in this study compared to common durations of ECMO therapy. To test long-term effects, experiments should be extended, and lung fluid content assessed. Lastly, right ventricular workload should also be considered.

Conclusion

We confirm that increase in EBF during VA ECMO therapy increases demands on LV performance, and our work extends this observation to conditions of decompensated chronic HF. We conclude that to protect the myocardium from harm, EBF of VA ECMO should be set with respect to not only systemic perfusion but also to LV parameters.

Abbreviations

ACT: Activated clotting time; CVP: Central venous blood pressure; EBF: Extracorporeal blood flow; (VA) ECMO: (Venoarterial) extracorporeal membrane oxygenation; EDP: LV end-diastolic pressure; EDV: LV end-diastolic volume; EF: LV ejection fraction; ESV: LV end-systolic volume; HF: Heart failure; HR: Heart rate; LV: Left ventricle; LVPP: LV peak pressure; PV (loop): Pressure–volume (loop); dP/dt_{max}: Maximal positive LV pressure change; dP/dt_{max}/EDV: dP/dt_{max} normalized to EDV; rSO_2: Regional tissue saturation; SV: LV stroke volume; SvO_2: Mixed venous oxygen saturation; SW: LV stroke work; TIC: Tachycardia-induced cardiomyopathy.

Acknowledgements

The authors wish to gratefully acknowledge the advice and assistance of Alena Dohnalová, for her help with statistical analysis, and of Jana Bortelová, Matěj Hrachovina, Tereza Vavříková, Karel Kypta, Alena Ehrlichová, and Maria Kim for their work and technical support.

Authors' contributions

PH, PO and OK: study design, statistical analysis, prepared and finalized the manuscript. PH, MM, DJ, MP, TB and SL: animal model preparation and performing the protocol procedures. PH, MM and MP: veterinary and intensive animal care. PO, JK, PN and OK: participated in study design, interpretation of the results. All authors read and approved the final manuscript.

Funding

This work was funded by Charles University research Grant GA UK No. 538216, Progres Q41/LF1, and SVV 260379.

Availability of data and materials

The datasets used and analyzed during the current study are available from the corresponding author on request. In "Discussion" section and Figs. 5 and 6 we reference to data from Ostadal et al. study [8] (https://doi.org/10.1186/s12967-015-0634-6) with generous permission of the author.

Ethics approval and consent to participate

Experimental protocol was reviewed and approved by the Institutional Animal Expert Committee of First Faculty of Medicine, Charles University and was performed at the University experimental laboratory, Department of Physiology, First Faculty of Medicine, Charles University, Prague, Czech Republic, in accordance with Act No. 246/1992 Coll., on the protection of animals against cruelty. All animals were treated and cared for in accordance with the Guide for the Care and Use of Laboratory Animals, 8th edition, published by National Academies Press, 2011.

Consent for publication

Not applicable.

Competing interests

The authors declare that they have no competing interests.

Author details

[1] Department of Physiology, First Faculty of Medicine, Charles University, Albertov 5, 128 00 Prague, Czech Republic. [2] Department of Cardiology, Na Homolce Hospital, Prague, Czech Republic. [3] Department of Cardiovascular Surgery, Second Faculty of Medicine, Charles University, Prague, Czech

Republic. [4] Department of Cardiovascular Medicine, First Faculty of Medicine, Charles University, Prague, Czech Republic.

Received: 29 August 2019 Accepted: 30 January 2020
Published online: 13 February 2020

References

1. Abrams D, Combes A, Brodie D. Extracorporeal membrane oxygenation in cardiopulmonary disease in adults. J Am Coll Cardiol. 2014;63:2769–78.
2. Brogan TV, Lequier L, Lorusso R, MacLaren G, Peek G. Extracorporeal life support: the ELSO red book. Ann Arbor: Extracorporeal Life Support Organization; 2017.
3. Combes A, Leprince P, Luyt CE, Bonnet N, Trouillet JL, Leger P, Pavie A, Chastre J. Outcomes and long-term quality-of-life of patients supported by extracorporeal membrane oxygenation for refractory cardiogenic shock. Crit Care Med. 2008;36:1404–11.
4. Pranikoff T, Hirschl RB, Steimle CN, Anderson HL 3rd, Bartlett RH. Efficacy of extracorporeal life support in the setting of adult cardiorespiratory failure. ASAIO J. 1994;40:M339–43.
5. Belohlavek J, Mlcek M, Huptych M, Svoboda T, Havranek S, Ost'adal P, Boucek T, Kovarnik T, Mlejnsky F, Mrazek V, Belohlavek M, Aschermann M, Linhart A, Kittnar O. Coronary versus carotid blood flow and coronary perfusion pressure in a pig model of prolonged cardiac arrest treated by different modes of venoarterial ECMO and intraaortic balloon counterpulsation. Crit Care. 2012;16:R50.
6. Mlcek M, Ostadal P, Belohlavek J, Havranek S, Hrachovina M, Huptych M, Hala P, Hrachovina V, Neuzil P, Kittnar O. Hemodynamic and metabolic parameters during prolonged cardiac arrest and reperfusion by extracorporeal circulation. Physiol Res. 2012;61(Suppl 2):S57–65.
7. Hala P, Mlcek M, Ostadal P, Janak D, Popkova M, Boucek T, Lacko S, Kudlicka J, Neuzil P, Kittnar O. Regional tissue oximetry reflects changes in arterial flow in porcine chronic heart failure treated with venoarterial extracorporeal membrane oxygenation. Physiol Res. 2016;65:S621–31.
8. Ostadal P, Mlcek M, Kruger A, Hala P, Lacko S, Mates M, Vondrakova D, Svoboda T, Hrachovina M, Janotka M, Psotova H, Strunina S, Kittnar O, Neuzil P. Increasing venoarterial extracorporeal membrane oxygenation flow negatively affects left ventricular performance in a porcine model of cardiogenic shock. J Transl Med. 2015;13:266.
9. Broome M, Donker DW. Individualized real-time clinical decision support to monitor cardiac loading during venoarterial ECMO. J Transl Med. 2016;14:4.
10. Seo T, Ito T, Iio K, Kato J, Takagi H. Experimental study on the hemodynamic effects of veno-arterial extracorporeal membrane oxygenation with an automatically driven blood pump on puppies. Artif Organs. 1991;15:402–7.
11. Aissaoui N, Guerot E, Combes A, Delouche A, Chastre J, Leprince P, Leger P, Diehl JL, Fagon JY, Diebold B. Two-dimensional strain rate and Doppler tissue myocardial velocities: analysis by echocardiography of hemodynamic and functional changes of the failed left ventricle during different degrees of extracorporeal life support. J Am Soc Echocardiogr. 2012;25:632–40.
12. Burkhoff D, Sayer G, Doshi D, Uriel N. Hemodynamics of mechanical circulatory support. J Am Coll Cardiol. 2015;66:2663–74.
13. Truby LK, Takeda K, Mauro C, Yuzefpolskaya M, Garan AR, Kirtane AJ, Topkara VK, Abrams D, Brodie D, Colombo PC, Naka Y, Takayama H. Incidence and implications of left ventricular distention during venoarterial extracorporeal membrane oxygenation support. ASAIO J. 2017;63:257–65.
14. Kato J, Seo T, Ando H, Takagi H, Ito T. Coronary arterial perfusion during venoarterial extracorporeal membrane oxygenation. J Thorac Cardiovasc Surg. 1996;111:630–6.
15. Fuhrman BP, Hernan LJ, Rotta AT, Heard CM, Rosenkranz ER. Pathophysiology of cardiac extracorporeal membrane oxygenation. Artif Organs. 1999;23:966–9.
16. Barbone A, Malvindi PG, Ferrara P, Tarelli G. Left ventricle unloading by percutaneous pigtail during extracorporeal membrane oxygenation. Interact Cardiovasc Thorac Surg. 2011;13:293–5.
17. Boulate D, Luyt CE, Pozzi M, Niculescu M, Combes A, Leprince P, Kirsch M. Acute lung injury after mechanical circulatory support implantation in patients on extracorporeal life support: an unrecognized problem. Eur J Cardiothorac Surg. 2013;44:544–9 **discussion 549–550**.
18. Soleimani B, Pae WE. Management of left ventricular distension during peripheral extracorporeal membrane oxygenation for cardiogenic shock. Perfusion. 2012;27:326–31.
19. Bavaria JE, Ratcliffe MB, Gupta KB, Wenger RK, Bogen DK, Edmunds LH Jr. Changes in left ventricular systolic wall stress during biventricular circulatory assistance. Ann Thorac Surg. 1988;45:526–32.
20. Ostadal P, Mlcek M, Strunina S, Hrachovina M, Kruger A, Vondrakova D, Janotka M, Hala P, Kittnar O, Neuzil P. Novel porcine model of acute severe cardiogenic shock developed by upper-body hypoxia. Physiol Res. 2016;65:711–5.
21. Ostadal P, Kruger A, Vondrakova D, Janotka M, Psotova H, Neuzil P. Noninvasive assessment of hemodynamic variables using near-infrared spectroscopy in patients experiencing cardiogenic shock and individuals undergoing venoarterial extracorporeal membrane oxygenation. J Crit Care. 2014;29(690):e611–95.
22. Shen I, Levy FH, Benak AM, Rothnie CL, O'Rourke PP, Duncan BW, Verrier ED. Left ventricular dysfunction during extracorporeal membrane oxygenation in a hypoxemic swine model. Ann Thorac Surg. 2001;71:868–71.
23. Tarzia V, Bortolussi G, Bianco R, Buratto E, Bejko J, Carrozzini M, De Franceschi M, Gregori D, Fichera D, Zanella F, Bottio T, Gerosa G. Extracorporeal life support in cardiogenic shock: impact of acute versus chronic etiology on outcome. J Thorac Cardiovasc Surg. 2015;150:333–40.
24. Howard RJ, Stopps TP, Moe GW, Gotlieb A, Armstrong PW. Recovery from heart failure: structural and functional analysis in a canine model. Can J Physiol Pharmacol. 1988;66:1505–12.
25. Moe GW, Armstrong P. Pacing-induced heart failure: a model to study the mechanism of disease progression and novel therapy in heart failure. Cardiovasc Res. 1999;42:591–9.
26. Power JM, Tonkin AM. Large animal models of heart failure. Aust N Z J Med. 1999;29:395–402.
27. Schmitto JD, Mokashi SA, Lee LS, Popov AF, Coskun KO, Sossalla S, Sohns C, Bolman RM 3rd, Cohn LH, Chen FY. Large animal models of chronic heart failure (CHF). J Surg Res. 2011;166:131–7.
28. Gossage AM, Braxton Hicks JA. On auricular fibrillation. Q J Med. 1913;6:435–40.
29. Whipple GH, Sheffield LT, Woodman EG, Theophilis C, Friedman S. Reversible congestive heart failure due to chronic rapid stimulation of the normal heart. Proc N Engl Cardiovasc Soci. 1962;20:39–40.
30. Shinbane JS, Wood MA, Jensen DN, Ellenbogen KA, Fitzpatrick AP, Scheinman MM. Tachycardia-induced cardiomyopathy: a review of animal models and clinical studies. J Am Coll Cardiol. 1997;29:709–15.
31. Takagaki M, McCarthy PM, Tabata T, Dessoffy R, Cardon LA, Connor J, Ochiai Y, Thomas JD, Francis GS, Young JB, Fukamachi K. Induction and maintenance of an experimental model of severe cardiomyopathy with a novel protocol of rapid ventricular pacing. J Thorac Cardiovasc Surg. 2002;123:544–9.
32. Hála P, Mlček M, Ošťádal P, Janák D, Popková M, Bouček T, Lacko S, Kudlička J, Neužil P, Kittnar O. Tachycardia-induced cardiomyopathy as a chronic heart failure model in swine. J Vis Exp. 2018;17(132):e57030.
33. Gupta S, Figueredo VM. Tachycardia mediated cardiomyopathy: pathophysiology, mechanisms, clinical features and management. Int J Cardiol. 2014;172:40–6.
34. Nikolaidis LA, Hentosz T, Doverspike A, Huerbin R, Stolarski C, Shen YT, Shannon RP. Mechanisms whereby rapid RV pacing causes LV dysfunction: perfusion-contraction matching and NO. Am J Physiol Heart Circ Physiol. 2001;281:H2270–81.
35. Spinale FG, Hendrick DA, Crawford FA, Smith AC, Hamada Y, Carabello BA. Chronic supraventricular tachycardia causes ventricular dysfunction and subendocardial injury in swine. Am J Physiol. 1990;259:H218–29.
36. Chow E, Woodard JC, Farrar DJ. Rapid ventricular pacing in pigs: an experimental model of congestive heart failure. Am J Physiol. 1990;258:H1603–5.
37. Hendrick DA, Smith AC, Kratz JM, Crawford FA, Spinale FG. The pig as a model of tachycardia and dilated cardiomyopathy. Lab Anim Sci. 1990;40:495–501.
38. Wyler F, Kaslin M, Hof R, Beglinger R, Becker M, Stalder G. The Gottinger minipig as a laboratory animal. 5. Communication: cardiac output, its

regional distribution and organ blood flow (author's transl). Res Exp Med (Berl). 1979;175:31–6.
39. Kass DA, Maughan WL, Guo ZM, Kono A, Sunagawa K, Sagawa K. Comparative influence of load versus inotropic states on indexes of ventricular contractility: experimental and theoretical analysis based on pressure–volume relationships. Circulation. 1987;76:1422–36.
40. Glower DD, Spratt JA, Snow ND, Kabas JS, Davis JW, Olsen CO, Tyson GS, Sabiston DC Jr, Rankin JS. Linearity of the Frank-Starling relationship in the intact heart: the concept of preload recruitable stroke work. Circulation. 1985;71:994–1009.
41. Burkhoff D, Mirsky I, Suga H. Assessment of systolic and diastolic ventricular properties via pressure–volume analysis: a guide for clinical, translational, and basic researchers. Am J Physiol Heart Circ Physiol. 2005;289:H501–12.
42. Walley KR. Left ventricular function: time-varying elastance and left ventricular aortic coupling. Crit Care. 2016;20:270.
43. Little WC. The left ventricular dP/dt_{max}-end-diastolic volume relation in closed-chest dogs. Circ Res. 1985;56:808–15.
44. Bartlett RH, Gazzaniga AB, Huxtable RF, Schippers HC, O'Connor MJ, Jefferies MR. Extracorporeal circulation (ECMO) in neonatal respiratory failure. J Thorac Cardiovasc Surg. 1977;74:826–33.
45. Tanke RB, Daniels O, van Heijst AF, van Lier H, Festen C. Cardiac dimensions during extracorporeal membrane oxygenation. Cardiol Young. 2005;15:373–8.
46. Cheng R, Hachamovitch R, Kittleson M, Patel J, Arabia F, Moriguchi J, Esmailian F, Azarbal B. Complications of extracorporeal membrane oxygenation for treatment of cardiogenic shock and cardiac arrest: a meta-analysis of 1,866 adult patients. Ann Thorac Surg. 2014;97:610–6.
47. Kim S, Kim JS, Shin JS, Shin HJ. How small is enough for the left heart decompression cannula during extracorporeal membrane oxygenation? Acute Crit Care. 2019;34:263–8.
48. Na SJ, Yang JH, Yang JH, Sung K, Choi JO, Hahn JY, Jeon ES, Cho YH. Left heart decompression at venoarterial extracorporeal membrane oxygenation initiation in cardiogenic shock: prophylactic versus therapeutic strategy. J Thorac Dis. 2019;11:3746–56.
49. Ostadal P, Mlcek M, Gorhan H, Simundic I, Strunina S, Hrachovina M, Kruger A, Vondrakova D, Janotka M, Hala P, Mates M, Ostadal M, Leiter JC, Kittnar O, Neuzil P. Electrocardiogram-synchronized pulsatile extracorporeal life support preserves left ventricular function and coronary flow in a porcine model of cardiogenic shock. PLoS ONE. 2018;13:e0196321.
50. Donker DW, Brodie D, Henriques JPS, Broome M. Left ventricular unloading during veno-arterial ECMO: a review of percutaneous and surgical unloading interventions. Perfusion. 2019;34:98–105.
51. Walther FJ, van de Bor M, Gangitano ES, Snyder JR. Left and right ventricular output in newborn infants undergoing extracorporeal membrane oxygenation. Crit Care Med. 1990;18:148–51.
52. Donker DW, Meuwese CL, Braithwaite SA, Broome M, van der Heijden JJ, Hermens JA, Platenkamp M, de Jong M, Janssen JGD, Balik M, Belohlavek J. Echocardiography in extracorporeal life support: a key player in procedural guidance, tailoring and monitoring. Perfusion. 2018;33:31–41.

Publisher's Note

Přiložený dokument 3

Video k tomuto dokumentu je dostupné na adrese:

https://www.jove.com/v/57030/

Video Article

Tachycardia-Induced Cardiomyopathy As a Chronic Heart Failure Model in Swine

Pavel Hála[1,2], Mikuláš Mlček[1], Petr Ošťádal[1,2], David Janák[1,3], Michaela Popková[1], Tomáš Bouček[1], Stanislav Lacko[1], Jaroslav Kudlička[1], Petr Neužil[1,2], Otomar Kittnar[1]

[1]Department of Physiology, First Faculty of Medicine, Charles University

[2]Department of Cardiology, Na Homolce Hospital

[3]Department of Cardiovascular Surgery, Second Faculty of Medicine, Charles University

Correspondence to: Pavel Hála at pavel.hala@gmx.com

URL: https://www.jove.com/video/57030
DOI: doi:10.3791/57030

Keywords: Medicine, Issue 132, Animal model, Chronic heart failure, Cardiomyopathy, Extracorporeal life support, Swine, Tachycardia

Date Published: 2/17/2018

Citation: Hála, P., Mlček, M., Ošťádal, P., Janák, D., Popková, M., Bouček, T., Lacko, S., Kudlička, J., Neužil, P., Kittnar, O. Tachycardia-Induced Cardiomyopathy As a Chronic Heart Failure Model in Swine. *J. Vis. Exp.* (132), e57030, doi:10.3791/57030 (2018).

Abstract

A stable and reliable model of chronic heart failure is required for many experiments to understand hemodynamics or to test effects of new treatment methods. Here, we present such a model by tachycardia-induced cardiomyopathy, which can be produced by rapid cardiac pacing in swine.

A single pacing lead is introduced transvenously into fully anaesthetized healthy swine, to the apex of the right ventricle, and fixated. Its other end is then tunneled dorsally to the paravertebral region. There, it is connected to an in-house modified heart pacemaker unit that is then implanted in a subcutaneous pocket.

After 4 - 8 weeks of rapid ventricular pacing at rates of 200 - 240 beats/min, physical examination revealed signs of severe heart failure - tachypnea, spontaneous sinus tachycardia, and fatigue. Echocardiography and X-ray showed dilation of all heart chambers, effusions, and severe systolic dysfunction. These findings correspond well to decompensated dilated cardiomyopathy and are also preserved after the cessation of pacing.

This model of tachycardia-induced cardiomyopathy can be used for studying the pathophysiology of progressive chronic heart failure, especially hemodynamic changes caused by new treatment modalities like mechanical circulatory supports. This methodology is easy to perform and the results are robust and reproducible.

Video Link

The video component of this article can be found at https://www.jove.com/video/57030/

Introduction

The variety of new treatment methods for heart failure (HF), especially the growing worldwide use of mechanical circulatory supports and extracorporeal membrane oxygenation (ECMO) in clinical practice, is reflecting in preclinical experimental testing. The main focus has been on hemodynamic changes caused by the examined treatment modalities, namely on systemic blood pressure[1], myocardial contractility, pressure and volume changes in heart chambers and heart work[2,3], arterial blood flow in systemic and peripheral arteries, along with metabolic compensation[4] - regional tissue saturation, pulmonary perfusion, and blood gas analysis. Other studies are directed on long-term effects of the circulatory support[5], concomitant inflammation, or occurrence of hemolysis. All these types of study need a stable biomodel of congestive HF.

Most of the published experiments on left ventricular (LV) performance and hemodynamics of mechanical circulatory support have been performed on experimental models of acute HF[2,6,7,8,9,10], or even on completely intact hearts. On the other hand, in clinical practice, mechanical circulatory supports are often being applied in a status of circulatory decompensation that develops on the grounds of previously present chronic heart disease. In such situations, the adaptation mechanisms are fully developed and can play important roles in inconsistency of outcomes observed according to the "acuteness or chronicity" of underlying cardiac disease[11]. Therefore, a stable model of chronic HF can offer new insights into pathophysiological mechanisms and hemodynamics. Although there are reasons why the use of chronic HF models is scarce - time consuming preparation, instability of heart rhythm, ethical questions, and mortality rate - their advantages are clear, as they offer presence of long-term neurohumoral activation, general systemic adaptation, functional changes of cardiomyocytes, and structural alterations of heart muscle and valves[12,13].

In general, the availability and variety of animal models used for hemodynamic studies is wide and offers choice for many specific needs. For these experiments, mostly porcine, canine, ovine, or with smaller settings murine models, are being chosen and offer a good simulation of expected human bodily reactions[14]. Furthermore, forms of single organ experiments are becoming more frequent[15]. To reliably mimic the

pathophysiology of HF, circulation is being artificially deteriorated. Damage to the heart can be caused by various methods, often by either ischemia, arrhythmia, pressure overload, or cardiotoxic effects of drugs, with any of these leading to hemodynamic deterioration of the model. To produce a true model of chronic HF, time has to be provided for developing the long-term adaptation of the whole organism. Such a reliable and stable model is represented well by tachycardia-induced cardiomyopathy (TIC), which can be produced by rapid cardiac pacing in experimental animals.

It has been shown that in predisposed hearts, long-lasting incessant tachyarrhythmias can lead to systolic dysfunction and dilation with decreased cardiac output. The condition referred to as TIC was first described in 1913[16], widely used in experiments since 1962[17], and is now a well-recognized disorder. Its origin can lie in various types of arrhythmias - both supraventricular and ventricular tachycardia can lead to progressive deterioration of systolic function, biventricular dilation, and progressive clinical signs of HF including ascites, edemas, lethargy, and ultimately cardiac decompensation leading to terminal HF and, if not treated, death.

Similar effects of circulatory suppression were observed by introduction of high rate cardiac pacing in animal models. In a porcine model, an atrial or ventricular heart rate over 200 beats/minute is potent enough to induce end-stage HF in a period of 3 - 5 weeks (progressive phase) with characteristics of TIC, though interindividual differences do exist[18,19]. These findings correspond well to decompensated cardiomyopathy and are, importantly, preserved also after the cessation of pacing (chronic phase)[19,20,21,22,23].

Porcine, canine, or ovine TIC models were repeatedly prepared to study the pathophysiology of HF[14], as changes to the LV mimic the characteristics of dilated cardiomyopathy[24]. The hemodynamic characteristics are well described - increased ventricular end-diastolic pressures, decreased cardiac output, increased systemic vascular resistance, and dilation of both ventricles. In contrast, wall hypertrophy is not observed consistently, and even wall thinning was described by some researchers[25,26]. With progression of ventricular dimensions, regurgitation on atrioventricular valves develops[26].

In this publication, we present a protocol to produce a TIC by long-term fast cardiac pacing in swine. This biomodel represents potent means to study decompensated dilated cardiomyopathy, hemodynamics of progressive chronic HF with low cardiac output, and effects of applied treatment.

Protocol

This experimental protocol was reviewed and approved by the Institutional Animal Expert Committee at First Faculty of Medicine, Charles University, and was performed at the University experimental laboratory, Department of Physiology, First Faculty of Medicine, Charles University in Prague, Czech Republic, in accordance with Act No. 246/1992 Coll., on the protection of animals against cruelty. All animals were treated and cared for in accordance with the Guide for the Care and Use of Laboratory Animals, 8th edition, published by National Academies Press, 2011. All procedures were performed according to standard veterinary conventions and at the completion of each study, the animal was sacrificed and a necropsy performed. Due to suitable anatomy, five healthy crossbred female swine (*Sus scrofa domestica*) up to 6 months of age were included in this experiment. Their mean body weight was 66 ± 20 kg at the day of data collection.

1. General Anesthesia

1. After 1 day of fasting, initiate anesthesia by intramuscular administration of midazolam (0.3 mg/kg) and ketamine hydrochloride (15 - 20 mg/kg) to the gluteal region.
2. Insert peripheral cannula into the marginal ear vein for intravenous drug applications.
3. Administer intravenous boluses of propofol (2 mg/kg) and morphine (0.1 - 0.2 mg/kg).
4. Provide animals with oxygen via a facial mask and advance orotracheal intubation with a cuffed endotracheal tube with a diameter of 6.5 - 7.5 mm.
5. Continue the total intravenous anesthesia by combination of propofol (6 - 12 mg/kg/h), midazolam (0.1 - 0.2 mg/kg/h), and morphine (0.1 - 0.2 mg/kg/h), adjusting the doses according to individual responses - suppress spontaneous breaths, corneal reflexes, and motoric response. Protect the animal's eyes with ointment to prevent dryness.
6. Operate the mechanical ventilation by a closed-loop automatic device set to adaptive support ventilation to maintain target end-tidal CO_2 of 38 - 42 mmHg and adequate hemoglobin saturation of 95 - 99%. Monitor all vital functions, especially heart rate and body temperature.
7. Attach the animal by securing its legs gently to the operation table in the supine position.
8. Administer wide spectrum antibiotics - 1 g of cefazolin intravenously through the ear vein cannula.

2. Ventricular Lead Implantation

1. Locate surgical sites and shave the skin properly using a razor at (1) the jugular region above the sternocleidomastoid muscle and (2) the unilateral paravertebral region on the back side of the animal's neck.
2. Using the ultrasound vascular probe, visualize the external jugular vein and mark its location on the skin. Locate the carotid artery as well to prevent its injury.
3. After the wide skin disinfection using povidone iodine, cover with a sterile surgical drape with the hole over the marked jugular region.
4. Prepare all necessary tools for pacemaker implantation and keep them sterile. It is crucial to maintain a sterile environment throughout the procedure.
5. Cut the skin parallel above the external jugular vein, form a shallow subcutaneous pocket in soft tissue not more than 10 mm deep. Do not expose any large vessels.
6. From the bottom of the preformed pocket, insert a sheath into the external jugular vein, using the standard Seldinger technique. First, insert a soft-tip guidewire through a 12G puncture needle, and then over the guidewire introduce a 7-French plastic tear away introducer sheath with a dilator.

7. Under fluoroscopic guidance, introduce a 58 cm pacing lead through this sheath and position its tip to the apex of the right ventricle. Then, remove the sheath and fixate the active tip of the electrode to the myocardium by screwing out its helix.
8. Test the pacing parameters - the lead sensed signal from ventricular electrocardiogram and impedance must be stable, the pacing threshold should be below an amplitude of 1 V with 0.4 ms of pulse duration.
9. Pull a rubber sleeve on the pacing lead and fix both together to the bottom of the preformed jugular subcutaneous pocket by two non-absorbable suture braided thread stitches. Importantly, enough length of the pacing lead must be inserted, considering the future possible growth of the animal.

3. Subcutaneous Lead Tunneling

1. Turn the animal over on its side and disinfect the previously shaved skin region lateral to the backbone, then cover with a sterile surgical drape with a hole. Make sure the jugular subcutaneous pocket and the lead remain sterile.
2. Cut the skin lateral to the backbone and form a deep, spacious, subcutaneous pocket. Use dull preparation and stop any possible bleeding.
3. Take a soft rubber extension tube from a sterile infusion set and cut off both its ends. Using a tunneling tool, preform a direct subcutaneous tunnel connecting the jugular and dorsal subcutaneous pockets with this extension tube.
4. Connect the tube's free end to the ventricular lead by pulling it onto its IS-1 connector and draw the lead through the preformed tunnel into the dorsal subcutaneous pocket by pulling the tube dorsally. It may be useful to secure the connection with a silk tie.
5. Remove both the tunneling tool and the extension tube, exposing the ventricular lead from the dorsal subcutaneous pocket.

4. Pacemaker Implantation

1. Set up the implantable dual-chamber heart pacemaker unit with the "Y" connecting part. The "Y" connection allows a convergent connection of both pacemaker outputs to be joined and connected together to the single pacing lead (**Figure 1** and **Figure 2**). This setting will later provide a wide range of pacing frequencies.
2. After connecting the pacing lead, fasten all the IS-1 connection screws in the pacemaker header unit and the "Y" lead connection.
3. Hide the whole pacing system in the deep dorsal pocket. There must be enough space to comfortably accommodate the pacemaker unit and any redundant lead.
4. Check the final pacing parameters. Make sure that cardiac ventricular pacing is possible from both pacemaker outputs.
5. Flush with povidone iodine and close both subcutaneous pockets. Use absorbable braided thread to suture fibrous tissue layers and non-absorbable suture for skin adaptation.

5. Postoperative Care

1. Observe the animal carefully until it regains sufficient consciousness.
2. Continue in a wide spectrum intravenous antibiotic regimen until the wounds are healed - cefazolin 1 g every 12 h. Administer analgesics in appropriate dosing, *e.g.,* morphine 0.2 mg/kg every 6 - 12 h for 3 days by subcutaneous injection. If necessary, make dose adjustments to adequately prevent pain.
3. Place the animal in a comfortable, calm facility at room temperature. Allow free access to water and suitable alimentation.
4. Dress the wounds with sterile scrubs regularly to preserve clean healing.
5. To provide rest after the surgical procedure, keep the pacemaker inhibited by native heart rhythm for at least 3 days.
6. Remove the non-absorbable skin sutures when fully healed, approximately 10 - 14 days after the procedure.

6. Pacing Protocol

1. Start the pacing protocol after an adequate resting period. Initially, increase the paced ventricular heart rate to 200 beats/min by setting the dual-chamber pacemaker to mode D00, 100 beats/min, and concomitantly adjusting the AV delay to 300 ms (to exactly match the pace to pace interval, see **Table 1**). Select the unipolar pacing in both outputs.
2. Increase stepwise the paced heart rate to 220 beats/min after 1 week and to 240 beats/min after 2 weeks (**Figure 3**). Keep continuous pacing at this frequency unless it is not hemodynamically tolerated. If the HF progresses too quickly, reduce the paced heart rate before increasing it again after another week.
3. Use auscultation of heart beat, ECG, and pacemaker interrogation daily to verify the heart rate and constant pacing parameters, including battery life.

7. Heart Failure Induction and Monitoring

1. Ensure regular care by a specialized veterinarian and monitor the animal's general health status. Clinical observations of increasing native heart and respiratory rates, evaluation of peripheral pulse oximetry, and reduction in spontaneous physical activity or appetite provide information about HF progression.
2. Use the advantage of wireless transcutaneous pacemaker interrogation and, if possible, continuous ECG recording - frequent non-sustained ventricular tachycardias (VT) are a sign of severe HF progression.
3. Use echocardiographic assessments to reveal the structural and functional heart changes. Pay attention to find an optimal image window according to porcine anatomy and heart dilation - for a typical 4 chamber view, place the transducer to the right just below the xiphoid and angle it to point to the neck or left shoulder. For short-axis views, use intercostal windows. Reduction of ventricular ejection fraction in native heart rhythm and atrioventricular regurgitations should be noticeable after a few weeks.
   NOTE: Significant interindividual differences of high rate ventricular pacing tolerance exist. Therefore, frequent monitoring and individually adapted adjustment of the pacing protocol are necessary.

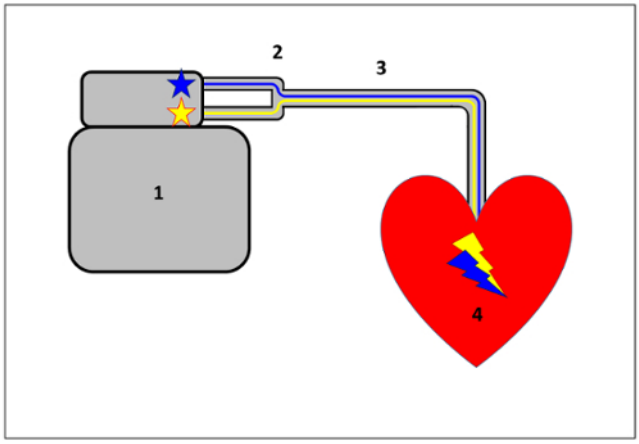

Figure 1: Heart pacing unit schematic. The dual-chamber pacemaker (1), a "Y" shaped adapter (2) conducting convergently both pacemaker outputs together to a single pacing lead (3). The tip of the lead is fixated into the apical part of the RV cavity (4). This setting provides a wide range of high pacing frequencies. Please click here to view a larger version of this figure.

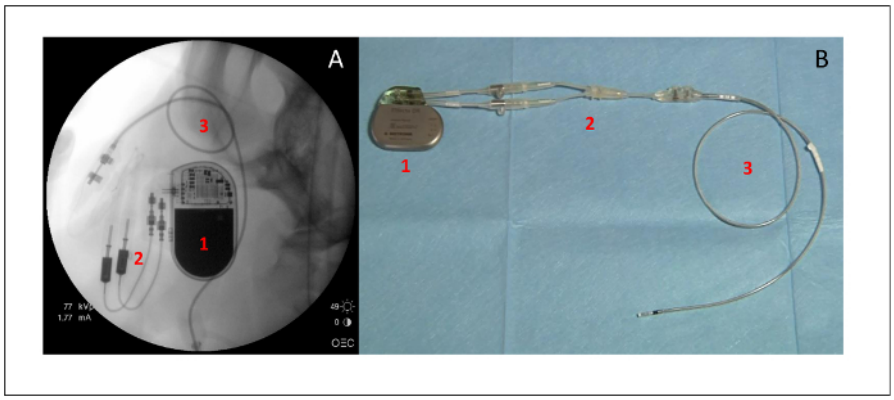

Figure 2: Heart pacing unit. X-ray (**A**) and photography (**B**) of the dual-chamber pacemaker (1), a "Y" shaped adapter (2), and the ventricular pacing lead (3). Please click here to view a larger version of this figure.

Desired HR	Set pacemaker rate	Pace to pace interval
beats/min	beats/min	ms
200	100	300
220	110	270
240	120	250
250	125	240

Table 1: Pacemaker parameters. To allow high rate cardiac pacing with the implanted in-house-modified dual-chamber pacemaker unit, the table shows the desired paced heart rate (HR) and matching pace to pace interval values. The pacemaker must be set to D00 operation mode at a rate of half of the desired HR, and the AV delay set to the corresponding pace to pace interval in milliseconds.

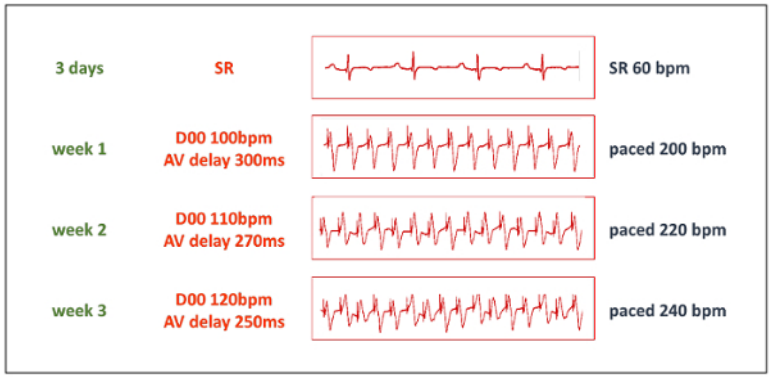

Figure 3: Pacing protocol. The progressive phase of the TIC induction starts after a resting period of 3 days. Then, the pacemaker is set to D00 mode with a pacing frequency of 50% of the desired paced frequency, and AV delay is set to the matching pace to pace interval (see Table 1). Thanks to the "Y" shaped adapter, both pacemaker outputs are conducted to a single pacing lead. bpm = beats/minute. Please click here to view a larger version of this figure.

Representative Results

Testing the model: After signs of decompensated chronic HF became prominent, anesthesia and artificial ventilation were administered again following the principles described above, but dosing was adjusted due to low cardiac output[27]. Due to possible cardiodepressive effects of anesthetics, careful intensive monitoring of vital functions is necessary.

The animal was attached in the supine position and all invasive approaches commenced. The femoral vein and artery and jugular vein were punctured and intravascular approaches ensured by standard percutaneous intraluminal sheaths. Right carotid and subclavian arteries were surgically exposed and circumjacent ultrasound flow probes of appropriate sizes were attached, enabling the obtainment of continuous blood flow measurements[28].

Central venous pressure (CVP) was measured via the jugular vein using a standard invasive method with a fluid-filled pressure transducer, but a high-sensitivity pressure sensor equipped catheter in the thoracic aorta was used for systemic arterial pressure measurements. Regional tissue oxygenation was monitored by near-infrared spectroscopy with sensors placed on the head and right forearm representing the brain and peripheral tissue oxygen saturation levels (rSO_2)[29]. A transthoracic echocardiographic probe was used for 2D and color Doppler imaging. Data from ECG, heart rate, pulse oximetry, blood pressures, capnometry, and rectal temperature were centralized on a bed-side monitor for immediate control. A balloon Swan-Ganz catheter was introduced through a femoral vein sheath to the pulmonary artery allowing readings of thermodilution derived continuous cardiac output (CO)[30] and mixed venous hemoglobin saturation (SvO_2). Through the aortic valve, a pressure-volume (PV) catheter was introduced retrogradely to the LV cavity. This PV conductance catheter enabled the registration of instant volume and pressure in the LV chamber[31,32,33,34], and its stable position was guided by fluoroscopy and echocardiography to obtain optimal PV loop morphology (**Figure 4** and **Figure 5**). Measured LV parameters included end-diastolic pressure and volume (EDP and EDV), end-systolic volume (ESV), LV peak pressure (LV PP), and maximal positive change of LV pressure, defined as the first time derivative of LV pressure normalized to EDV (dP/dt_{max} / EDV), which then represents a preload independent index of LV contractility[35,36]. Additional calculated parameters were stroke volume (SV = EDV - ESV), left ventricular ejection fraction (EF = SV / EDV), and averaged arterial flow in the carotid and subclavian arteries. Fluoroscopic guidance and X-ray imaging were conducted by a C-arm throughout the protocol. After conclusion of the experimental measurements, euthanasia by intravenous potassium overdose and autopsy were performed. The heart was exposed, cut out from the chest, emptied of blood, weighed, and investigated for structural abnormalities.

All data were acquired in native sinus rhythm after the rapid ventricular pacing had been stopped abruptly and time had been provided for stabilization to steady state conditions. Parameters were then recorded and sets of data averaged from three end-expiratory time points. If present, premature beats were omitted from the analyses. All values are expressed as mean ± standard deviation.

Measured results: Physical examination revealed severe clinical signs of chronic HF in all animals after 4 - 8 weeks of pacing protocol. Detailed results are summarized in **Table 2**.

Initial mean heart rate of sinus rhythm was 100 ± 38 beats/min, the mean aortic blood pressure reached 47 ± 38 mmHg and CVP 14 ± 4 mmHg. Chest X-rays showed heart shadow dilation, with a cardiothoracic ratio of 0.64 ± 0.04 (**Figure 5A**). This is in concordance with transthoracic echocardiography findings. Dilation of all heart chambers, severe systolic dysfunction of both ventricles, and significant mitral and tricuspid regurgitations were apparent on echocardiography. Mean ejection fraction of the left ventricle was below 30% in all animals, the LV wall was judged non-hypertrophic with a thickness of 7 - 10 mm and dyssynchrony of LV contraction was obvious (**Figure 6**).

Thermodilution measured cardiac output in the resting state was 2.9 ± 0.8 L/min and mixed venous blood saturation 62 ± 18% corresponded with inadequate tissue oxygen delivery in this model. Average arterial blood flow in the carotid artery was 211 ± 144 mL/min and in the subclavian artery was 103 ± 108 mL/min. Similarly, regional tissue saturation recorded transcutaneously on the head was only 57 ± 13%, and it was even lower on the right forearm, at 37 ± 13%.

The pressure volume loop obtained from the PV catheter illustrates the detailed hemodynamic measures and work produced by the mechanical activity of the left ventricle during each cardiac cycle (**Figure 4**). Maximum LV peak pressure was reduced to 49 ± 32 mmHg, but EDP remained low at 7 ± 4 mmHg. The measured volumes of the left ventricular chamber were reflective of its dilation and systolic dysfunction. EDV was increased to 189 ± 59 mL and ESV to 139 ± 37 mL. Averaged SV was 51 ± 45 mL and the mean LV ejection fraction was calculated to be 25 ± 16%. In addition, a preload independent index of LV contractility can be represented by a dP/dt_{max} / EDV ratio, which was averaged to 2.2 ± 1.7 mmHg/s/mL.

An autopsy confirmed cardiomegaly (**Figure 7**) with a mean heart weight of 471 ± 127 g, which formed 0.7% of body weight. Dilation of all heart chambers and LV wall thinning were stated, and fluid collections were described in pericardial and peritoneal spaces. No shunt or other cardiac anomaly was found in any of the animals.

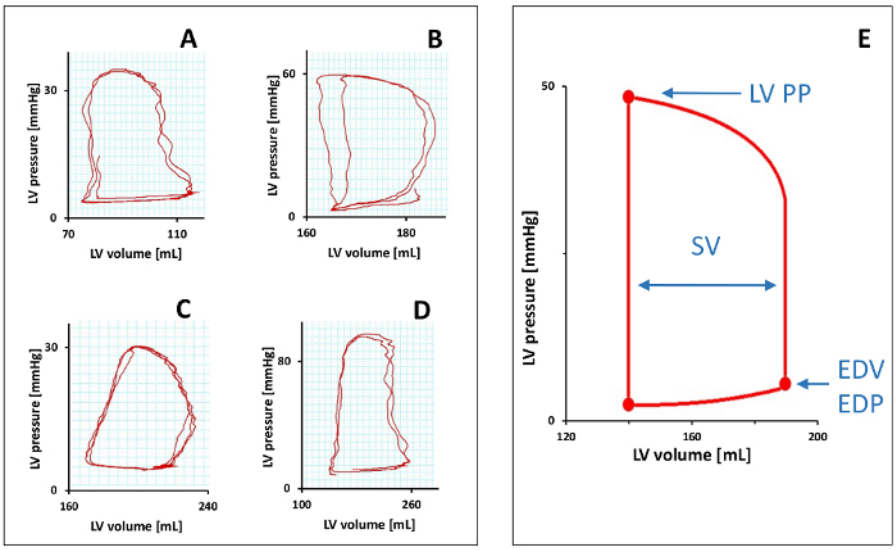

Figure 4: **Pressure-volume measurements.** Samples of direct left ventricular PV loops (**A-D**) and schematic averaged PV loop of all TIC subjects (**E**). LV PP = LV peak pressure, EDP = end-diastolic pressure, EDV = end-diastolic volume, and SV = stroke volume. Please click here to view a larger version of this figure.

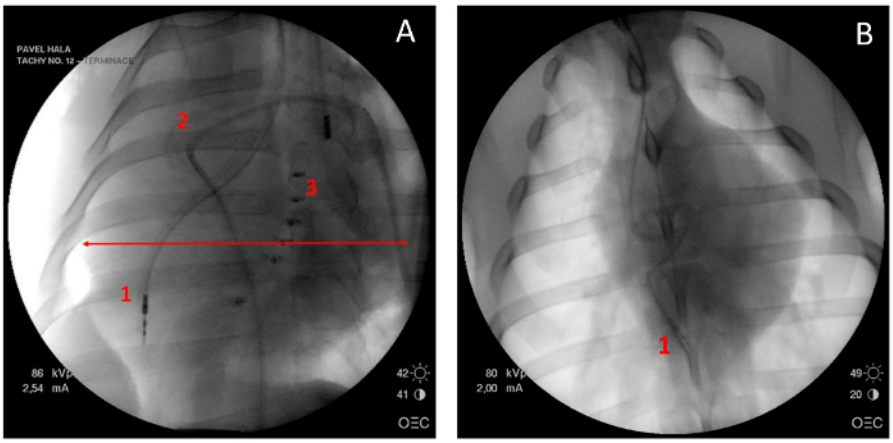

Figure 5: Chest X-rays. Enlarged heart shadow (red arrow) and increased cardiothoracic ratio (**A**). Note the pacing lead introduced to the apex of right ventricle (1), Swan-Ganz catheter placed in the pulmonary artery (2), and PV catheter with 5 electrodes in left ventricular chamber (3). For comparison, a chest X-ray of the normal heart from the day of pacemaker implantation (**B**). Please click here to view a larger version of this figure.

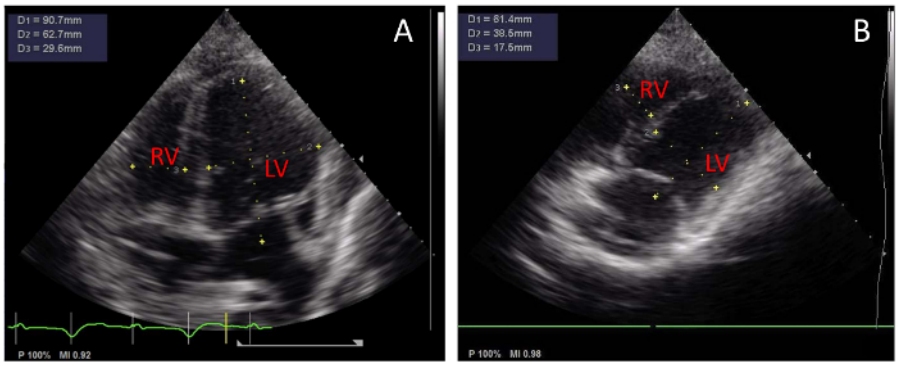

Figure 6: Transthoracic echocardiography. Representative tachycardia-induced cardiomyopathy with severe dilation of all heart chambers (**A**) and a similar view obtained before the pacemaker was implanted (**B**), for comparison. Both acquisitions were taken at end-diastole. Notice the visible tip of pacing lead in RV apex in (**A**). RV = right ventricle, and LV = left ventricle. Please click here to view a larger version of this figure.

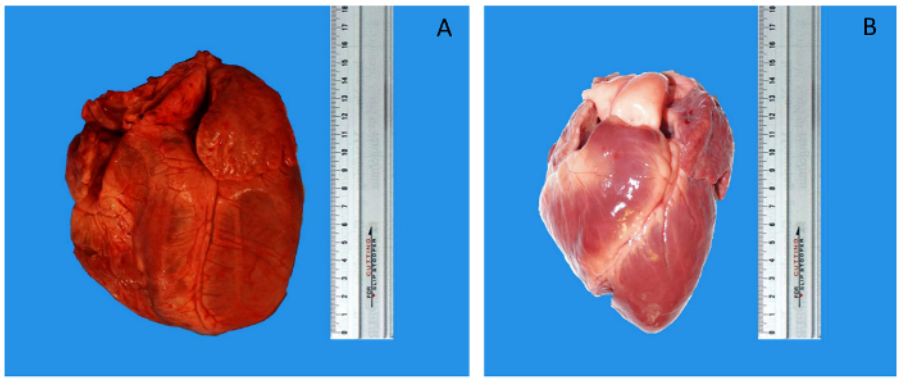

Figure 7: Photographs of exposed heart. Cardiomegaly (**A**) after the TIC induction. Normal porcine heart sample for size comparison (**B**) (scales in cm). Please click here to view a larger version of this figure.

Parameter	TIC value			Units
Imaging				
CTR	0.64	±	0.04	
LV EF		< 30		%
LV EDD	66	±	3	mm
RV EDD	40	±	6	mm
AV regurgitations		severe		
Circulation parameters				
HR	100	±	38	beats/min
MAP	47	±	38	mmHg
CO	2.9	±	0.8	L/min
SvO_2	62	±	18	%
rSO_2 head	57	±	13	%
rSO_2 right forearm	37	±	13	%
Carotid flow	211	±	144	mL/min
Subclavian flow	103	±	108	mL/min
CVP	14	±	4	mmHg
Pressure-volume acquisition				
LV PP	49	±	32	mmHg
LV EDP	7	±	4	mmHg
LV EDV	189	±	59	mL
LV ESV	139	±	37	mL
SV	51	±	45	mL
LV EF	25	±	16	%
dP/dt_{max} / EDV ratio	2.2	±	1.7	mmHg/s/mL
Autopsy				
mean heart weight	471	±	127	g
cardiomegaly, dilation of heart chambers, LV wall thinning, pericardial fluid collections				

Table 2: Numerical results of the TIC model after cessation of pacing protocol. All values expressed as mean ± standard deviation. CTR = cardiothoracic ratio, LV EF = LV ejection fraction, LV EDD / RV EDD = LV / RV end-diastolic diameter, AV regurgitations = atrioventricular valve regurgitations, HR = heart rate, MAP = mean aortic pressure, CO = cardiac output, SvO_2 = mixed venous hemoglobin saturation, rSO_2 = regional tissue saturation, CVP = central venous pressure, LV PP = LV peak pressure, LV EDP / LV EDV = LV end-diastolic pressure/volume, LV ESV = LV end-systolic volume, and SV = stroke volume.

Discussion

Chronic HF is a major health problem that contributes greatly to morbidity and mortality. The pathogenesis and progression of HF in humans is complex, so an appropriate animal model is critical to investigate the underlying mechanisms and to test novel therapeutics that aim to interfere with native severe disease progression. To study its pathogenesis, large animal models are being used for experimental testing.

In general, surgical models of chronic HF closely mimic this disease. When compared to models of acute HF, chronic HF models offer more insight into the pathophysiology, but at the cost of time consuming experimental preparation or higher mortality rate. From the variety of known chronic HF models, we are referring to an appropriate and easily manageable model, represented here by decompensated chronic HF induced by paced tachycardia.

Tachycardia-induced cardiomyopathy as a form of dilated cardiomyopathy is inducible by fast cardiac pacing. The pacing electrode can be located in the ventricles or atria[19,24]. We omitted the supraventricular pacing site to prevent problems possibly caused by atrioventricular block during high pacing frequencies. The ventricular position also improved the stability of the pacing lead fixated in the ventricular apex compared to the atrial position and reduced occurrence of its dislocation. The presented methodology is specifically designed for easy performance, use of widely available equipment, and prevention of complications. Another goal of this method was to easily control chronic HF progression by titration of the pacing protocol.

Bacterial infection complications are a major problem of implants in experimental settings. Generator pocket infections and infective endocarditis are both associated with poor prognoses and would make the experiment futile. Due to porcine anatomy, the jugular region is exposed and if a

pacemaker generator was placed here, healing and preventing contamination would be a difficult task in long-survival experiments. The usage of subcutaneous tunneling enables the location of the pacemaker generator pocket to the dorsal region, which is accessible and can be kept in a hygienic state. The pacemaker is also not within the animal's reach, which considerably improves healing. An alternative approach could be the use of an extracorporeal pacemaker generator attached to the skin surface, but this tactic was shown to be mechanically vulnerable, if long-term animal survival was intended.

All equipment necessary for the described protocol are widely available, and this method is reproducible with basic surgical and catheterization skills. The purpose of the "Y" shaped connection unit is to use a regular dual-chamber pacemaker, as it converges both of its outputs (atrial and ventricular) to the tip of the single pacing lead. These settings allow a wide range of high rate pacing frequencies (200 - 300 beats/min, **Figure 1** and **Table 1**).

The most critical step is the titration of pacing frequencies. Too high from the beginning would cause acute decompensation with no time for the adaptation mechanisms to develop; conversely, titrating the pacing too low would be well tolerated and would prolong the HF induction.

According to previous publications[22,25,37] and the authors' experience, the pacing protocol was defined and started with pacing rate of 200 beats/min, which is above physiological rate of healthy swine in exercise or stress. Subsequently, the frequency was escalated and titrated between 200 and 240 beats/min with respect to individual HF progression[13,19]. Due to interindividual differences in response to fast pacing, the time needed to produce chronic HF with profound signs of decompensation varied from 4 to 8 weeks. An issue here can become the battery life, as such high rate pacing increases energy demands. Especially when the pacing threshold is elevated, regular interrogations are important.

After the pacing protocol, symptoms of chronic HF were prominent consistently in all animals - tachypnea, fatigue, spontaneous tachycardia of >150 beats/min, and systolic murmurs. After further clinical investigation, ascites, pericardial and pleural effusions, non-sustained ventricular tachycardias, dilation of all heart chambers, and significant mitral and tricuspid regurgitations were described. Failing hemodynamics was indicated by arterial hypotension, poor myocardial contractility, low stroke volume, and cardiac output reduced to approximately 50% of a healthy animal's expected normal value[38]. This developed model of tachycardia induced cardiomyopathy matched well to poorly compensated dilated cardiomyopathy and was also preserved after the cessation of pacing[21,39,40].

The fact that systolic function continues to be severely deteriorated after cessation of pacing makes the model an excellent choice to examine HF in native sinus rhythm. It has been previously shown that tachycardia-induced systolic dysfunction is at least partially reversible in the so-called recovery phase, but the time needed for it to improve or normalize varies significantly between individuals. The pacing protocol duration and aggressiveness of rate titration may be a significant contributor too, as permanent ischemic and fibrotic changes are produced in the myocardium[22,39,40,41]. The persistence of severe systolic dysfunction in the presented model was tested at least for 12 h after the pacing had been ceased[4] and the qualities of the prepared model including neurohumoral dynamics, peripheral vascular abnormalities, and cardiac dysfunction were reflective of human chronic HF[14].

The presented results demonstrate severely deteriorated hemodynamics, both clinical investigation and measured values indicate induction of HF syndrome. Cardiomegaly was consistently observed by clinical examination, imaging, and autopsy. Heart rate of sinus rhythm after the cessation of fast pacing was elevated from normal resting frequency, but we assume that the influence of cardiodepressive effects of anesthetics could limit this spontaneous tachycardia. Aortic pressures show deep hypotension[42] and CVP was elevated.

Functional reflection is then the failing circulation and tissue hypoperfusion. These are primarily caused by impaired myocardial contraction, as indicated by the low ejection fraction of the left ventricle. Both ventricles were dilated with no extension in wall thickness, and this heart remodeling was grounds for progressive atrioventricular regurgitations and consequently low cardiac output. As no anatomical shunts were found postmortem, the cardiac output was equally low in systemic as well as in pulmonary circulation, and so the thermodilution derived cardiac output measurements in the pulmonary artery were used to calibrate the PV loop volume characteristics.

The brachial and brain regional tissue oxygen saturation as well as the regional blood flow in subclavian and carotid artery suggests centralization of the blood circulation. Their low values show severely reduced tissue perfusion in peripheral as well as in vital organs, which was confirmed by low SvO_2 when compared to the expected normal value of at least 65%[42]. The general low tissue perfusion was in concordance with the measurements of low cardiac output.

Hemodynamics and mechanical work during each cardiac cycle of the left ventricle was well documented by the PV diagram obtained from PV catheter instant measurements. Poor myocardial strength was denoted by maximum LV peak pressure during systole and the dP/dt_{max} / EDV ratio, a preload independent index of LV contractility. LV chamber volumes were enlarged during the whole cycle, thus the image of dilated cardiomyopathy. The end-diastolic LV pressure was not increased as high as would be expected in cardiogenic shock. The LV filling pressure remains low, most likely due to high compliance of the LV thin myocardial wall[43].

In the vast majority of previous TIC studies, porcine and canine models have been used[19]. However, rapid pacing can be used to induce cardiomyopathy in other species, even in small animals. Few studies have demonstrated metabolic effects of acute TIC in rats[44] or myocardial contractility impairment after long-term fast pacing in rabbits[45].

Although this model is adequately reliable, it has several limitations. Non-sustained ventricular tachycardias are a sign of successful HF induction, but long-lasting VT produce risks of sudden cardiac death. During anesthesia, one of the animals required resuscitation and defibrillation. The wide dispersion of results was partly due to differences in animal body weight. Also, the necessity of anesthesia has to be taken under consideration when reporting the results, especially its influence on heart rate and blood pressure. Blood levels of porcine-specific markers could be useful for assessment of the degree of cardiac remodeling, but the evidence on this front is still lacking. As most of these measurement methods were invasive and thus unrepeatable, we did not provide a baseline or sham subject measurement.

A model of progressive chronic heart failure can be produced by the presented methodology. This technique is easy to perform with widely available equipment, and the results are robust and reproducible. This tachycardia-induced cardiomyopathy offers a valuable object for further experimental studies on hemodynamics, investigation of disease mechanisms and effects of applied treatments.

positives	negatives
chronic heart failure syndrome with systemic adaptation	time consuming model preparation
easy control of disease progression	close monitoring necessary
lead tunneling prevents infective complications	risk of lead dislocation
done with basic surgical and cathetrization skills	risk of malignant arrhythmia
potentially transferable to different animal species	

Table 3: Overview summarizing the positives and negatives of the presented methodology for tachycardia-induced cardiomyopathy in swine as a model of chronic heart failure.

Disclosures

The authors have nothing to disclose.

Acknowledgements

This work was supported by Charles University research grants GA UK No. 538216 and GA UK No. 1114213.

References

1. Ostadal, P. *et al.* Direct comparison of percutaneous circulatory support systems in specific hemodynamic conditions in a porcine model. *Circ Arrhythm Electrophysiol.* **5** (6), 1202-1206 (2012).
2. Ostadal, P. *et al.* Increasing venoarterial extracorporeal membrane oxygenation flow negatively affects left ventricular performance in a porcine model of cardiogenic shock. *J Transl Med.* **13** 266 (2015).
3. Shen, I. *et al.* Left ventricular dysfunction during extracorporeal membrane oxygenation in a hypoxemic swine model. *Ann Thorac Surg.* **71** (3), 868-871 (2001).
4. Hala, P. *et al.* Regional tissue oximetry reflects changes in arterial flow in porcine chronic heart failure treated with venoarterial extracorporeal membrane oxygenation. *Physiol Res.* **65** (Supplementum 5), S621-S631 (2016).
5. Church, J. T. *et al.* Normothermic Ex-Vivo Heart Perfusion: Effects of Live Animal Blood and Plasma Cross-Circulation. *ASAIO J.* (2017).
6. Bavaria, J. E. *et al.* Changes in left ventricular systolic wall stress during biventricular circulatory assistance. *Ann Thorac Surg.* **45** (5), 526-532 (1988).
7. Shen, I. *et al.* Effect of extracorporeal membrane oxygenation on left ventricular function of swine. *Ann Thorac Surg.* **71** (3), 862-867 (2001).
8. Ostadal, P. *et al.* Novel porcine model of acute severe cardiogenic shock developed by upper-body hypoxia. *Physiol Res.* **65** (4), 711-715 (2016).
9. Ostadal, P. *et al.* Noninvasive assessment of hemodynamic variables using near-infrared spectroscopy in patients experiencing cardiogenic shock and individuals undergoing venoarterial extracorporeal membrane oxygenation. *J Crit Care.* **29** (4), 690 e611-695 (2014).
10. Mlcek, M. *et al.* Hemodynamic and metabolic parameters during prolonged cardiac arrest and reperfusion by extracorporeal circulation. *Physiol Res.* **61** (Suppl 2) S57-65 (2012).
11. Tarzia, V. *et al.* Extracorporeal life support in cardiogenic shock: Impact of acute versus chronic etiology on outcome. *J Thorac Cardiovasc Surg.* **150** (2), 333-340 (2015).
12. Howard, R. J., Stopps, T. P., Moe, G. W., Gotlieb, A., Armstrong, P. W. Recovery from heart failure: structural and functional analysis in a canine model. *Can J Physiol Pharmacol.* **66** (12), 1505-1512 (1988).
13. Moe, G. W., Armstrong, P. Pacing-induced heart failure: a model to study the mechanism of disease progression and novel therapy in heart failure. *Cardiovasc Res.* **42** (3), 591-599 (1999).
14. Power, J. M., Tonkin, A. M. Large animal models of heart failure. *Aust N Z J Med.* **29** (3), 395-402 (1999).
15. Trahanas, J. M. *et al.* Achieving 12 Hour Normothermic Ex Situ Heart Perfusion: An Experience of 40 Porcine Hearts. *ASAIO J.* **62** (4), 470-476 (2016).
16. Gossage, A. M., Braxton Hicks, J. A. On auricular fibrillation. *Quarterly Journal of Medicine.* **6** 435-440 (1913).
17. Whipple, G. H., Sheffield, L. T., Woodman, E. G., Theophilis, C., Friedman, S. Reversible congestive heart failure due to chronic rapid stimulation of the normal heart. *Proceedings of the New England Cardiovascular Society.* **20** (1), 39-40 (1962).
18. Spinale, F. G., Grine, R. C., Tempel, G. E., Crawford, F. A., Zile, M. R. Alterations in the myocardial capillary vasculature accompany tachycardia-induced cardiomyopathy. *Basic Res Cardiol.* **87** (1), 65-79 (1992).
19. Shinbane, J. S. *et al.* Tachycardia-induced cardiomyopathy: a review of animal models and clinical studies. *J Am Coll Cardiol.* **29** (4), 709-715 (1997).
20. Moe, G. W., Stopps, T. P., Howard, R. J., Armstrong, P. W. Early recovery from heart failure: insights into the pathogenesis of experimental chronic pacing-induced heart failure. *J Lab Clin Med.* **112** (4), 426-432 (1988).
21. Takagaki, M. *et al.* Induction and maintenance of an experimental model of severe cardiomyopathy with a novel protocol of rapid ventricular pacing. *J Thorac Cardiovasc Surg.* **123** (3), 544-549 (2002).
22. Tomita, M., Spinale, F. G., Crawford, F. A., Zile, M. R. Changes in left ventricular volume, mass, and function during the development and regression of supraventricular tachycardia-induced cardiomyopathy. Disparity between recovery of systolic versus diastolic function. *Circulation.* **83** (2), 635-644 (1991).
23. Schmitto, J. D. *et al.* Large animal models of chronic heart failure (CHF). *J Surg Res.* **166** (1), 131-137 (2011).
24. Spinale, F. G. *et al.* Chronic supraventricular tachycardia causes ventricular dysfunction and subendocardial injury in swine. *Am J Physiol.* **259** (1 Pt 2), H218-229 (1990).

25. Chow, E., Woodard, J. C., Farrar, D. J. Rapid ventricular pacing in pigs: an experimental model of congestive heart failure. *Am J Physiol.* **258** (5 Pt 2), H1603-1605 (1990).
26. Howard, R. J., Moe, G. W., Armstrong, P. W. Sequential echocardiographic-Doppler assessment of left ventricular remodelling and mitral regurgitation during evolving experimental heart failure. *Cardiovasc Res.* **25** (6), 468-474 (1991).
27. Roberts, F., Freshwater-Turner, D. Pharmacokinetics and anaesthesia. *Contin Educ Anaesth Crit Care Pain 7 (1): 25-29.* (2007).
28. Carter, B. S., Farrell, C., Owen, C. Microsurgical clip obliteration of middle cerebral aneurysm using intraoperative flow assessment. *J Vis Exp.* (31) (2009).
29. Wolf, M., Ferrari, M., Quaresima, V. Progress of near-infrared spectroscopy and topography for brain and muscle clinical applications. *J Biomed Opt.* **12** (6), 062104 (2007).
30. Mateu Campos, M. L. *et al.* [Techniques available for hemodynamic monitoring. Advantages and limitations]. *Med Intensiva.* **36** (6), 434-444 (2012).
31. Baan, J. *et al.* Continuous measurement of left ventricular volume in animals and humans by conductance catheter. *Circulation.* **70** (5), 812-823 (1984).
32. Ellenbroek, G. H. *et al.* Primary Outcome Assessment in a Pig Model of Acute Myocardial Infarction. *J Vis Exp.* (116) (2016).
33. Townsend, D. Measuring Pressure Volume Loops in the Mouse. *J Vis Exp.* (111) (2016).
34. van Hout, G. P. *et al.* Admittance-based pressure-volume loops versus gold standard cardiac magnetic resonance imaging in a porcine model of myocardial infarction. *Physiol Rep.* **2** (4), e00287 (2014).
35. Kass, D. A. *et al.* Comparative influence of load versus inotropic states on indexes of ventricular contractility: experimental and theoretical analysis based on pressure-volume relationships. *Circulation.* **76** (6), 1422-1436 (1987).
36. Glower, D. D. *et al.* Linearity of the Frank-Starling relationship in the intact heart: the concept of preload recruitable stroke work. *Circulation.* **71** (5), 994-1009 (1985).
37. Hendrick, D. A., Smith, A. C., Kratz, J. M., Crawford, F. A., Spinale, F. G. The pig as a model of tachycardia and dilated cardiomyopathy. *Lab Anim Sci.* **40** (5), 495-501 (1990).
38. Wyler, F. *et al.* [The Gottinger minipig as a laboratory animal. 5. Communication: cardiac output, its regional distribution and organ blood flow (author's transl)]. *Res Exp Med (Berl).* **175** (1), 31-36 (1979).
39. Cruz, F. E. *et al.* Reversibility of tachycardia-induced cardiomyopathy after cure of incessant supraventricular tachycardia. *J Am Coll Cardiol.* **16** (3), 739-744 (1990).
40. Umana, E., Solares, C. A., Alpert, M. A. Tachycardia-induced cardiomyopathy. *Am J Med.* **114** (1), 51-55 (2003).
41. Dixon, J. A., Spinale, F. G. Large animal models of heart failure: a critical link in the translation of basic science to clinical practice. *Circ Heart Fail.* **2** (3), 262-271 (2009).
42. Xanthos, T. *et al.* Baseline hemodynamics in anesthetized landrace-large white swine: reference values for research in cardiac arrest and cardiopulmonary resuscitation models. *J Am Assoc Lab Anim Sci.* **46** (5), 21-25 (2007).
43. Little, W. C. Diastolic dysfunction beyond distensibility: adverse effects of ventricular dilatation. *Circulation.* **112** (19), 2888-2890 (2005).
44. Montgomery, C., Hamilton, N., Ianuzzo, C. D. Effects of different rates of cardiac pacing on rat myocardial energy status. *Mol Cell Biochem.* **102** (2), 95-100 (1991).
45. Qin, F., Shite, J., Mao, W., Liang, C. S. Selegiline attenuates cardiac oxidative stress and apoptosis in heart failure: association with improvement of cardiac function. *Eur J Pharmacol.* **461** (2-3), 149-158 (2003).

Přiložený dokument 4

Regional Tissue Oximetry Reflects Changes in Arterial Flow in Porcine Chronic Heart Failure Treated With Venoarterial Extracorporeal Membrane Oxygenation

P. HÁLA[1,2], M. MLČEK[2], P. OŠŤÁDAL[1], D. JANÁK[2], M. POPKOVÁ[2], T. BOUČEK[3], S. LACKO[2], J. KUDLIČKA[2], P. NEUŽIL[1], O. KITTNAR[2]

[1]Department of Cardiology, Na Homolce Hospital, Prague, Czech Republic, [2]Department of Physiology, First Faculty of Medicine, Charles University, Prague, Czech Republic, [3]Second Department of Internal Medicine, First Faculty of Medicine, Charles University, Prague, Czech Republic

Received March 26, 2016
Accepted October 26, 2016

Summary

Venoarterial extracorporeal membrane oxygenation (VA ECMO) is widely used in treatment of decompensated heart failure. Our aim was to investigate its effects on regional perfusion and tissue oxygenation with respect to extracorporeal blood flow (EBF). In five swine, decompensated low-output chronic heart failure was induced by long-term rapid ventricular pacing. Subsequently, VA ECMO was introduced and left ventricular (LV) volume, aortic blood pressure, regional arterial flow and tissue oxygenation were continuously recorded at different levels of EBF. With increasing EBF from minimal to 5 l/min, mean arterial pressure increased from 47±22 to 84±12 mm Hg ($P<0.001$) and arterial blood flow increased in carotid artery from 211±72 to 479±58 ml/min ($P<0.01$) and in subclavian artery from 103±49 to 296±54 ml/min ($P<0.001$). Corresponding brain and brachial tissue oxygenation increased promptly from 57±6 to 74±3 % and from 37±6 to 77±6 %, respectively (both $P<0.01$). Presented results confirm that VA ECMO is a capable form of heart support. Regional arterial flow and tissue oxygenation suggest that partial circulatory support may be sufficient to supply brain and peripheral tissue by oxygen.

Key words

Extracorporeal membrane oxygenation • Chronic heart failure • Swine • Perfusion • Oximetry

Corresponding author

P. Hála, Department of Physiology, First Faculty of Medicine, Charles University, Albertov 5, 128 00 Prague 2, Czech Republic. E-mail: pavel.hala@lf1.cuni.cz

Introduction

Extracorporeal membrane oxygenation in venoarterial settings (VA ECMO) represents a well-established percutaneously introduced circulatory support used in refractory but potentially recoverable cardiogenic shock. It can fully substitute the functions of lungs and heart to maintain sufficient gas exchange and systemic blood circulation (Pranikoff *et al.* 1994, Abrams *et al.* 2014). When applied, VA ECMO forms a circulatory bypass as it drains blood from right atrium and after passing it through the gas exchange unit, the oxygenated blood is returned to the thoracic aorta. VA ECMO is proofed beneficial for improved survival, neurologic outcome and resuscitability (Belohlavek *et al.* 2012, Mlcek *et al.* 2012).

On the other hand, VA ECMO has significant effects on systemic circulation. Increasing VA ECMO flow negatively affects left ventricular (LV) performance and hence it has been recently suggested to use only lowest possible rate of circulatory support (Ostadal *et al.* 2015, Broome and Donker 2016). Especially in this context of increasing LV demands during high bypass flow, evaluation of systemic cerebral and peripheral

Fax +420 241 062 164, e-mail: physres@biomed.cas.cz, www.biomed.cas.cz/physiolres

arterial flow, its characteristics and regional tissue oxygen supply become important.

VA ECMO has been studied in number of experiments, but to our knowledge, only intact or acute heart failure (HF) models have been used (Bavaria *et al.* 1988, Shen *et al.* 2001, Mlcek *et al.* 2012, Ostadal *et al.* 2013) and therefore the heart and whole cardiovascular system was untouched prior to the investigations. In contrast, significant part of VA ECMO applications from real life are due to acute circulatory decompensation which develops on grounds of previously present chronic heart disease. Furthermore, retrospective clinical studies have also revealed that outcome of patients treated by ECMO differs according to the "acuteness or chronicity" of underlying cardiac disease (Tarzia *et al.* 2015).

Although there are reasons why models of chronic heart failure are being used rarely – their time-consuming preparation, instability of heart rhythm, ethical questions or mortality rate – their advantage is clearly documented as they offer long-term neurohormonal activation, general systemic adaptation and structural and functional alterations of myocytes (Moe and Armstrong 1999). In presented experiment chronic HF model was developed by fast cardiac pacing. This tachycardia-induced cardiomyopathy (TIC), first described by Gossage and Braxton Hicks (1913) and widely used in experiments since 1962 (Whipple *et al.* 1962), reliably mimics decompensated dilated cardiomyopathy with low cardiac output which persists also after cessation of pacing (Shinbane *et al.* 1997, Takagaki *et al.* 2002, Schmitto *et al.* 2011).

The aim of our study was to describe cerebral and peripheral blood supply in swine model of decompensated chronic HF supported by increasing flow of VA ECMO in a stepwise protocol. We focused on arterial flow speed, its characteristics represented by pulsatility index and possible association with tissue oxygen saturation. Based on published data it is expected that VA ECMO should be able to supply both cerebral and peripheral tissue adequately, but the optimal flow rate of circulatory support remains unclear. At the same time reduction of pulsatility indices was expected in arterial flow and pressure.

Methods

Experimental protocol was reviewed and approved by the Institutional Animal Expert Committee of First Faculty of Medicine, Charles University and was performed at the University experimental laboratory, Department of Physiology, First Faculty of Medicine, Charles University, Prague, Czech Republic, in accordance with Act No. 246/1992 Coll., on the protection of animals against cruelty. All animals were treated and cared for in accordance with the Guide for the Care and Use of Laboratory Animals published by the US National Institutes of Health (NIH Publication No. 85-23, revised 1985).

At the completion of each study the animal was sacrificed and a necropsy performed to look for potential cardiac anomalies.

Animal model

According to large evidence, TIC as a form of dilated cardiomyopathy was generated by long-term rapid cardiac pacing (Spinale *et al.* 1990, Nikolaidis *et al.* 2001, Gupta and Figueredo 2014).

Five healthy crossbred female swine (*Sus scrofa domestica*) up to 6 months of age with initial weight of 37-46 kg were included in this experiment. After 1 day of fasting, general anesthesia was initiated by intramuscular administration of midazolam (0.3 mg/kg) and ketamine hydrochloride (15-20 mg/kg). Intravenous boluses of propofol (2 mg/kg) and morphine (0.1-0.2 mg/kg) were administered and animals were provided with oxygen and orotracheally intubated with a cuffed endotracheal tube. Total intravenous anesthesia was then continued by combination of propofol (6-12 mg/kg/h), midazolam (0.1-0.2 mg/kg/h) and morphine (0.1-0.2 mg/kg/h), the doses adjusted according to individual responses. Mechanical ventilation was operated by a Hamilton G5 closed-loop automatic device (Hamilton Medical AG, Switzerland) set to adaptive support ventilation to maintain target end-tidal CO_2 of 38-42 mm Hg and adequate hemoglobin saturation of 95-99 %. All procedures were performed according to standard veterinary conventions.

Under aseptic conditions and antibiotic prophylaxis (cefazolin 1 g) a single pacing lead with active fixation was placed transvenously under fluoroscopic guidance in the apical part of right ventricle and subcutaneously tunneled to connect with an in-house modified heart pacemaker (Effecta, Biotronik SE & Co. KG, Germany) which was then implanted into a dorsal subcutaneous pocket. These arrangements proved to prevent device-related complications and allowed a wide range of high rate pacing frequencies.

Additional permanent catheter (Groshong PICC, Bard AS, USA of Arteriofix, B. Braun, Germany) was inserted through the marginal ear vein; animals were then kept in chronic care facility under the care of veterinary specialist. They were provided with free access to water and continued antibiotic regimen of cefazolin for total of 5 days.

Pacing protocol and chronic heart failure induction

After the necessary resting period of two to five days reserved for recovery from the surgical procedure, the rapid ventricular pacing was initiated. According to publications of previous frequent experiments and our own experience, the pacing protocol was defined and started with pacing rate of 200 beats/min. Subsequently, the frequency was escalated and titrated between 200 and 240 beats/min with respect to the heart failure progression (Moe *et al.* 1988, Chow *et al.* 1990, Hendrick *et al.* 1990, Tomita *et al.* 1991). Veterinary surveillance and clinical check-ups including echocardiographic evaluations were kept regularly. Due to interindividual differences in response to fast pacing, time needed to produce chronic heart failure with profound signs of decompensation varied from 4 to 8 weeks.

At the end of pacing protocol, all animals showed consistently significant symptoms of chronic HF – tachypnea, fatigue, spontaneous sinus tachycardia of >150 beats/min and systolic murmurs. At further investigation ascites, pericardial and pleural effusions, nonsustained ventricular tachycardias, dilation of all heart chambers and significant mitral and tricuspid regurgitations were apparent. Hemodynamics of failing circulation was denoted by arterial hypotension and due to poor contractility and low stroke volume, cardiac output was reduced to approximately 50 % of healthy animal's expected normal value. This developed model of tachycardia induced cardiomyopathy corresponds well to poorly compensated dilated cardiomyopathy and was preserved also after the cessation of pacing (Cruz *et al.* 1990, Takagaki *et al.* 2002, Umana *et al.* 2003). Qualities of prepared model including neurohormonal dynamics, peripheral vascular abnormalities and cardiac dysfunction are reflecting human chronic HF (Power and Tonkin 1999).

Experimental preparation and monitoring

At this stage of decompensated chronic heart failure, again anesthesia and artificial ventilation were administered following principles described above, but dosing was adjusted due to low cardiac output (Roberts and Freshwater-Turner 2007).

Anesthetized animals were then connected to bed-side monitor (Life Scope TR, Nihon Kohden, Japan) and all invasive approaches commenced. Bilateral femoral veins and arteries, jugular vein and left carotid artery were punctured and intravascular approaches ensured by standard percutaneous intraluminal sheaths. Right carotid and subclavian arteries were surgically exposed and circumjacent ultrasound flow probes of appropriate sizes attached (3PSB, 4PSB or 6PSB, Scisense, Transonic Systems, USA) enabling to obtain continuous blood flow measurements.

Intravenous anticoagulation was initiated by unfractionated heparin bolus (100 IU/kg) followed by continual infusion maintaining an activated clotting time (ACT) of 200 s (Hemochron Junior+, International Technidyne Corporation, USA) and following invasive catheters were introduced. A balloon Swan-Ganz catheter through femoral vein to the pulmonary artery allowing thermodilution derived continuous cardiac output (CCO Combo Catheter; Vigilance II, Edwards Lifesciences, USA), mixed venous hemoglobin saturation, pulmonary artery and pulmonary arterial wedge pressure assessments. Through the aortic valve a pressure-volume catheter (7F VSL Pigtail, Scisense, Transonic Systems, USA) was introduced to the LV cavity. Central venous pressure was measured *via* jugular vein using a standard invasive method with pressure transducer (TruWave, Edwards Lifesciences, USA), but a high sensitive pressure sensor equipped pigtail catheter in aortic arch (7F VSL Pigtail, Scisense, Transonic Systems, USA) was used for systemic arterial pressure measurement.

Regional tissue oxygenation was monitored by near-infrared spectroscopy (INVOS Oximeter, Somanetics, USA) with sensors placed on forehead and right arm region representing brain and peripheral tissue oxygen saturation levels (Wolf *et al.* 2007).

Intracardiac and transthoracic echocardiography probes (AcuNav IPX8, Acuson P5-1 and X300 ultrasound system, Siemens, USA) were used for 2D and color Doppler imaging. ECG, heart rate, pulse oximetry, capnometry, rectal temperature, mixed central venous hemoglobin saturation were measured continuously. Blood gas parameters were evaluated by a bedside analysis system (AVL Compact 3, Roche Diagnostics, Germany).

VA ECMO

After intravenous systemic heparinization, extracorporeal circulation was maintained by a femoral venoarterial extracorporeal oxygenation system (VA ECMO) compounded of Levitronix Centrimag console (Thoratec, USA) with centrifugal pump, hollow fiber microporous membrane oxygenator (QUADROX-i Adult, Maquet Cardiopulmonary, Germany) and tubing set with two percutaneous cannulas (Medtronic, USA) introduced by the Seldinger technic through punctures of the unilateral femoral vein and artery (Fig. 1). Tip of venous inflow cannula (23 Fr) was advanced to the right atrium and the tip of arterial outflow cannula (18 Fr) reached the thoracic descending aorta, the position of both being verified by fluoroscopy. Fully assembled ECMO circuit was primed with saline solution and extracorporeal blood flow (EBF) initiated at flow of 300 ml/min being considered the minimal flow necessary to prevent thrombus formation inside ECMO circuit and having a neglectable impact to the systemic circulation at the same time. This rate of EBF was later referred to EBF 0 category. EBF was registered by a separate circumjacent flow probe (ME 9PXL, Transonic Systems, USA) attached to the ECMO outflow cannula.

Blood gas analysis was monitored continuously (CDI Blood Parameter Monitoring System 500, Terumo Cardiovascular Systems Corporation, USA) and the partial oxygen pressure and air flow through the oxygenator adjusted to maintain pO_2 100-120 mm Hg, pCO_2 35-45 mm Hg and pH 7.35-7.45 in the blood leaving the oxygenator throughout the whole experiment.

Experimental protocol

After instrumentation was completed, ventricular pacing was discontinued, so all animals were further studied in sinus rhythm.

Under the conditions of profound chronic HF, ECMO protocol was initiated. Mechanical ventilation was repeatedly adjusted (both partial pressure of oxygen and minute ventilation) to reach hemoglobin saturation in arterial blood of 95-99 % and end-tidal CO_2 between 38-42 mm Hg. Crystalloid infusion was administered (100-500 ml/h) to reach and maintain a mean baseline CVP at least 5 mm Hg, ACT kept in range of 200-300 s by continuous intravenous heparin administration.

According to our standardized ramp protocol, the speed of EBF was set by changing the VA ECMO pump rotation speed. We gradually changed the EBF by steps of 1 l/min every 10-15 min and these stepwise

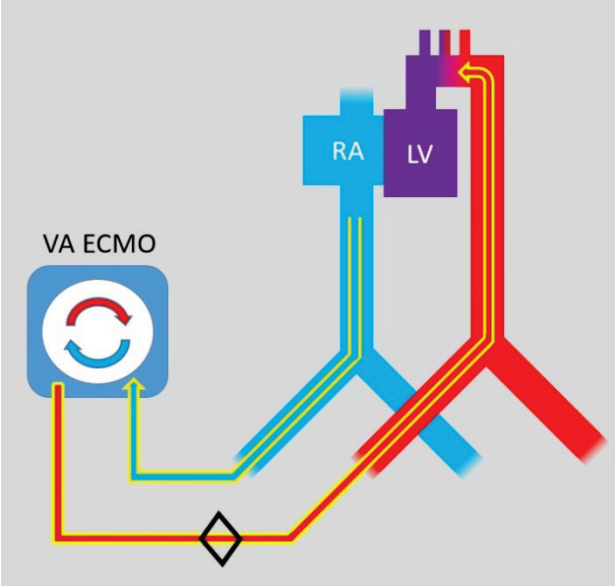

Fig. 1. Femoro-femoral VA ECMO scheme. Venous blood is drawn by inflow cannula from right atrium (RA). It then continuous through the gas exchange unit by the force of centrifugal pump and oxygenated is returned to the descending part of thoracic aorta. LV – left ventricle. Black diamond showing the placement of EBF flow probe.

categories with constant EBF were referred to as EBF 0, 1, 2, 3, 4 and 5.

Data acquisition

In sinus rhythm, time was provided for stabilization of all measured parameters and the baseline values were collected before ECMO introduction. Then ECMO was started and at each EBF step animals were allowed to stabilize for 10-15 min to reach steady state conditions. Parameters were then recorded and sets of data averaged from three end-expiratory time points. If present, premature beats were omitted from the analyses.

Statistical analysis

All data are expressed as mean ± standard error of mean (SEM). Comparisons between different levels of EBF were analyzed by using the Friedman test with Dunn's multiple comparison. Nonparametric Spearman correlation was used for statistical relationship of groups. A P-value of <0.05 was considered statistically significant.

Recordings were sampled at 400 Hz by PowerLab A/D converter and continuously recorded to LabChart Pro Software (ADInstruments, Australia), statistical analyses and graphical interpretations were performed in GraphPad Prism 6 (GraphPad, USA) and Excel (Microsoft, USA).

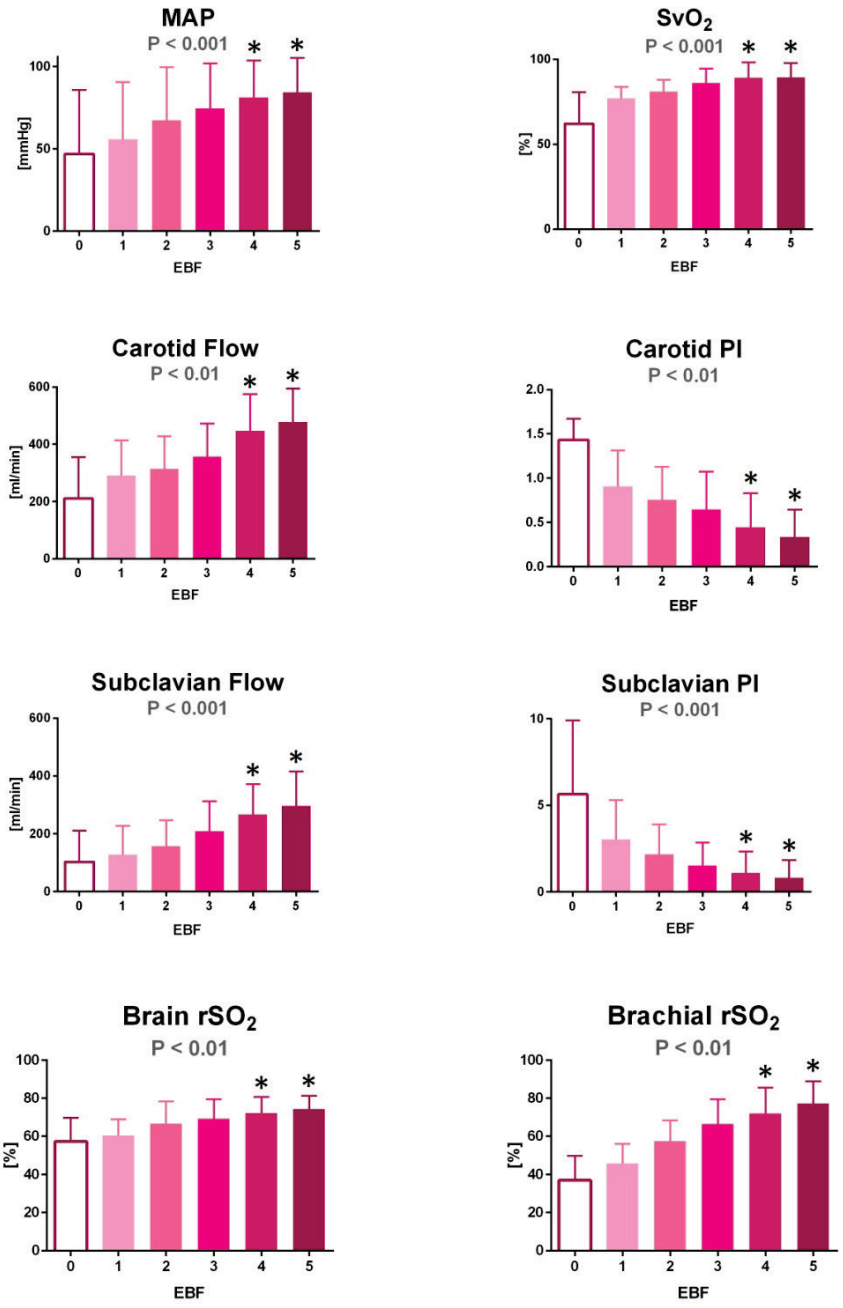

Fig. 2. The effect of venoarterial extracorporeal membrane oxygenation blood flow (EBF) on selected hemodynamic parameters in a porcine model of chronic heart failure. * marks significant change from EBF 0. MAP – mean aortic pressure, SvO_2 – mixed venous oxygenation, PI – pulsatility index, rSO_2 – regional tissue oxygenation.

Results

Detailed results are summarized in Table 1 and Figure 2. In all animals included in our study fast ventricular pacing for 4-8 weeks generated TIC with signs of decompensated heart failure which was denoted by baseline values of cardiac output at rest 2.9±0.4 l/min, severe dilation of all heart chambers and mean aortic pressure 47±22 mm Hg. Left ventricular ejection fraction evaluated by echocardiography and pressure-volume catheter was below 30 % in all animals and initial mean heart rate of sinus rhythm was 100±19 beats/min. Baseline SvO_2 value of 62±8 % corresponds with inadequate tissue oxygen delivery in our model.

With stepwise increase of EBF from minimal to maximal flow, we observed gradual increase in mean aortic blood pressure by 79 % – from baseline 47±22 mm Hg to 84±12 mm Hg (for EBF 0 to EBF 5, P<0.001). Similarly, arterial blood flow increased with every increase of EBF. In carotid artery it changed from 211±72 ml/min to 479±58 ml/min (by 127 % from EBF 0 to EBF 5, P<0.01) and in subclavian artery from 103±49 ml/min to 296±54 ml/min (by 187 % from EBF 0 to EBF 5, P<0.001). For both arteries the pulsatility index (PI) was defined as calculated difference between the peak systolic and minimum diastolic velocities divided

by the mean velocity during each cardiac cycle and as such represents the variability of arterial flow during cardiac cycle. Interestingly, baseline PI was considerably higher in subclavian than in carotid artery. A reduction of pulsatility indices by 76 % (from 1.43±0.12 to 0.34±0.15, P<0.05) in the carotid and by 85 % (from 5.7±1.9 to 0.8±0.5, P<0.001) in the subclavian artery was observed from EBF 0 to EBF 5.

Mean heart rate (HR) tended to decline with every increase in EBF – from 101±22 beats/min to 86±14 beats/min (for EBF 0-5, P=0.34). Left ventricular stroke work (SW) was calculated from measured pressure-volume loops and exhibits flow-dependent increase from 1434±941 mm Hg*ml to 1892±1036 mm Hg*ml (for EBF 0-5, P<0.05), but reaching its maximal value of 2105±1060 mm Hg*ml at EBF 4. Baseline mixed venous blood saturation (SvO_2) was 62±8 %, but increased to 77±3 % with EBF 1 and reached >80 % with all higher EBF steps (P<0.01). With increasing of EBF, the average value of CVP did gradually fall, but not under 7 mm Hg, avoiding ECMO underfilling.

Regional tissue oxygenation (rSO_2) both on forehead and right arm was on low level at baseline, but increased promptly with increase of EBF. Forehead rSO_2 changed by 30 % from 57±6 % to 74±3 % and right brachial rSO_2 changed in total by 108 % from 37±6 % to 77±6 % (both P<0.01).

Graphs of regional perfusion and tissue oxygenation are visualized on Figure 3 and demonstrate linear relationship – carotid flow correlated significantly with brain oxygenation (r=0.75, P<0.001) and subclavian flow correlated significantly with corresponding brachial oxygenation (r=0.94, P<0.001).

Table 1. Hemodynamic parameters and oximetry data for each step of increasing extracorporeal blood flow (EBF in l/min).

Parameter	VA ECMO blood flow						Relative change
	EBF 0	**EBF 1**	**EBF 2**	**EBF 3**	**EBF 4**	**EBF 5**	*EBF 0-5*
MAP, mm Hg	47±22	56±20	67±19	75±16	81±13*	84±12*	79 %
Carotid flow, ml/min	211±72	291±62	314±57	356±57	447±64*	479±58*	127 %
Carotid pulsatility index	1.43±0.12	0.91±0.20	0.75±0.19	0.64±0.21	0.44±0.19*	0.34±0.15*	-76 %
Subclavian flow, ml/min	103±49	128±44	158±40	208±47	266±47*	296±54*	187 %
Subclavian pulsatility index	5.7±1.9	3.0±1.0	2.2±0.8	1.5±0.6	1.1±0.5*	0.8±0.5*	-86 %
HR, beats/min	101±22	96±19	93±17	90±13	90±14	86±14	-15 %
*SW, mm Hg*ml*	1434±941	1595±987	1867±1102	2014±1062	2105±1060*	1892±1036	32 %
SvO_2, %	62±8	77±3	81±3	86±4	89±4*	89±4*	44 %
CVP, mm Hg	14±2	11±2	10±2	8±2*	9±2*	8±2*	-43 %
rSO_2 forehead, %	57±6	60±4	67±5	69±5	72±4*	74±3*	30 %
rSO_2 right arm, %	37±6	46±5	58±5	67±6	72±7*	77±6*	108 %

Values expressed as mean ± SEM. Values significantly different from EBF 0 marked with *. MAP – mean aortic pressure, HR – heart rate, SW – left ventricular stroke work, SvO_2 – mixed venous blood oxygenation, CVP – central venous pressure, rSO_2 – regional tissue oxygenation.

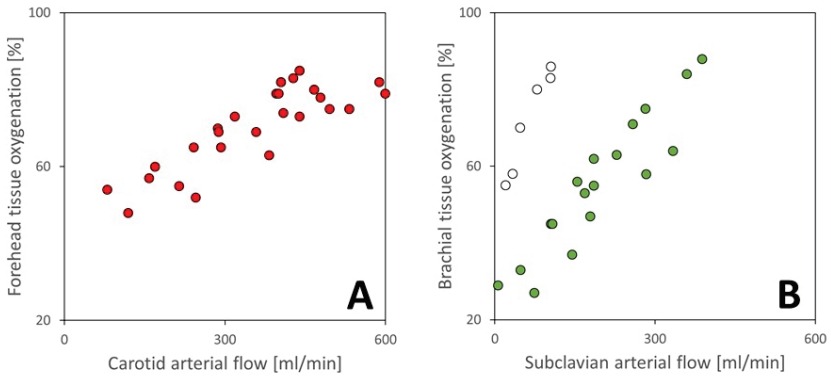

Fig. 3. Correlation of carotid (**A**) and subclavian (**B**) arterial flow and corresponding regional tissue oxygenation. Correlation coefficients r=0.75 (for A) and r=0.94 (for B), P<0.001 for both; omitting one outlying subject – empty circles in B.

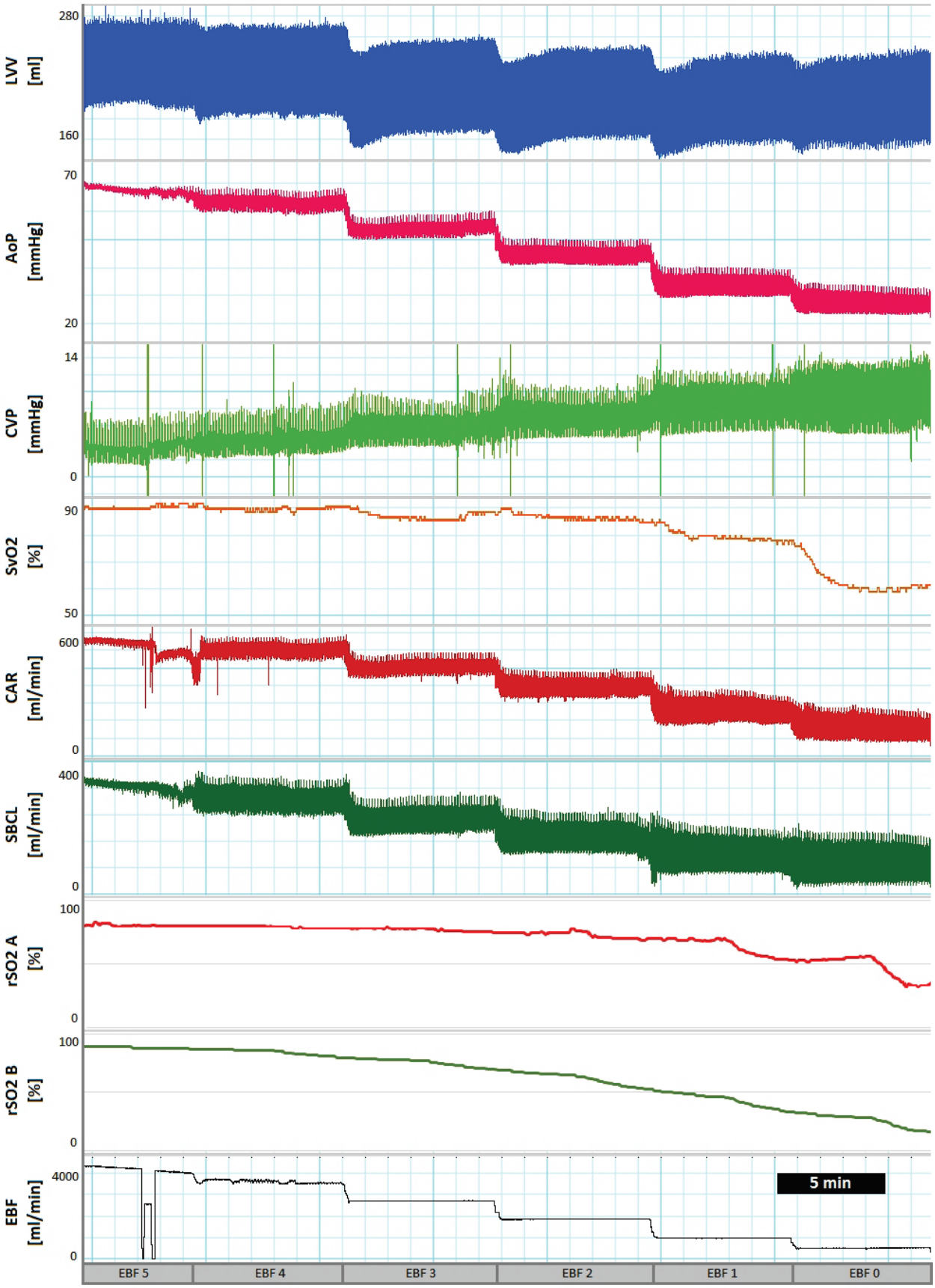

Fig. 4. Continuous data records from one animal (reversed protocol EBF 5-0). With time (horizontal axis) the EBF changed in stepwise manner. LVV – left ventricular volume, AoP – aortic blood pressure, CVP – central venous pressure, SvO_2 – mixed venous blood oxygenation, CAR – carotid arterial flow, SBCL – subclavian arterial flow, rSO_2 A – forehead tissue oxygenation, rSO_2 B – brachial tissue oxygenation, EBF – extracorporeal blood flow.

Continuous data samples acquired from one animal model are shown on Figure 4. After each change of EBF, presented parameters change abruptly, then stabilize during 1-5 min reaching steady-state. Volumetric and hemodynamic parameters demonstrate only partial compensation. Postmortem autopsies did not reveal any shunt or other cardiac anomaly, but significant myocardial hypertrophy (mean heart weight of 471±127 g).

Discussion

VA ECMO serves as an efficient circulatory support in cases of cardiac decompensation. In recent studies, it has been reported that increasing inflow of oxygenated blood from ECMO circuit to the thoracic aorta significantly increases afterload and demands on work of LV and therefore oxygen consumption of the myocardium. By the same authors, setting VA ECMO flow as low as possible was proposed (Ostadal *et al.* 2015, Broome and Donker 2016). Based on SW measurements, this is in agreement with our observations. On the other hand, adequate vital organ perfusion and tissue oxygenation has to be ensured. Thus, the optimal rate of support from extracorporeal circulation remains unclear. In presented study, we focused on influence of VA ECMO on brain and peripheral arterial flow and corresponding tissue oxygenation in a stepwise protocol of increasing EBF.

As in current healthcare practice, VA ECMO is used to treat acute circulatory decompensation which often develops on grounds of previously present chronic heart disease. The use of a chronic HF model to study effects of VA ECMO on systemic circulation is a novel approach of our experimental work. We chose to individualize the pacing protocol as interindividual differences in response have been reported. For TIC induction we paced the apex of right ventricle of each animal at a rate between 200 and 240 beats/min and the TIC model was developed in a period of 4-8 weeks. After this time, persistent changes of myocardium were expected and circulatory failure persisted after cessation of pacing. Also neurohormonal response and compensatory mechanisms were activated during this period. In agreement with literature mentioned above, this porcine model of tachycardia-induced heart failure represented a form of dilated cardiomyopathy with symptoms of profound circulatory decompensation which was denoted by low-flow heart failure, low central venous and regional tissue oxygenation.

Brain and peripheral tissue oxygenation levels were represented by near-infrared spectroscopy with sensors placed on forehead and right arm. This transcutaneous technique is widely used for bedside monitoring of relative local oxyhemoglobin concentration changes. As a non-invasive method it has been validated both in experimental and clinical studies for microcirculation assessments (Ito *et al.* 2012, Ostadal *et al.* 2014). Blood flow to matching regions was measured by circumjacent probes on right carotid and right subclavian artery.

Overlook of our results confirms that with stepwise increase of the EBF, arterial blood flow in carotid and subclavian artery increase in a manner respecting the increase of mean aortic blood pressure. As both pulsatile systemic and non-pulsatile extracorporeal circulations are concomitantly meeting in the thoracic aorta, with increasing of EBF, the relative contribution of LV ejection to arterial flow is decreasing. Due to the increase of LV end-diastolic pressure, excessive afterload may not be accompanied by an increase in coronary perfusion, which may further contribute to the loss of pulsatility observed in both arteries (Kato *et al.* 1996).

Whether deficiency of pulsatile flow in arteries negatively affects organ perfusion remains a controversial topic. At baseline before ECMO initiation, pulsatility index of carotid flow was considerably lower compared to subclavian, but with increase of EBF to 5 l/min, the carotid PI dropped less than in subclavian artery (by 76 % vs. 85 %). In general, PI is to be influenced by transaortic LV ejection, vascular resistance, arterial carbon dioxide tension and aortic and arterial wall stiffness, which can be considered low as we studied young animals. To suppress their effects, blood gas parameters were maintained in physiological ranges in extracorporeal and also native circulation. Insufficiency of the aortic valve, another contributor to pulsatility, was present in our model due to the insertion of transaortic catheter. But, according to echocardiography, this was of little significance. Similar gradual decline of PI in newborns was observed at higher EBF and remained low also shortly after the VA ECMO decannulation, suggesting changes in vascular resistance (Van De Bor *et al.* 1990).

In our results, baseline cerebral perfusion through the right carotid artery was 211±72 ml/min, which is approximately 59 % of flow reported previously in healthy animals with identical methodology (Mlcek *et al.* 2015). Interindividual variability of carotid flow does

not seem to correlate with body size. Instantaneous increase of arterial flow is provided by setting higher EBF. This increase is again more prominent in subclavian compared to carotid artery (by 187 % vs. 127 %). Similarly, respecting the local flow, baseline regional tissue oxygenation of the arm is lower compared to the forehead (P=0.08), but it increases by 108 % compared to only 30 % increase on the forehead. These observations are reflecting peripheral hypoperfusion and the ability to compensate intracranial circulation at baseline in conditions of cardiogenic shock. Both brain and brachial tissue oxygenation demonstrate linear correlation with local perfusion throughout the whole protocol, which supports the constant local oxygen consumption.

Our results of cerebral perfusion are similar to clinical study reported by Liem *et al.* (1995). In infants undergoing VA ECMO for cardiorespiratory failure, they evidenced increased total cerebral blood flow accompanied by increased cerebral blood volume and also loss of PI assessed by transcranial Doppler ultrasound. On contrary, different observations were reported by Stolar and Reyes (1988) in healthy lambs – two hours of high flow VA ECMO narrowed pulse pressure, but caused no significant changes of carotid flow. The use of healthy animals, absence of increase in mean arterial pressure or cannulas' position can explain this discrepancy. Notably, link of cerebral hyperperfusion and intracranial hemorrhage is suspected (Van De Bor *et al.* 1990).

Mean brain oxygenation in healthy animal is referred to reach 65 % (Xanthos *et al.* 2007). In our work, already during low to mild circulatory support of EBF 2 or 3 l/min, the tissue oxygenation, arterial flow and mixed venous oxygen saturation steeply comes close to normal values. Further increase to high rates of EBF then seems to provide only moderate improvement. These experimental results could imply that in decompensated chronic heart failure of matching severity, low to mild EBF may be of enough circulatory support to cover adequate tissue needs and at the same time protecting the LV from possibly harming overload.

Although the main parameters followed trends significantly, only five animals were included in the study. Despite our maximal effort, presented results should be tempered by several limitations. First, the animal model can represent only one form of decompensated chronic heart failure, but VA ECMO would be employed in broad spectrum of patients who may differ in response. Next, near-infrared spectroscopy provides good information about regional tissue oxygenation, but due to technical limitations, only its relative change in time should be evaluated. Also, we could not measure the total brain perfusion as it is served by both carotid and vertebral arteries. Lastly, because we used circulatory support of VA ECMO only for short-term period of hours, its chronic effects cannot be determined. Upcoming studies can answer some of these interesting questions.

Conclusions

Our results imply that even low to mild circulatory support of VA ECMO provides sufficient cerebral and peripheral perfusion in conditions of decompensated chronic heart failure. In these settings high rates of EBF may not be necessary.

Conflict of Interest

There is no conflict of interest.

Acknowledgements

The authors wish to gratefully acknowledge the advice and assistance of Alena Dohnalová, for her help with statistical analysis, of Jana Bortelová for help with animal care and of Matěj Hrachovina, Tereza Vavříková, Alena Ehrlichová and Karel Kypta for their technical support. This work was supported by Charles University research grant GA UK No. 1114213 and SVV 260255/2016.

Abbreviations

CVP – central venous pressure, EBF – extracorporeal blood flow, HF – heart failure, HR – heart rate, LV – left ventricle, PI – pulsatility index, rSO_2 – regional tissue oxygenation, SvO_2 – mixed venous blood saturation, SW – stroke work, TIC – tachycardia-induced cardio-myopathy, VA ECMO – venoarterial extracorporeal membrane oxygenation,.

References

ABRAMS D, COMBES A, BRODIE D: Extracorporeal membrane oxygenation in cardiopulmonary disease in adults. *J Am Coll Cardiol* **63**: 2769-2778, 2014.

BAVARIA JE, RATCLIFFE MB, GUPTA KB, WENGER RK, BOGEN DK, EDMUNDS LH JR: Changes in left ventricular systolic wall stress during biventricular circulatory assistance. *Ann Thorac Surg* **45**: 526-532, 1988.

BELOHLAVEK J, MLCEK M, HUPTYCH M, SVOBODA T, HAVRANEK S, OSTADAL P, BOUCEK T, KOVARNIK T, MLEJNSKY F, MRAZEK V, BELOHLAVEK M, ASCHERMANN M, LINHART A, KITTNAR O: Coronary versus carotid blood flow and coronary perfusion pressure in a pig model of prolonged cardiac arrest treated by different modes of venoarterial ECMO and intraaortic balloon counterpulsation. *Crit Care* **16**: R50, 2012.

BROOME M, DONKER DW: Individualized real-time clinical decision support to monitor cardiac loading during venoarterial ECMO. *J Transl Med* **14**: 4, 2016.

CHOW E, WOODARD JC, FARRAR DJ: Rapid ventricular pacing in pigs: an experimental model of congestive heart failure. *Am J Physiol* **258**: H1603-H1605, 1990.

CRUZ FE, CHERIEX EC, SMEETS JL, ATIE J, PERES AK, PENN OC, BRUGADA P, WELLENS HJ: Reversibility of tachycardia-induced cardiomyopathy after cure of incessant supraventricular tachycardia. *J Am Coll Cardiol* **16**: 739-744, 1990.

GOSSAGE AM, BRAXTON HICKS JA: On auricular fibrillation. *Q J Med* **6**: 435-440, 1913.

GUPTA S, FIGUEREDO VM: Tachycardia mediated cardiomyopathy: pathophysiology, mechanisms, clinical features and management. *Int J Cardiol* **172**: 40-46, 2014.

HENDRICK DA, SMITH AC, KRATZ JM, CRAWFORD FA, SPINALE FG: The pig as a model of tachycardia and dilated cardiomyopathy. *Lab Anim Sci* **40**: 495-501, 1990.

ITO N, NANTO S, NAGAO K, HATANAKA T, NISHIYAMA K, KAI T: Regional cerebral oxygen saturation on hospital arrival is a potential novel predictor of neurological outcomes at hospital discharge in patients with out-of-hospital cardiac arrest. *Resuscitation* **83**: 46-50, 2012.

KATO J, SEO T, ANDO H, TAKAGI H, ITO T: Coronary arterial perfusion during venoarterial extracorporeal membrane oxygenation. *J Thorac Cardiovasc Surg* **111**: 630-636, 1996.

LIEM KD, HOPMAN JC, OESEBURG B, DE HAAN AF, FESTEN C, KOLLEE LA: Cerebral oxygenation and hemodynamics during induction of extracorporeal membrane oxygenation as investigated by near infrared spectrophotometry. *Pediatrics* **95**: 555-561, 1995.

MLCEK M, OSTADAL P, BELOHLAVEK J, HAVRANEK S, HRACHOVINA M, HUPTYCH M, HALA P, HRACHOVINA V, NEUZIL P, KITTNAR O: Hemodynamic and metabolic parameters during prolonged cardiac arrest and reperfusion by extracorporeal circulation. *Physiol Res* **61** (Suppl 2): S57-S65, 2012.

MLCEK M, BELOHLAVEK J, HUPTYCH M, BOUCEK T, BELZA T, LACKO S, KRUPICKOVA P, HRACHOVINA M, POPKOVA M, NEUZIL P, KITTNAR O: Head-up tilt rapidly compromises hemodynamics in healthy anesthetized swine. *Physiol Res* **64** (Suppl 5): S677-S683, 2015.

MOE GW, STOPPS TP, HOWARD RJ, ARMSTRONG PW: Early recovery from heart failure: insights into the pathogenesis of experimental chronic pacing-induced heart failure. *J Lab Clin Med* **112**: 426-432, 1988.

MOE GW, ARMSTRONG P: Pacing-induced heart failure: a model to study the mechanism of disease progression and novel therapy in heart failure. *Cardiovasc Res* **42**: 591-599, 1999.

NIKOLAIDIS LA, HENTOSZ T, DOVERSPIKE A, HUERBIN R, STOLARSKI C, SHEN YT, SHANNON RP: Mechanisms whereby rapid RV pacing causes LV dysfunction: perfusion-contraction matching and NO. *Am J Physiol Heart Circ Physiol* **281**: H2270-H2281, 2001.

OSTADAL P, MLCEK M, KRUGER A, HORAKOVA S, SKABRADOVA M, HOLY F, SVOBODA T, BELOHLAVEK J, HRACHOVINA V, TABORSKY L, DUDKOVA V, PSOTOVA H, KITTNAR O, NEUZIL P: Mild therapeutic hypothermia is superior to controlled normothermia for the maintenance of blood pressure and cerebral oxygenation, prevention of organ damage and suppression of oxidative stress after cardiac arrest in a porcine model. *J Transl Med* **11**: 124, 2013.

OSTADAL P, KRUGER A, VONDRAKOVA D, JANOTKA M, PSOTOVA H, NEUZIL P: Noninvasive assessment of hemodynamic variables using near-infrared spectroscopy in patients experiencing cardiogenic shock and individuals undergoing venoarterial extracorporeal membrane oxygenation. *J Crit Care* **29**: 690.e11-690.e15, 2014.

OSTADAL P, MLCEK M, KRUGER A, HALA P, LACKO S, MATES M, VONDRAKOVA D, SVOBODA T, HRACHOVINA M, JANOTKA M, PSOTOVA H, STRUNINA S, KITTNAR O, NEUZIL P: Increasing venoarterial extracorporeal membrane oxygenation flow negatively affects left ventricular performance in a porcine model of cardiogenic shock. *J Transl Med* **13**: 266, 2015.

POWER JM, TONKIN AM: Large animal models of heart failure. *Aust N Z J Med* **29**: 395-402, 1999.

PRANIKOFF T, HIRSCHL RB, STEIMLE CN, ANDERSON HL 3RD, BARTLETT RH: Efficacy of extracorporeal life support in the setting of adult cardiorespiratory failure. *ASAIO J* **40**: M339-M343, 1994.

ROBERTS F, FRESHWATER-TURNER D: Pharmacokinetics and anaesthesia. *Contin Educ Anaesth Crit Care Pain* **7**: 25-29, 2007.

SCHMITTO JD, MOKASHI SA, LEE LS, POPOV AF, COSKUN KO, SOSSALLA S, SOHNS C, BOLMAN RM 3RD, COHN LH, CHEN FY: Large animal models of chronic heart failure (CHF). *J Surg Res* **166**: 131-137, 2011.

SHEN I, LEVY FH, VOCELKA CR, O'ROURKE PP, DUNCAN BW, THOMAS R, VERRIER ED: Effect of extracorporeal membrane oxygenation on left ventricular function of swine. *Ann Thorac Surg* **71**: 862-867, 2001.

SHINBANE JS, WOOD MA, JENSEN DN, ELLENBOGEN KA, FITZPATRICK AP, SCHEINMAN MM: Tachycardia-induced cardiomyopathy: a review of animal models and clinical studies. *J Am Coll Cardiol* **29**: 709-715, 1997.

SPINALE FG, HENDRICK DA, CRAWFORD FA, SMITH AC, HAMADA Y, CARABELLO BA: Chronic supraventricular tachycardia causes ventricular dysfunction and subendocardial injury in swine. *Am J Physiol* **259**: H218-H229, 1990.

STOLAR CJ, REYES C: Extracorporeal membrane oxygenation causes significant changes in intracranial pressure and carotid artery blood flow in newborn lambs. *J Pediatr Surg* **23**: 1163-1168, 1988.

TAKAGAKI M, MCCARTHY PM, TABATA T, DESSOFFY R, CARDON LA, CONNOR J, OCHIAI Y, THOMAS JD, FRANCIS GS, YOUNG JB, FUKAMACHI K: Induction and maintenance of an experimental model of severe cardiomyopathy with a novel protocol of rapid ventricular pacing. *J Thorac Cardiovasc Surg* **123**: 544-549, 2002.

TARZIA V, BORTOLUSSI G, BIANCO R, BURATTO E, BEJKO J, CARROZZINI M, DE FRANCESCHI M, GREGORI D, FICHERA D, ZANELLA F, BOTTIO T, GEROSA G: Extracorporeal life support in cardiogenic shock: impact of acute versus chronic etiology on outcome. *J Thorac Cardiovasc Surg* **150**: 333-340, 2015.

TOMITA M, SPINALE FG, CRAWFORD FA, ZILE MR: Changes in left ventricular volume, mass, and function during the development and regression of supraventricular tachycardia-induced cardiomyopathy. Disparity between recovery of systolic versus diastolic function. *Circulation* **83**: 635-644, 1991.

UMANA E, SOLARES CA, ALPERT MA: Tachycardia-induced cardiomyopathy. *Am J Med* **114**: 51-55, 2003.

VAN DE BOR M, WALTHER FJ, GANGITANO ES, SNYDER JR: Extracorporeal membrane oxygenation and cerebral blood flow velocity in newborn infants. *Crit Care Med* **18**: 10-13, 1990.

WHIPPLE GH, SHEFFIELD LT, WOODMAN EG, THEOPHILIS C, FRIEDMAN S: Reversible congestive heart failure due to chronic rapid stimulation of the normal heart. *Proceedings of the New England Cardiovascular Society* **20**: 39-40, 1962.

WOLF M, FERRARI M, QUARESIMA V: Progress of near-infrared spectroscopy and topography for brain and muscle clinical applications. *J Biomed Opt* **12**: 062104, 2007.

XANTHOS T, BASSIAKOU E, KOUDOUNA E, TSIRIKOS-KARAPANOS N, LELOVAS P, PAPADIMITRIOU D, DONTAS I, PAPADIMITRIOU L: Baseline hemodynamics in anesthetized landrace-large white swine: reference values for research in cardiac arrest and cardiopulmonary resuscitation models. *J Am Assoc Lab Anim Sci* **46**: 21-25, 2007.